



Prifysgol
Abertawe
Swansea
University



Treatment of Emerging Contaminants in
Wastewater by Advanced Oxidation Processes

Anna Catton, BSc

Supervisors: Prof Chedly Tizaoui, Dr Michael Gerardo

Submitted to Swansea University in fulfilment of the
requirements for the Degree of Master of Science by
research

Swansea University

2023

Abstract

This study evaluated the effectiveness of ozonation and activated carbon for the degradation and removal of three main emerging contaminants (ECs) in wastewater; fluoranthene (FLT), di (2- ethyl hexyl) phthalate (DEHP) and cypermethrin (CYM). The effects of key semi-batch ozonation parameters related to gas-liquid mass transfer and reaction kinetics were identified for all contaminants.

The degradation rates were evaluated in solutions of DI water, using concentration change of ozone and EC versus time. With an ozone gas concentration of 20 g/m³ NTP, the change in concentration from an initial concentration of 0.05 mg/L over time was measured using HPLC. To decrease by 75 %, it took less than a minute for FLT, two minutes for DEHP and six minutes for CYM.

The adsorption of the emerging contaminants with granulated activated carbon (GAC) were evaluated in solutions of DI water at an initial concentration of 1 mg/L. For the decrease in concentration of 60 %, the time for each contaminant varied. For FLT this was achieved in 5 minutes, DEHP was decreased within 20 minutes, and it took CYM 20 minutes to reach this decrease.

The effects of ozonation and adsorption onto GAC were also investigated in samples of final wastewater effluent.

Declarations and Statements

This work has not previously been accepted in substance for any degree and is not being concurrently submitted in candidature for any degree.

Signed: *A. Catton*

Date: 17/01/2024

This thesis is the result of my own investigations, except where otherwise stated. Other sources are acknowledged by footnotes giving explicit references. A bibliography is appended.

Signed: *A. Catton*

Date: 17/01/2024

I hereby give consent for my thesis, if accepted, to be available for electronic sharing

Signed: *A. Catton*

Date: 17/01/2024

The University's ethical procedures have been followed and, where appropriate, that ethical approval has been granted.

Signed: *A. Catton*

Date: 17/01/2024

Acknowledgements

I would like to thank Prof Chedly Tizaoui for his support throughout my project and for assisting in the further development of my understanding and experimental skills. Without his support the outcomes from my project would not have been possible.

I also would like to thank Dr Michael Gerardo with Welsh Water for his continued support with my project and for providing an insight from an industrial point of view into the research I was undertaking.

The M2A programme, I would like to thank, for their support throughout this year, and the additional activities they conducted throughout the year to ensure I finished my masters with a well-rounded set of skills.

My family and have friends have provided me with so much support throughout this year that has helped and enabled me to complete my research and thesis within the time frame and to the best of my abilities.

And finally, thank you to everyone else who has helped me in any capacity throughout this year, there are too many to mention individually, without all of you I would not have been able to complete this project to the level I have. Thank you.

Table of Contents

Abstract	2
Declarations and Statements	3
Acknowledgements	4
Table of Contents	5
Table of Figures	10
Table of Tables	12
Abbreviations	14
Chapter 1 – Introduction	15
Aims and Objectives	18
Chapter 2 – Literature Review	19
2.1 - Water crisis	19
2.2 - Emerging contaminants	19
2.3 – Emerging contaminants of interest to this study	20
2.3.1 - Fluoranthene	21
2.3.2 – Di (2-ethyl hexyl) phthalate	23
2.3.3 - Cypermethrin	25
2.4 - Advanced oxidation processes and alternative processes	27
2.4.1 – Coagulation and flocculation	28
2.4.2 - Biological	29
2.4.3 – Ozone	31
2.4.3.1 - Direct ozonation	32
2.4.3.2 - Indirect ozonation	33
2.4.3.3 – Radical scavengers	37
2.4.3.4 – By-products	37
2.4.3.5 - Ozone toxicology	39
2.4.3.6 - Ozone mass transfer	39
2.4.3.7 - Bubble coalescence	40
2.4.3.9 - Surface tension	40
2.4.3.10 - Effects of pH and temperature on ozonation	42
2.4.4 - Ozonation of the emerging contaminants	42
2.4.4.1 - Fluoranthene ozonation	42
2.4.4.2 - Di (2- ethyl hexyl) phthalate ozonation	42
2.4.4.3 - Cypermethrin ozonation	43

2.4.5 - Hybrid processes	43
2.4.5.1 - UV/H ₂ O ₂	44
2.4.5.2 - Ozone/H ₂ O ₂	44
2.4.5.3 - Ozone/UV	45
2.4.5.4- Fenton's reaction	46
2.4.6 - Adsorption.....	47
2.4.6.1 - Activated carbon	47
2.4.6.2 - Ozone/activated carbon	48
2.4.6.3 - BET Isotherm	49
2.4.6.4 – TOC.....	50
2.4.6.5 - Iodine Number	51
2.4.7 - Isotherms.....	52
2.4.7.1 - Langmuir Isotherm.....	53
2.4.7.2 - Freundlich isotherm	54
2.5 - Rate theory.....	55
2.5.2 - Arrhenius equation	56
2.6 - Analytical techniques	57
2.6.1.1 - Indigo Method.....	57
2.6.1.2 - Beer Lambert Law	59
2.6.2 – Sample preparation.....	60
Chapter 3 – Materials and Methods.....	61
3.1 – Materials.....	61
3.1.1 - Emerging contaminants of interest:.....	61
3.1.2 - Contaminant Solution Preparation	61
3.2 - Analytical	62
3.2.1 - UV-Vis Analysis.....	62
3.2.2 - Fluorescence Analysis	62
3.2.3 - High Performance Liquid Chromatography Analysis	62
3.3 - Ozonation Experiments.....	63
3.4 - Mass transfer of ozone in DI water	63
3.4.1 - Ozonation of chemical contaminants.....	65
3.4.1.1 - Fluoranthene	66
3.4.1.2 - Di (2- ethyl hexyl) phthalate	67
3.4.1.3 - Cypermethrin	68
3.4.1.4 - Stoichiometric Analysis.....	69
3.4.2 - Indigo Method.....	69

3.5 - Adsorption experimentation	71
3.5.1 - Iodine Number	71
3.5.1.1 - Preparation of solutions	71
3.5.1.2 - Standardisation of solutions	72
3.5.1.3 - Iodine number procedure	72
3.5.1.4 - Adsorption with GAC	72
3.6 - Wastewater Analysis	74
Chapter 4 – Ozone Mass Transfer Analysis	76
4.1 - Indigo Method	76
4.2 - Ozone mass transfer	76
4.2.1 - Effects of pH on ozone mass transfer	79
4.2.2 - Effect of temperature	81
4.2.3 - Effect of flow rate	83
4.2.4 - Effect of scavengers	88
Chapter 5 - Ozone Degradation of Chemical Contaminants	90
5.1 - FLT analysis	91
5.1.1 - UV-Vis Analysis	91
5.1.2 - Fluorescence Analysis	91
5.1.3 - HPLC Analysis	92
5.1.3.1 - Calibration Curve	92
5.1.4 - Effect of oxygenating solution	94
5.1.5 - Effect of ozone concentration	95
5.1.6 - Effect of pH	95
5.1.7 - Effects of temperature	99
5.1.9 - Stoichiometric Effects	103
5.1.10 - Summary of findings	105
5.2 - DEHP analysis	106
5.2.1 - UV-Vis Analysis	106
5.2.2 - Fluorescence Analysis	106
5.2.3 - HPLC Analysis	107
5.2.3.1 - Calibration Curve	107
5.2.4 - Oxygenation of DEHP	109
5.2.5 - Ozonation of DEHP	109
5.2.6 - Effect of pH	110
5.2.7 - Effect of temperature	113
5.2.8 - Effect of scavengers	115

5.2.9 - Stoichiometric Analysis.....	116
5.2.10 - Summary of findings.....	118
5.3 - CYM Analysis.....	119
5.3.1 - UV-Vis Analysis.....	119
5.3.2 - Fluorescence Analysis.....	120
5.3.3 - HPLC Analysis.....	120
5.3.3.1 - Calibration Curve.....	120
5.3.4 - Oxygenation of CYM.....	122
5.3.5 - Ozonation of CYM.....	122
5.3.6 - Effect of pH.....	124
5.3.7 - Effect of temperature.....	124
5.3.8 - Effect of scavengers.....	126
5.3.9 - Stoichiometric Analysis.....	128
5.3.10 - Summary of findings.....	129
5.4 - Combined Ozonation.....	130
5.5 - Ozonation Summary.....	132
Chapter 6 - Adsorption onto Activated Carbon.....	133
6.1 - FLT Adsorption.....	133
6.2 - CYM Adsorption.....	136
6.3 - DEHP Adsorption.....	139
6.5 - Iodine Number.....	142
6.6 - Summary of findings.....	145
Chapter 7 – Wastewater Analysis.....	146
7.1 - Ozonation of wastewater.....	147
7.2 - Adsorption onto GAC in wastewater.....	148
Chapter 8 – Conclusion and Future Work.....	151
8.1 - Ozone Mass Transfer.....	151
8.2 - Ozonation of emerging contaminants.....	151
8.2.1 - FLT.....	151
8.2.2 - DEHP.....	152
8.2.3 - CYM.....	153
8.3 - Adsorption by Granulated Activated Carbon.....	154
8.4 - Wastewater Analysis.....	154
8.4.1 - Ozonation of chemical contaminants in wastewater.....	154
8.4.2 - Adsorption of chemical contaminants in wastewater.....	155
References.....	157

Glossary	171
Appendices	173
Appendix 1 – Iodine Number Calculations	173
Standardisation of 0.100 N Sodium Thiosulfate	173
Standardisation of 0.100 N Iodine Solution	173
Calculating the iodine number	174
Calculating the carbon dosage	175
Appendix 2 – deriving the equation relating C_{AL} and k_La	176

Table of Figures

Figure 1: Skeletal structure of fluoranthene	21
Figure 2: Skeletal structure of di (2- ethyl hexyl) phthalate	24
Figure 3: Skeletal structure of cypermethrin.....	26
Figure 4: schematic of the process of coagulation and flocculation	28
Figure 5: Schematic showing the process of biological degradation.....	30
Figure 6: Mechanism for the oxidation of a compound by direct ozonation, where M presents a compound, and M _{oxid} is the compound oxidised.	32
Figure 7: Chemical equation to show the generation of hydroxyl radicals from a chemical oxidation process	33
Figure 8: Diagram to show the generation of hydroxyl radicals from a photocatalytic process, figure generated from (Nosaka & Nosaka, 2016), where S is a substrate molecule.	34
Figure 9: Diagram to show the generation of hydroxyl radicals from a sonochemical process, figure generated from (Ziembowicz et al., 2017)	35
Figure 10: Mechanism for the production of hydroxyl radicals from ozone, where MP is a product.....	36
Figure 11: A schematic showing the cohesive factors between molecules in a liquid.	41
Figure 12: Equation showing the degradation of ozone with hydrogen peroxide to produce hydroxyl radicals	44
Figure 13: The chemical reactions that occur within the Fenton's reaction process	46
Figure 14: an equilibrium between the gas phase and the adsorbate phase	53
Figure 15: within the Freundlich isotherm, there is variety in the amount of gas adsorbed depending on the temperature and pressure.	54
Figure 16: mechanism for the reaction of indigo sulphonate solution with ozone	58
Figure 17: reaction scheme for the reaction with indigo trisulphonate.....	70
Figure 18: effect of gas ozone concentration on absorption into solution (pH = 6, temperature ~ 20 °C, oxygen gas flow = 0.5 L/min)	77
Figure 19: effect of pH on absorption of ozone into solution (ozone gas concentration = 50 g/m ³ NTP, temp = ~ 20 °C, oxygen flow rate = 0.5 L/min)	80
Figure 20: effect of temperature on absorption of ozone into the liquid phase (ozone gas concentration = 50 g/m ³ NTP, pH = 6, oxygen flow rate = 0.5 L/min)	82
Figure 21: (a) effect of flow rate on absorption of ozone into solution; (b) effect of flow rate on kLa, (ozone gas concentration = 50 g/m ³ NTP, pH = 6, temp = ~ 20 °C).....	84
Figure 22: effect of radical scavengers on absorption of ozone into solution (ozone gas concentration = 50 g/m ³ NTP, pH = 6, temp = ~ 20 oC, oxygen flow rate = 0.5 L/min)	88
Figure 23: Chemical reactions for the conversion of radicals to ozone by carbonate	89
Figure 24: Calibration curve obtained for FLT once guards were installed on the column... ..	93
Figure 25: Graph depicting the effect of flowing oxygen into solution on FLT degradation (oxygen flow rate = 0.5 L/min, pH = 6, temp = ~ 20 °C).....	94
Figure 26: Graph comparing the effects of pH on FLT degradation (ozone gas concentration = 20 g/m ³ NTP, temp = ~ 20 oC, oxygen flow rate = 0.5 L/min)	96
Figure 27: Effect of pH on ozone concentration (ozone gas concentration = 20 g/m ³ NTP, temp = ~ 20 oC, oxygen flow rate = 0.5 L/min).....	98
Figure 28: Effect of temperature on FLT degradation (ozone gas concentration = 20 g/m ³ NTP, pH = 6, oxygen flow rate = 0.5 L/min)	99

Figure 29: Effect of tert-butanol on FLT degradation (ozone gas concentration = 20 g/m ³ NTP, temp = ~ 20 oC, oxygen flow rate = 0.5 L/min, pH = 6)	102
Figure 30: Relationship between the volume of ozonated water used in the reaction and the ratio of change of moles of ozone throughout the reaction and change of moles of FLT throughout the reaction	104
Figure 31: calibration curve for the first peak shown in the HPLC analysis for DEHP concentration.....	108
Figure 32: ozonation of DEHP (ozone gas concentration = 20 g/m ³ NTP, temp = ~ 20 °C, oxygen flow rate = 0.5 L/min, pH = 6).....	110
Figure 33: effect of pH (ozone gas concentration = 20 g/m ³ NTP, temp = ~ 20 oC, oxygen flow rate = 0.5 L/min)	111
Figure 34: effect of temperature on DEHP degradation (ozone gas concentration = 20 g/m ³ NTP, pH = 6, oxygen flow rate = 0.5 L/min)	113
Figure 35: effect of the presence of a radical scavenger (ozone gas concentration = 20 g/m ³ NTP, temp = ~ 20 °C, oxygen flow rate = 0.5 L/min, pH = 6).....	115
Figure 36: stoichiometric relationship between DEHP concentration and ozone concentration.....	117
Figure 37: UV-Vis spectrum	119
Figure 38: calibration curve for the HPLC analysis of CYM.....	121
Figure 39: ozonation of CYM (ozone gas concentration = 20 g/m ³ NTP, temp = ~ 20 °C, oxygen flow rate = 0.5 L/min, pH = 6).....	123
Figure 40: degradation of CYM by ozonation at different temperatures (ozone gas concentration = 20 g/m ³ NTP, oxygen flow rate = 0.5 L/min, pH = 6)	125
Figure 41: ozonation of CYM comparing the reaction with the presence of tert-butanol as a radical scavenger and with no scavenger present (ozone gas concentration = 20 g/m ³ NTP, temp = ~ 20 °C, oxygen flow rate = 0.5 L/min, pH = 6)	127
Figure 42: Relationship between the volume of ozonated water used within the reaction and the ratio of change of moles of ozone throughout the reaction compared to the change in moles of CYM throughout the reaction	128
Figure 43: ozonation degradation rates of all contaminants when ozonated in a solution of DI water containing all three contaminants (ozone concentration = 20 g/m ³ NTP, oxygen flow rate = 0.5 L/min, pH = 6, temperature = 20 oC).....	130
Figure 44: effect of different masses of GAC on adsorption of FLT onto the surface of GAC	133
Figure 45: plot of Q against time for the adsorption of FLT onto GAC (T = 20 oC).....	135
Figure 46: change in concentration of CYM over time due to adsorption onto GAC.....	137
Figure 47: plot pf Q against time for the adsorption of CYM onto GAC.....	138
Figure 48: change in concentration of DEHP over time due to adsorption onto the surface of GAC	140
Figure 49: plot of Q against time for the adsorption of DEHP onto the surface of GAC	141
Figure 50: graph representing the iodine number of different samples of granulated activated carbon	144
Figure 51: Degradation of the three emerging contaminants in final wastewater effluent by ozonation. (T = 20 °C, pH = 6, ozone concentration = 20 g/m ³ NTP, oxygen flow rate = 0.5 L/min).....	147
Figure 52: Rate of concentration decrease over time of (a) DEHP, (b) FLT, and (c) CYM from adsorption onto GAC (mass GAC = 0.015 g, T = 20 °C)	149

Table of Tables

Table 1: Oxidation Potentials (Leusink, 2014).	48
Table 2: HPLC conditions used for analysis	63
Table 3: conditions used for each experiment investigating ozone mass transfer into 500 mL DI water.....	64
Table 4: Reaction conditions used when analysing the effect of different conditions on the ozonation of Fluoranthene.	66
Table 5: Reaction conditions used when analysing the effect of different conditions on the ozonation of Di (2- ethyl hexyl) phthalate.	67
Table 6: Reaction conditions used when analysing the effect of different conditions on the ozonation of Cypermethrin.....	68
Table 7: Volumes used to analyse the stoichiometric relationship of the chemical contaminants and ozone.	69
Table 8: Reaction conditions used for the analysis of adsorption rates of the chemical contaminants onto different masses of GAC.....	73
Table 9: Reaction conditions used for each experiment when investigating the ozonation of the chemical contaminants in wastewater.....	74
Table 10: k_{La} values and C_{AL}^* values for each experiment comparing ozone gas concentration.....	79
Table 11: Effect of pH on mass transfer parameters C_{AL}^* and k_{La}	81
Table 12: comparison of C_{AL}^* and k_{La} values from the effect of temperature	82
Table 13: comparison of C_{AL}^* and k_{La} values looking at the effect of flow rate	85
Table 14: comparison of C_{AL}^* and k_{La} values from different scavengers.....	89
Table 15: temperature effects on rate constants.....	100
Table 16: rate constants calculated for the different temperatures used to investigate the degradation of DEHP.....	114
Table 17: rate constants determined from the different temperatures used to affect the rate of degradation	126
Table 18: values for the rate constant calculated for each mass of GAC.....	136
Table 19: rate constants for the different masses of GAC used.....	139
Table 20: rate constants obtained for the kinetics of DEHP sorption onto GAC.....	141
Table 21: Iodine numbers calculated for different GAC samples.....	143
Table 22: Results for the characterisation of the wastewater final treated effluent from Welsh Water	146
Table 23: Summary of results comparing the ozonation of the contaminants in solutions of DI water and wastewater effluent.....	155
Table 24: Summary of results comparing the adsorption in solutions of DI water and solutions of final wastewater effluent.....	155

Table of Equations

Equation 1.....	50
Equation 2.....	50
Equation 3.....	51
Equation 4.....	51
Equation 5.....	51
Equation 6.....	53
Equation 7.....	53
Equation 8.....	54
Equation 9.....	55
Equation 10.....	55
Equation 11.....	57
Equation 12.....	58
Equation 13.....	59
Equation 15.....	78
Equation 16.....	78
Equation 17.....	87
Equation 18.....	93
Equation 19.....	101
Equation 20.....	108
Equation 21.....	121
Equation 22.....	134
Equation 23.....	135

Abbreviations

AC	Activated Carbon
AOP	Advanced Oxidation Processes
ATP	Adenosine triphosphate
BET	Brunauer-Emmett-Teller Theory
CAL	ozone liquid phase concentration
CO ₂	Carbon dioxide
COD	Chemical oxygen demand
CYM	Cypermethrin
DAD	Diode array detection
DEHP	Di (2- ethyl hexyl) phthalate
DI	Deionised Water
EC	Emerging Contaminants
EPA	Environmental Protection Agency
FLD	Fluorescence detector
FLT	Fluoranthene
GAC	Granulated Activated Carbon
H ₂ O ₂	Hydrogen Peroxide
HPLC	High performance liquid chromatography
IES-Ps-1	Pseudomonas aeruginosa
IN	Iodine Number
NTP	Normal Temperature and Pressure
O ₃	Ozone
PAH	Polycyclic Aromatic Hydrocarbons
PVC	Polyvinyl Chloride
SDG	Sustainable Development Goals
TOC	Total Organic Carbon
UN	United Nations
UV	Ultra Violet
UV-Vis	Ultra Violet - Visible

Chapter 1 – Introduction

One of the main concerns regarding wastewater and the health and safety of the human population is the occurrence of many newly identified contaminants found within the water. These compounds are more commonly referred to as emerging contaminants (Bolong et al., 2009). Emerging contaminants (ECs) may include pharmaceuticals, hormones, antibiotics, and many other categories. They are classified as contaminants due to the adverse health effects they are associated with (Tran et al., 2018). The detection of emerging contaminants has attracted lots of attention, due to the increased prevalence of them, as well as the adverse side effects on both human health and the environment. As these compounds are released continuously into the environment, the overall concentration cannot be known precisely (Taheran et al., 2018).

ECs are not completely removed by conventional wastewater treatment processes, meaning there is currently high demand around finding solutions to remove ECs from the wastewater. Solutions need to be found to reduce the concentrations of these ECs and ensure the wastewater is safe for discharge into the receiving environment or reuse once treated (Ahmed et al., 2017).

Amongst the large list of ECs, three organic chemicals of concern to the industrial sponsor were investigated in this project: (i) fluoranthene, (ii) di (2- ethyl hexyl) phthalate, and (iii) cypermethrin:

- (i) Fluoranthene (FLT) is a polycyclic aromatic hydrocarbon released to the environment through combustion of coal and is of concern due to its mutagenic and carcinogenic potential. This chemical has been found to have detrimental health effects on humans and animals, including kidney and liver damage (Zhang et al., 2013). Wastewater treatment plants are a major source of FLT in the environment (Edokpayi et al., 2016). Current research highlights a gap in the understanding of treatment of this chemical, with the majority of research focusing on the removal of fluoranthene instead of the breakdown of the structure into safer chemicals. As polycyclic aromatic hydrocarbons are very resistant to biodegradation, this process is not favourable. There are also problems associated with the standard chemical removal process such as coagulation and flocculation, as these processes are not very efficient at

fluoranthene removal. There is promise within the ability to break down the structure into safer chemicals; using oxidation, which is a process that is less intrusive and easier to perform (Hao et al., 2012). Research on the breakdown of FLT is scarce, which means that an oxidative technique needs to be developed to effectively degrade the chemical within a wastewater solution.

- (ii) Di (2- ethyl hexyl) phthalate (DEHP) is a commonly used plasticiser in interactions with poly (vinyl chloride) to make it more malleable. PVC consists of up to 40 % di (2- ethyl hexyl) phthalate (Koch et al., 2006). Within this structure, the two chemical compounds are not chemically bound, which has benefits as it allows the structure to be more malleable, however, it also has negative aspects as the matrix of the structure can alter over time. The di (2- ethyl hexyl) phthalate can leach out over time, resulting in the chemical entering the environment in many unmonitored and unregulated ways (Hammad & Jung, 2008). The fact that the compound can enter the environment in different ways, also means that human exposure is unregulated, therefore, it can enter the human body through inhalation, oral, dermal and intravenous routes (Caldwell, 2012). Within the environment and wastewater, di (2- ethyl hexyl) phthalate is commonly found within sewage sludge. Due to the structure of the compound, it is very resistant to biodegradation, so alternative processes must be found to degrade and remove this chemical from the wastewater system.
- (iii) Cypermethrin (CYM) is a synthetic pesticide, commonly used for the control of ectoparasites (Velisek et al., 2006). The toxicity of cypermethrin is selective, and affects neuronal sodium channels and metabolic degradation (Giray et al., 2001). The use of cypermethrin as a pesticide has previously been associated with adverse effects to ecosystems. CYM has been seen to cause poisoning in humans through inhalation, as well as causing nervous and digestive disorders in cats and dogs (Grewal et al., 2010). Due to CYM having low water solubility and being very hydrophobic, large quantities of CYM can be found accumulated on the surface of soil, therefore resulting in higher concentrations in the water supplies. Hydrolysis and photolysis can be used for the degradation of CYM, with the trans isomer being hydrolysed faster than the cis isomer (Jones, 1995). It is possible that algae can be used for the bioremediation of CYM from within water, (Nastuneac et al., 2019), however, this does not destroy the pesticide, merely

absorbs it into the algae. Therefore, better techniques are required to degrade and destruct the chemical contaminants. (Yilmaz, 2021)

These emerging contaminants are all currently found within the wastewater cycle, with different concentration of the chemicals being found at different stages throughout the wastewater treatment process. The concentrations before and after treatment can be compared to identify the areas where improvement is still required within the treatment process.

Looking at data obtained for a specific site provided by Welsh Water, the differences in the concentration of the chemicals before and after treatment can be compared. Looking at fluoranthene, the concentration in the crude sewage was found to be 0.254 µg/L and after treatment the concentration in the final effluent had decreased to a concentration of 0.034 µg/L. The value for the concentration of di (2- ethyl hexyl) phthalate in the crude sewage sample was 11.1 µg/L, in comparison to a highest value of 0.96 µg/L after treatment. In crude sewage, the concentration of cypermethrin was 0.09793 µg/L, and after treatment this concentration decreased to 0.00038 µg/L in the final effluent. This shows that there is a large percentage of these contaminants removed in the treatment process. However, there are still traces present, therefore, there is still room to improve the treatment process to produce safe levels of the contaminants in the final treated effluent.

The purpose of this research is to investigate the use of ozone and activated carbon as advanced oxidation processes to assist in the degradation and removal of these chemical contaminants. Ozone is a strong oxidant that been used previously in water disinfection and organic pollutant degradation (Liu et al., 2021). It works effectively through the formation of hydroxyl radicals which can further increase the oxidation potential. Ozonation is a popular oxidation process used for treatment of water contaminants through the decrease in costs associated with the process, as well as the environmental advantages that have been shown, (Rekhate & Srivastava, 2020). Activated carbon is a common adsorbent for use in the treatment of wastewater, due to the high surface area that its porous structure provides (Bhatnagar et al., 2013). The adsorption capability can be altered through the functionalisation of the carbon, as well as the presence of additional heteroatoms within the structure. The activated carbon is very susceptible to pollutants being adsorbed into the structure, and therefore these contaminants can be easily extracted from within the wastewater (Karnib et al., 2014).

Aims and Objectives

- To investigate the degradation of the three ECs using ozonation under different operating conditions.
- To investigate the adsorption properties of the three ECs on granular activated carbon.
- To investigate the degradation and adsorption of the three ECs in multicomponent solutions.
- To investigate whether the defined process is effective in real wastewater samples.

Chapter 2 – Literature Review

2.1 - Water crisis

The United Nations (UN) outlined the UN sustainable development goals (SDG) in September 2015. These goals aimed to eliminate discrimination and inequality, end poverty and overcome climate change by 2030. There are 17 goals set out and these include many economic and social-developmental concerns such as water and sanitation (Alawneh et al., 2018). The availability of water is of utmost importance for human existence and well-being, meaning that two of the sustainable development goals relate to the availability of water. SDG 6 states to ensure availability and sustainable management of water and sanitation for all and SDG 14 states the need to conserve and sustainably use the oceans, seas and marine resources for sustainable development. Both of these SDGs are targeting explicitly sustainable water policies (Tsani et al., 2020). The availability of clean water is a basic human right; however, billions of people are denied this across the globe. The rate of water consumption is also increasing at a rate of 1 % per year (Arora & Mishra, 2019).

The reusability of wastewater and the recycling of water has been shown to be crucial in finding a solution for the lack of availability of clean water. However, the contaminants found within the wastewater supply can be problematic if not removed effectively, or reduced to a safe concentration for human consumption (David et al., 2023).

2.2 - Emerging contaminants

One of the main concerns regarding wastewater and the health and safety of the human population is the occurrence of many newly identified contaminants found in water. These compounds are more commonly referred to as emerging contaminants (Bolong et al., 2009). These contaminants tend to be unregulated as they have not been previously identified within the water supply as a point of concern. This means that their effects have not been seen or researched thoroughly. The appearance of these emerging contaminants may therefore lead to legislative intervention in the future (Petrović et al., 2003).

Emerging contaminants may include pharmaceuticals, hormones, antibiotics, and many other categories. They are classified as contaminants due to the adverse health effects they are associated with (Tran et al., 2018).

The detection of emerging contaminants has attracted lots of attention, due to their increased prevalence, as well as the adverse side effects on both human health and the environment. As these compounds are released continuously into the environment, the overall concentration cannot be precisely known. However, the release into the environment does not need to be continuous to have a severe impact on the environment (Taheran et al., 2018). Many emerging contaminants have been classified as endocrine disruptors, which are difficult to remove within current wastewater treatment plants. Improvements need to be made to processes that occur within these wastewater treatment plants to counteract the increase of emerging contaminants within the water supply (Rout et al., 2021).

There are several different processes that have been studied and investigated for the removal of emerging contaminants, and some of these are discussed in following sections.

2.3 – Emerging contaminants of interest to this study

There are many chemicals within water that may become a problem in the future with rising concentrations and new information about their toxicity. For this research, three main chemicals will be focused on, these being fluoranthene, cypermethrin, and di (2- ethyl hexyl) phthalate. The concentration of these emerging contaminants is rising in wastewater and so there is increased interest for their removal from the water supply.

2.3.1 - Fluoranthene

Fluoranthene (FLT) is a member of the polycyclic aromatic hydrocarbons (PAHs), released into the environment through the combustion of coal. These compounds are of great environmental concern, because of their mutagenic and carcinogenic potential. Fluoranthene is commonly found within the sediment, as opposed to water, due to the hydrophobicity of PAHs and strong sorption within the environment (Somtrakoon et al., 2014). The molecular weight of PAHs can vary, as they can have differing numbers of benzene rings. The PAHs having a higher molecular weight are very lipophilic and chemically stable. The half-lives of these chemicals are very large, meaning the concentration within the environment is high. This results in an accumulation of fluoranthene within the environment, therefore, the removal and degradation are important to reduce the concentration within the environment and various ecosystems (Luo et al., 2014).

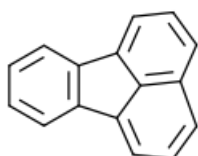


Figure 1: Skeletal structure of fluoranthene

PAHs contain two or more fused benzene rings, which are formed during the incomplete combustion of carbon-containing fuels, including coal. Currently, there is little technology available for the removal and degradation of fluoranthene, the technologies that are available remove the compound as opposed to degrade them (Hao et al., 2012). There are many long-term health effects that fluoranthene can cause to humans and animals, some of these include cataracts, kidney and liver damage and jaundice (Zhang et al., 2013). PAHs have been shown to cause genetic defects and tumours. As FLT can easily penetrate the food chain, this may cause further problems including potential carcinogens and other hazardous and toxic side effects, harmful to animals and humanity (Rababah & Matsuzawa, 2002).

There is currently interest in the removal and degradation of fluoranthene and other PAHs, due to their strong toxicity, persistence, and accumulation within ecosystems. Fluoranthene is bio accumulative and persistent to avoid microbial degradation, the compound is also one of the 16 priority PAHs that have been set out by the United States – Environmental Protection Agency (Kahla et al., 2021). Due to the poor solubility of fluoranthene within water, there are high concentrations found within soil and bottom sediments. This means that removal and degradation techniques are not aggressive enough to combat the high concentrations within the sediment and soil (Małachowska-Jutysz & Niesler, 2015).

Technology involving microorganisms to remove PAH via biosorption, and biotransformation have been proposed. Microalgae can be used to remove some toxic organic pollutants by autotrophic growth (Lei et al., 2007). Different ways for the removal and degradation of PAHs have been developed, however, some result in more toxic by-products, leading to further ecological imbalance and negatively affecting human health. Many of these processes incur additional costs, long operating hours and complicated procedures, making these techniques unfavourable (C. Li et al., 2022). There is a type of bacteria that can degrade some PAHs, including fluoranthene, to produce carbon dioxide and metabolic intermediates. However, little research has been carried out in this area, and the metabolic intermediates produced could be equally as or more hazardous to the environment, meaning that this is not a popular technique due to the lack of understanding (Giraud et al., 2001).

Bioremediation is a technique that has the advantages of being both environmentally friendly and cost effective. This includes the use of earthworms for fluoranthene removal. However, this method is hindered by the low bioavailability of PAHs and their biotoxicity. These chemicals are toxic to earthworms which is a negative aspect of this process (Shi et al., 2020).

As PAHs tend to be resistant to biodegradation, as well as the traditional physical methods, such as coagulation and flocculation not being very efficient for removal, more chemical processes need to be determined. Sorption is one of the most effective processes for fluoranthene removal, as well as the removal of many persistent organic contaminants. Activated carbon has shown to be beneficial for this purpose, with a high surface area to maximise adsorption (Nkansah et al., 2012). Many adsorbents that can be used to assist in the removal and degradation of fluoranthene are costly and synthetic, providing their own problems.

2.3.2 – Di (2-ethyl hexyl) phthalate

Di (2- ethyl hexyl) phthalate (DEHP) is a polluting phthalate that occurs at high concentrations in the aquatic environment. Phthalates have many uses, including plasticisers, solvents, toys and cosmetics. Due to the number of uses, the evidence of phthalates within the environment is high, meaning the safety regarding these chemicals is being questioned (Bodzek et al., 2004). To show the extent of the use of DEHP, around 2 million tonnes of DEHP are produced each year worldwide (Koch et al., 2003).

DEHP is a commonly used plasticiser to interact with poly (vinyl chloride) (PVC) to render it malleable. PVC consists of up to 40 % DEHP (Koch et al., 2006). The process of plasticisation occurs through the interactions of the plasticiser with the polymer, there is no chemical combination between the two compounds. DEHP is highly hydrophobic so does not produce covalent bonds with PVC (F. Li et al., 2022). The plasticiser is much smaller than the polymer used. DEHP contains polar carbonyl groups, these moieties interact with the polar chloride bonds that are within the chain in PVC, ensuring that these two compounds are compatible. However, this is contradicted by the nonpolar functionalities of DEHP, leaving the structure to be ductile and malleable (Erythropel et al., 2014). As they are not chemically bonded to each other, it means that the polymer matrix can alter over time, and the DEHP can leach out into the surrounding medium. This causes more hazards, as the DEHP can enter the environment in an unmonitored way (Hammad & Jung, 2008). As DEHP can enter the environment in many ways, human exposure can also occur in a variety of pathways, including, but not limited to, inhalation, oral, dermal, and intravenous routes (Caldwell, 2012). When the exposure is from a medical route, the levels can be very high.

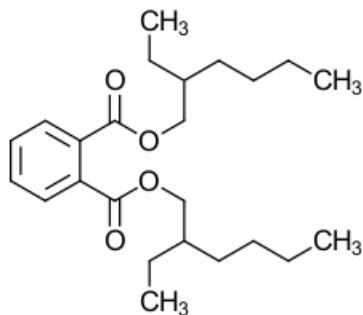


Figure 2: Skeletal structure of di (2- ethyl hexyl) phthalate

The combination of PVC and DEHP is commonly found within the medical industry, as the plastic structure formed has considerable benefits, including flexibility, strength, low cost, and resistance to kinking (Tickner et al., 2001).

The environmental concerns around DEHP arise from its ability to act as an endocrine disruptor, since the chemical has effects similar to that of the hormone oestrogen (Manikkam et al., 2013). The DEHP can bind to hormone receptors resulting in side effects, including a reduction in immunity and endocrine disorders. This can lead to health effects including reproductive issues (Zhang et al., 2023). DEHP interferes with hormone production, meaning that certain hormones are either produced in too large or too low a quantity. In terms of oestrogen, the levels within the body are very important, especially during pregnancy, and even minute changes in the concentration could have drastically negative effects. Endocrine disrupting chemicals can be transferred through the placenta to the foetus and to a baby through breast milk (Ason et al., 2022). DEHP can alter the production of testosterone within the body, and within a male foetus this has very negative effects. These can include malformations in the external genitalia, as well as decreased sperm production throughout life (Beckera et al., 2004). Side effects of increased exposure can also include reduced foetal survival (Manikkam et al., 2013).

The largest release of DEHP to the environment comes from poorly managed industrial waste, meaning that chemical contamination is becoming a major problem in industrial regions. Amongst the largest industrial contributors are agricultural and textile industries (Daiem et al., 2012).

As DEHP is not chemically bound to its polymers, it leaches out in contact with water, but as it is also highly hydrophobic, DEHP can normally be found within sewage sludge. The DEHP currently within treatment plants is not found in high concentrations within the water as it adsorbs into the sludge produced within the treatment process. Common end destinations for sewage sludge are energy production, agricultural use, and landfill (Marttinen et al., 2004). Biodegradation has been trialled for use in the treatment of DEHP, however, due to the structure of DEHP and its long side chains, it is very stable making it more resistant to biodegradation processes. These processes are also very time consuming (Chen et al., 2009). Nanofiltration has some positives for the possibility of its use for DEHP removal, including, lower energy consumption, however, nanofiltration does not work very effectively for molecules of a high molecular weight (Wei et al., 2016).

The most promising technique for DEHP degradation and removal appears to be the use of advanced oxidation processes. There are many different approaches within this branch of techniques which will be discussed in later sections. The main downside of these techniques is the potential higher cost.

2.3.3 - Cypermethrin

Across the world there are many new chemicals that have been synthesised and are being used as pesticides. Pesticides are used for a wide variety of industries; including, but not limited to, agricultural, livestock and households (Ullah et al., 2018). Synthetic pesticides are very potent, and these equate to over 30 % of global pesticide and insecticide use (Shukla et al., 2002).

Cypermethrin (CYM) is an example of a synthetic pesticide that is based on pyrethroids and is one of the most effective of this family. Cypermethrin is commonly used for the control of ectoparasites. These parasites commonly infect livestock such as cattle, sheep and poultry (Velisek et al., 2006). The toxicity of cypermethrin is selective, and effects neuronal sodium channels and metabolic degradation. Pyrethroids are more hydrophobic than many other classes of insecticides (Giray et al., 2001). Cypermethrin is a complex structure, which can be seen below in Figure 3.

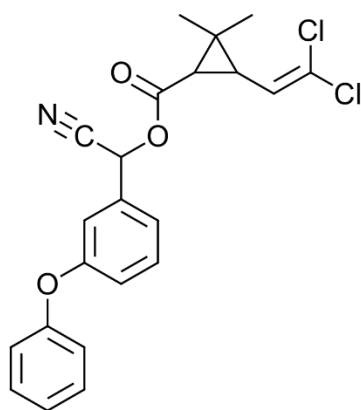


Figure 3: Skeletal structure of cypermethrin

The use of cypermethrin (CYM) as a pesticide has already been associated with adverse effects to ecosystems. CYM has been seen to cause poisoning in humans through inhalation, as well as causing nervous and digestive disorders in cats and dogs (Grewal et al., 2010). CYM can cause a variety of toxic effects in mammals, including lack of coordination, increased salivation, muscle tremors and tonic-clonic convulsions (Elbetieha et al., 2001). CYM is very lipophilic, therefore has a high rate of gill absorption when in water. This means that fish are at a higher risk of CYM poisoning than some other aquatic life. The effects on fish have not been fully investigated, due to the differing impacts on different species of fish, however CYM is known to be toxic to aquatic life (Saha & Kaviraj, 2008).

Cypermethrin is classified as a stomach poison as well as a contact insecticide. This results in unwanted side effects within the body, including inhibiting the production of ATPase enzymes which regulate the movement of ions against concentration gradients (Yousef et al., 2003). There are many medical cases associated to the use and presence of pesticides, and approximately 87,000 cancer cases occur annually that can be associated with the use of pesticides in developing countries (Kanyika-Mbewe et al., 2020).

Within solutions of cypermethrin, the compound exists as both the cis and trans isomers. The cis isomers are more active than the trans isomers which represents the highest concern. Due to CYM having low water solubility, and being very hydrophobic, large quantities of CYM can be found accumulated on the soil surface and therefore high concentrations can be seen. Hydrolysis and photolysis can be used for the degradation of CYM, with the trans isomer being hydrolysed faster than the cis isomer (Jones, 1995).

Due to the prevalence of CYM within the environment, there are novel techniques under investigation for the removal of CYM from areas of high concentration. One such technique is the use of different materials for adsorption. The use of natural materials for this is preferable due to their renewable nature, as well as the low costs associated with them. Different algae have been investigated for their use in the removal of CYM (Nastuneac et al., 2019). Algae are promising for use in water decontamination since they can act as environmental indicators of contamination. It is possible that algae can be used for the bioremediation of CYM from within water, however, this does not destroy the pesticide, merely absorbs it into the algae. Therefore, more preferable techniques are required to result in the degradation and destruction of CYM (Yilmaz & Tas, 2021).

A selection of techniques involving advanced oxidation processes have been investigated. These include, for example photocatalysis with titanium dioxide (Affam & Chaudhuri, 2013). The combination of titanium dioxide assisted photocatalysis and ozonation, has potential for the degradation of many pollutants including CYM. Ozone has been reported to reduce the concentration of CYM on contaminated surfaces, however, was proven to be more effective when combined with another technique, for example, the use of UV (Lin et al., 2012). Many pesticides have been shown to have varying levels of degradation when exposed to ozone. (Wu et al., 2007).

2.4 - Advanced oxidation processes and alternative processes

The removal of emerging contaminants by conventional processes, for example biological treatments, are often very limited, due to many of these chemicals having lower solubility, being unreactive or resistant to certain treatments or too persistent within the wastewater to react to any treatment. Thus leading to inefficient removal from the sample (Borikar et al., 2015). In some cases, the treatment does not dispose of the emerging contaminants, merely takes them from one place to another, for example when using algae, and the problem remains of how to remove the contaminants.

There are also other reasons as to why different techniques for contaminant removal are required. In the past, chemical and biological approaches have been used to remove emerging contaminants from within the wastewater. However, due to high operational costs and low efficiency of these techniques, advanced oxidation processes are gaining interest to either replace or use in combination with.

The following sections will discuss typical processes commonly used to address emerging contaminants in water.

2.4.1 – Coagulation and flocculation

Coagulation and flocculation are two chemical processes that can assist in the treatment of wastewater. Coagulation and flocculation occur successively to one another, allowing particle collision and growth of floc. Particles that are suspended within water tend to have a negative charge, which means when these particles within water are too close to each other, they repel. Within a sample of water, the solid within it will not clump together and settle until coagulation and flocculation occur (Prakash et al., 2014). The combination of coagulation and flocculation have been shown to work effectively for contaminant removal. This can be seen through the use of these processes for microplastic removal from wastewater (Lapointe et al., 2020). The schematic shown in Figure 4 depicts a simplistic process of coagulation and flocculation of colloids in a solution.

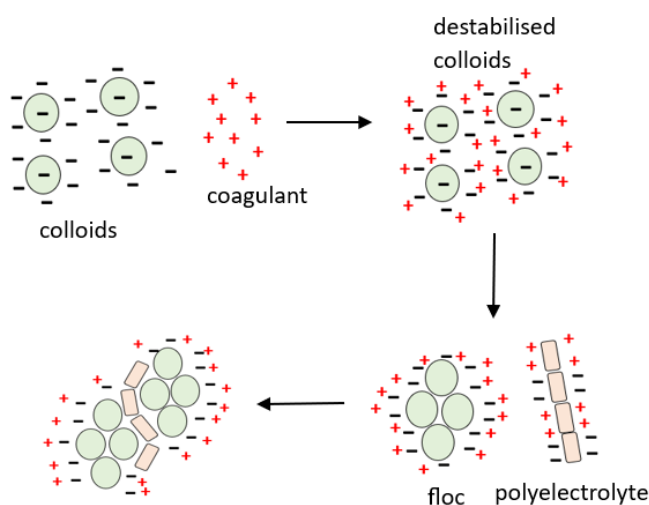


Figure 4: schematic of the process of coagulation and flocculation

Different types of coagulants can be used for the coagulation of different contaminants within the wastewater, and this will depend on certain criteria for the contaminant's removal. These coagulants can be inorganic, synthetic polymers or biological coagulants (Muruganandam et al., 2017). Many factors can affect the efficiency of the process, including pH, coagulant type, and effluent quality. These factors can be difficult to control, meaning that the process of coagulation and flocculation is not always efficient (Saritha et al., 2017).

Due to the volumes of chemicals required to appropriately separate the contaminants from the water, high operating costs tend to be associated with this process, as well as a difficult disposal route for the toxic sludge generated, generating further cost. New processes are being investigated appear to be more favourable at disposing of the organic contaminants found within wastewater (Iwuozor, 2019).

When looking at the use of coagulation and flocculation for the removal of emerging contaminants, there is little research to support the use of these techniques. The processes are found to be ineffective in the removal of emerging contaminants within wastewater treatment plants, as they predominantly are able to remove suspended solids within the solution. The only way that emerging contaminants can be removed through these techniques would be the adsorption of the contaminants onto pre prepared flocs within the solution (Shahid et al., 2021).

2.4.2 - Biological

The process bioremediation is a popular technique for the removal of chemicals that are of environmental and human concern. The ability to effectively remove the chemicals of concern depends on the ecosystem as an entirety (Fester et al., 2014). Aerobic respiration has been used to assist with the degradation of organic pollutants, although, for some organic contaminants, anaerobic respiration through biological processes has shown promise (Ghattas et al., 2017). Biodegradation has great potential for use to reduce levels of pollutants within wastewater at low costs, as well as the potential for full degradation of the pollutants. Biodegradation involves the use of microorganisms to facilitate the degradation of emerging organic contaminants within water and sediment (Tran et al., 2013). The schematic shown in Figure 5 shows a simplistic process of biodegradation.

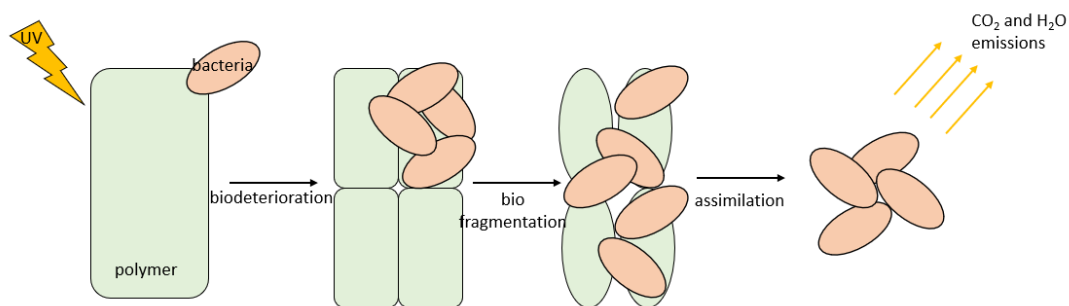


Figure 5: Schematic showing the process of biological degradation

One of the main challenges for biodegradation is the low availability of the contaminants within the samples. The concentration of the contaminants needs to be at a certain level for the biodegradation via microorganisms to occur. Therefore, this is not always an appropriate technique to utilise to decrease the concentration of organic contaminants within the wastewater and sediment (Cébron et al., 2013). When the process of biodegradation is taking place, the conditions must be favourable to allow biodegradation to occur effectively, this includes oxygen and nutrient availability, as well as pH and temperature (Hickman & Reid, 2008).

PAHs are resistant to biological and environmental degradation, this is due to the low solubility these molecules possess (Lutsinge & Chirwa, 2018). This means that chemical processes tend to be more favourable for the removal of FLT, as biological degradation cannot occur if the compound is not dissolved within the ecosystem.

DEHP has been found to have removal rates during specific sections of the treatment plant. This degradation mainly occurs in the activated sludge treatment, where DEHP has been adsorbed into the sludge before it undergoes treatment. An example of this treatment is the combination of primary sedimentation followed by aerobic biological treatment. In a study, it was found that this process removed 29 % of DEHP from the wastewater (Marttinen et al., 2003). There is also potential for the removal of DEHP in composting, combined with the aeration of the sludge from wastewater. In the process of aeration of the wastewater, biodegradable material becomes oxidised (Marttinen et al., 2004).

CYM can also be degraded through the activated sludge treatment pathway, however, for degradation of CYM to occur, *Pseudomonas aeruginosa* (*IES-Ps-1*) is required within the solution. *IES-Ps-1* is a toxic organic compound degrader that can be used in many treatments, for many chemicals (Hasan & Jabeen, 2015). When *IES-Ps-1* was added to the activated sludge, efficient degradation of CYM was seen at a degradation rate of 82 %, at concentrations of 40 mg/L (Jilani & Khan, 2006). Once optimising the reaction conditions, *IES-Ps-1* assisted in the degradation of cypermethrin within activated sludge treatment processes. Without *IES-Ps-1*, there would be no biological degradation of CYM within the wastewater treatment process (Jilani, 2013).

2.4.3 – Ozone

Ozone (O₃) is a strong oxidant which has many uses, including water disinfection and organic pollutant degradation. Ozone can be used for organic pollutant degradation through the formation of hydroxyl radicals from ozone decomposition (Liu et al., 2021). Ozone can oxidise organics with moieties that are electron rich, this means that specific organics can be eliminated by direct ozonation. Other organic compounds that are lower in ozone reactivity cannot be oxidised by ozone alone, and instead can be oxidised by hydroxyl radicals which are produced from ozone decomposition (Wang et al., 2018).

Ozone is produced through passing a stream of air or oxygen through a high voltage discharge system. This system will convert the oxygen into ozone, which can then be used for the water treatment. The main problem associated with O₃ production is the high energy consumption required, which makes the process less favourable. However, when combined with other AOPs, the energy requirement for ozonation can be reduced (Presumido et al., 2022). The ozone technology has evolved in the past decade and highly efficient ozone generators are available on a large scale. Therefore, ozone has become an increasingly popular AOP in recent years, due partly to decreasing costs, as well as the environmental advantages it offers over many other accepted techniques (Rekhate & Srivastava, 2020).

The ozone reactions can proceed through two different routes of oxidation; (i) direct ozonation, where the oxidation occurs from just the ozone, and (ii) indirect ozonation, where the oxidation occurs from reactive radicals generated as a result of ozone decomposition. These are further discussed below.

2.4.3.1 - Direct ozonation

Ozone acts as a selective electrophile and reacts very quickly with certain organic groups, for example, amines and phenols (Snyder et al., 2006).

Although the ozonation of organic contaminants appear promising, the direct ozonation can result in the formation of oxidative by-products, where there is a chance that these by-products could be more toxic than the original compound. The complete degradation of certain organic compounds by this method is limited (Almomani et al., 2016).

For the reaction of compounds with ozone via direct ozonation, the mechanism quite simply involves adding ozone to the compound requiring oxidation. The mechanism is shown below in Figure 6 (Drozdova et al., 2014).

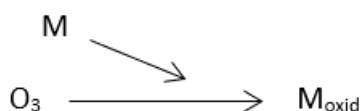


Figure 6: Mechanism for the oxidation of a compound by direct ozonation, where *M* presents a compound, and *M_{oxid}* is the compound oxidised.

Direct ozonation is the most important path of oxidation in wastewater, especially when the production of hydroxyl radicals is inhibited, due to a lack of initiating compounds to begin the chain reaction process. Direct ozonation can also be preferable when there are too many hydroxyl radicals in the solution. There are many compounds that have been found to directly degrade with ozone, and these include pesticides, taste and odour compounds and phenolic compounds (Avery et al.).

2.4.3.2 - Indirect ozonation

Ozonation normally occurs through direct ozonation and the reactions of molecular ozone. However, occasionally indirect ozonation is preferable. This is due to the hydroxyl radicals not reacting selectively and not targeting specific bonds within a molecule (Benitez et al., 2013). Hydroxyl radicals are species with a very small half-life that have a very high oxidation potential, therefore they are favourable in the oxidation processes used for wastewater treatment. Hydroxyl radicals react unselectively with both organic and inorganic materials present within water (Beltrán & Rey, 2018). Ozone decomposition forms hydroxyl radicals or other molecules that are in an excited state, making them more reactive. These molecules can then react with each other and other molecules and act as oxidants within the solution (Ibáñez et al., 2013).

There are many techniques that can be used to generate hydroxyl radicals, some of these include the following; (i) chemical oxidation process in homogenous phase, (ii) photocatalytic processes in homogenous or heterogenous phases, (iii) sonochemical processes and (iv) electrochemical processes (Cretin & Huong, 2015).

- (i) Reactions for the oxidative generation of radicals, for example the Fenton reaction, which is further discussed later in this literature review, are an important source of hydroxyl radicals. An example of a chemical oxidative reaction for production of hydroxyl radicals is shown below in Figure 7. The oxidative power of radicals can be preferable in pollutant and wastewater treatment processes (Lyngsie et al., 2018).

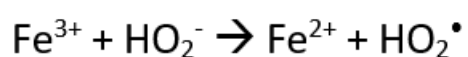


Figure 7: Chemical equation to show the generation of hydroxyl radicals from a chemical oxidation process

- (ii) Photocatalysis is a popular technique that can be used for the decomposition of harmful pollutants in water. The photocatalytic activity can correlate to the production of hydroxyl radicals. This is because the radicals generated at the photocatalyst surface can diffuse into the solution, increasing the oxidative potential in the solution. The process of generating hydroxyl radicals at the surface of photocatalysts can be seen below in Figure 8 (Nosaka & Nosaka, 2016).

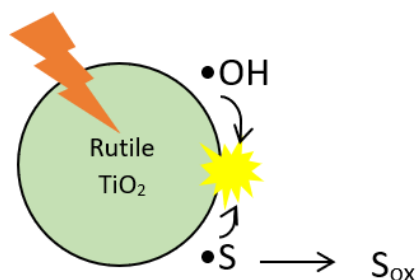


Figure 8: Diagram to show the generation of hydroxyl radicals from a photocatalytic process, figure generated from (Nosaka & Nosaka, 2016), where *S* is a substrate molecule.

- (iii) A sonochemical process involves reactions that occur because of the application of powerful ultrasound radiation (Savun-Hekimoglu, 2020). The sonochemical process for pollutant degradation relies on the generation of radicals that are generated in violent cavitation events. The hydroxyl radical reactions can occur at the bubble-liquid interface, as well as in the liquid itself. The high temperatures generated by a collapsing bubble also contributes to the generation of radicals. The chemical reactions within sonochemical processes leading to the generation of hydroxyl radicals can be seen in Figure 9 (Ziembowicz et al., 2017).

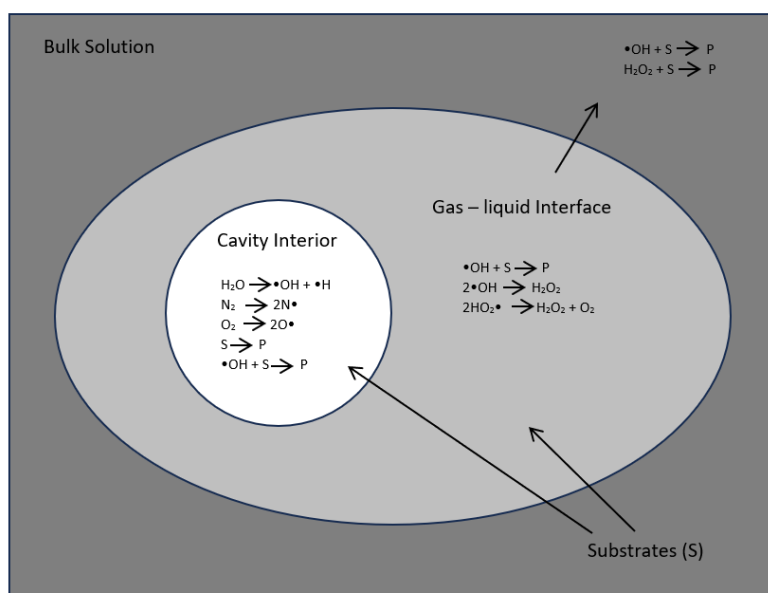


Figure 9: Diagram to show the generation of hydroxyl radicals from a sonochemical process, figure generated from (Ziembowicz et al., 2017)

- (iv) The electrochemical process of generating hydroxyl radicals is sometimes more preferable, as it counteracts the costs and complexity associated with several of the reactions used. For example, an electro-Fenton reaction has been developed which involves the generation of hydroxyl radicals through the Fenton reaction at the surface of an electrode. The mechanism for this reaction can be seen in Figure 10. The addition of the electrode enables reactions to occur at more specific times and eliminates the opportunity for any direct oxidation to occur (Monroe & Heien, 2013).

The mechanism to produce hydroxyl radicals from ozone can be seen in Figure 10. The production of hydroxyl radicals occurs through a three-step reaction including the initiation reaction, when a negatively charged hydroxyl ion is generated, followed by a series of chain reactions producing HO_3 radicals and HO_4 radicals. Finally, there is a termination reaction, where the hydroxyl radicals are produced (Drozdova et al., 2014).

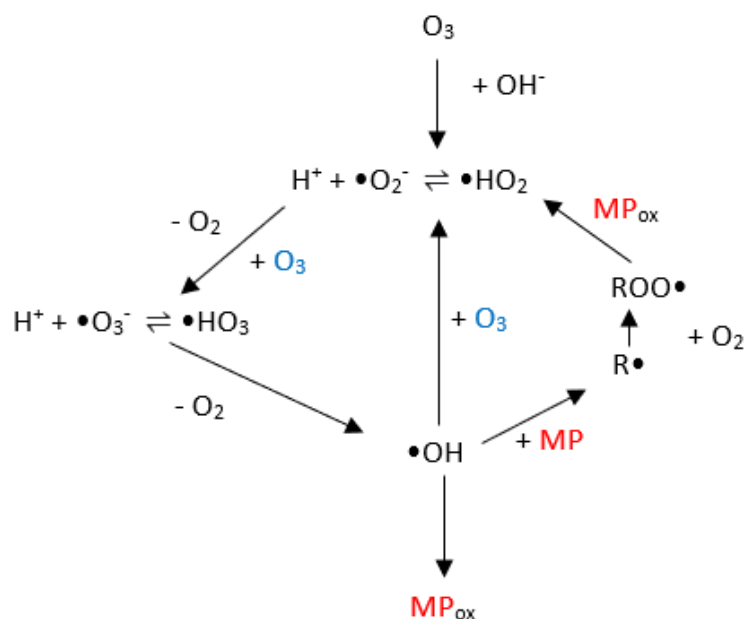


Figure 10: Mechanism for the production of hydroxyl radicals from ozone, where MP is a product

The use of hydroxyl radicals in wastewater treatment can be favourable. However, this does depend on which mechanism the oxidation of the compound of interest will occur. This could be either direct ozonation with molecular ozone, or indirect ozonation with hydroxyl radicals.

To increase the amount of hydroxyl radicals within the solution, activated carbon has been shown to provide many benefits, acting as both an adsorbent and as a catalyst. The pyrrol groups found on the carbon surface are able to interact with the ozone to increase the number of hydroxyl radicals produced, making the ozonation process more efficient (Liu et al., 2016; Sanchez-Polo et al., 2005).

The two processes of ozonation are effective in different ways, depending on the molecules being ozonated. To investigate the effect of both indirect and direct ozonation, radical scavengers can be used to compare the rates of oxidation.

2.4.3.3 – Radical scavengers

Through the oxidation reaction of ozone, reactive oxygen species are generated. These species are commonly O_2 , H_2O_2 , $O_2^{\cdot-}$, OH^{\cdot} (Das & Roychoudhury, 2014). There are a variety of chemicals that can be used as reactive oxygen species scavengers, an example of this is tert-butanol, which can quench the amount of reactive oxygen species formed in the ozonation system (Guo et al., 2021). Carbon nanotubes have ability to react with free radicals, most commonly through electron transfer processes and adduct formation. Carbon nanotubes can be used as a scavenger to capture radicals, which would decrease the oxidising potential of the mixture (Galano, 2008).

The process of radical scavenging involves the reaction of free radicals with non-target chemical species. These radical scavengers can either be soluble and react within the aqueous phase, or solid and react on the surface of the solid phase (Crincoli & Huling, 2020).

There are radical scavengers present within wastewater. These scavengers have some beneficial properties within the wastewater treatment process, for example, within the treatment of landfill leach solution and solutions of high pH. In these scenarios, a lower concentration of hydroxyl radicals would be favourable, allowing oxidation to occur more effectively with molecular ozone (Kishimoto, 2007).

2.4.3.4 – By-products

When degrading organic contaminants in wastewater by processes such as ozonation, potentially toxic oxidative products can be formed when the pollutants within the water are not completely degraded or decomposed. These by-products could become a problem within the environment. Therefore, it is important to have an understanding of the oxidation of each chemical pollutant and the different by-products formed (Tay et al., 2013). The by-products formed from ozonation tend to be organic, such as carbonyl compounds, or inorganic, like bromate (Papageorgiou et al., 2017). Using ozonation as an oxidation process removes the generation of chlorination by-products which were present from the previous accepted technologies used for organic pollutant removal discussed in the following sections (Papageorgiou et al., 2014).

It is important to understand the mechanisms of reaction, to be able to identify potential ozonation transformation products. This will give a better understanding of the type of by-products to expect; their toxicity and the most successful way to then remove them from the wastewater. The majority of the by-products occurring are formed from the indirect ozonation, as opposed to the direct reaction (Schollée et al., 2018).

One of the most significant by-products of ozonation is bromate, resulting from the reaction of ozone with bromide in water.

Bromide is a chemical that is present within all water sources and samples at varying concentrations. Although concentrations are low within water sources, the concentration can increase through the treatment of water samples (Ruffino et al., 2020). The presence of bromide within wastewater samples is a concern, due to the ability of bromide to be oxidised to become bromate, a toxic ion. This process occurs rapidly with the ozonation of water (Gounden & Jonnalagadda, 2019). As bromate is the main by-product associated with the ozonation of wastewater, the concentration within the wastewater samples should be monitored. The presence of bromate ions can also react with organic matter within the water sample to form total organic bromine, which is of an even higher toxicity (Liu et al., 2022). The level of bromate ions formed through the ozonation process can vary depending on ozone dosage, as well as water pH (Tawabini & Zubair, 2011).

One way to monitor the levels of bromate ions within the water samples could be the use of ultraviolet radiation, which, over time, would break down the bromate ions into bromine atoms and oxygen (Zhao et al., 2013). The use of a pre-ozonation treatment process to the water samples being treated could have a positive impact on the bromate generation, meaning that the concentration of bromate ions in the final effluent would be significantly decreased (Selcuk et al., 2005).

2.4.3.5 - Ozone toxicology

Ozone is a relatively insoluble gas. Humans exposed to acute amounts, can experience pulmonary function decrements, as well as acute tissue damage within the lung and trachea. When ozone is inhaled, it proceeds to a deeper airway with higher inhalation rates, this means that when exposed to higher doses of ozone, there is an increased risk of tissue damage to the respiratory system (Mautz, 2003). Ozone is a secondary air pollutant, naturally formed in the troposphere from primary pollutants (Bromberga & Korenb, 1995). Ozone can decompose once it has entered the body and can be dangerous at high concentrations due to its toxicity (Batakliiev et al., 2014).

2.4.3.6 - Ozone mass transfer

Although ozone is significantly more soluble in water than oxygen itself, the solubility it presents is still poor, it has limited equilibrium concentrations, as well as a low mass transfer efficiency (Wang et al., 2021). To increase the amount of ozone dissolved within wastewater, different techniques can be used. These include good gas dispersion, large interfacial area and an increased contact time (Biñ et al., 2001). The most common apparatus used to increase the dispersion of ozone throughout the water sample are diffusers, static mixers, or injectors (Bin & Roustan, 2000). A high mass transfer coefficient of ozone would be preferable, showing more ozone is dissolved within the water. This can also be affected by the operating conditions, including water quality and facility setup. Therefore, the optimal conditions of operation need to be considered to maximise ozone presence within the reaction mixture (Zhou & Smith, 2000).

2.4.3.7 - Bubble coalescence

When bubbling a gas, for example ozone, through a liquid, the reaction rate can depend on the size of the bubbles themselves. To increase the rate of reaction, a smaller bubble would be preferable. This is because more smaller bubbles would increase the surface area per unit volume, increasing the likelihood of an interaction between the contaminants and the ozone (Oliveira et al., 2019). During the process of coalescence, when two or more bubbles or droplets collide, they will merge into one, meaning the bubbles have increased in size, but overall, the surface area has decreased (Anthony et al., 2017). Electrolytes can be added into the solution to reduce coalescence of the bubbles. Coalescence tends to occur very easily in pure water, however, the higher the concentration of electrolytes or other alternative preventative techniques present, the amount of bubble coalescence occurring greatly decreases due to differing surface tensions being present (Christenson et al., 2008). Alternatively, another way to minimise the coalescence, is to reduce the flow rate of gas through the liquid sample.

2.4.3.9 - Surface tension

When ozone is applied to reaction systems, the surface tension during treatment can be changed, this would have an impact on the reaction schemes, due to the change to the property of the water (Luo & Wong, 2001).

Surface tension is a property of water that occurs between the bulk of the solution and the surfactant layer of the solution, it is a property of water that allows an object with a higher density than water to float. The reason that this can occur is because of adsorption of hydroxide ions at the interface between the surfactant layer (if present) and the bulk of the liquid (Beattie et al., 2014). When water is investigated, the surface tension alters depending on the level of treatment, as chemicals within the wastewater sample can affect the relationship between the bulk of the liquid and the surfactant layer (Amiri & Dadkhah, 2006). When comparing the surface tension of a liquid, the numerical value would always be positive. This is because the particles in the surfactant layer have fewer van der Waals interactions between adjacent molecules, as opposed to the molecules that are within the bulk of the solution (Hauer et al., 2017). These cohesive forces between the molecules within the solution are an essential component of surface tension, and a diagram showing this is shown in Figure 11.

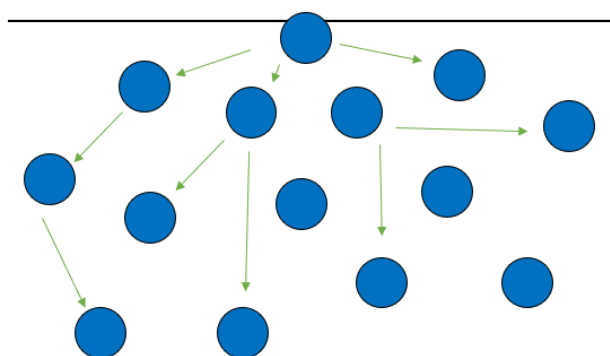


Figure 11: A schematic showing the cohesive factors between molecules in a liquid.

Surface tension can be altered through wetting. This is the spread of a liquid over a surface so that the surfactant layer is larger, and the bulk is smaller. This increases the contact area of the liquid and the solid support, which can affect the reaction rate (Luo & Wong, 2001). Surface tension can also be affected by the volume of bubbles produced within the reaction, or the addition of a solid into the reaction mixture that will increase the amount of water that is in the surfactant layer, therefore increasing the rate of reaction and efficiency of the reaction scheme (George et al., 2017).

2.4.3.10 - Effects of pH and temperature on ozonation

The pH of the solution can have an effect on the adsorption and oxidising potential of ozone. If the pH is decreased, then the abundance of hydroxyl radicals is inhibited, meaning oxidation via hydroxyl radicals and therefore indirect oxidation cannot occur effectively (Kishimoto & Nakamura, 2011). Hydroxyl radicals tend to be prevalent at pH levels above 7 or 8. So therefore, if oxidation via ozone is only to occur via direct ozonation processes, a lower pH level would be preferable (Adams & Gorg, 2002). When ozonating water, the effect of temperature can be seen through the generation of bromoform. The higher the temperature, the higher the formation of bromoform (Zhang et al., 2005). Effect of temperature can also be seen through ozonation decay. The decay rate of ozone tends to increase with an increase of temperature (Jung et al., 2017).

2.4.4 - Ozonation of the emerging contaminants

2.4.4.1 - Fluoranthene ozonation

The fluoranthene within the wastewater industry can be found concentrated within the soil sediment. Ozone has been found to be a promising technique for the treatment of the fluoranthene within this sedimentation. The efficiency of treating the soil sediment with ozone has been investigated, but, while being an effective form of treatment, the process is reliant on a number of variables. These include the ozone dose, flow rate and contact time (Rivas et al., 2009). A study showed following 2 hours of ozonation to a soil sediment contaminated with fluoranthene, there was a 50 – 100 % removal of fluoranthene in a variety of soil and liquid phases (Zeng & Hong, 2002).

2.4.4.2 - Di (2- ethyl hexyl) phthalate ozonation

The ozonation of DEHP has been investigated within wastewater. The removal of DEHP in solution using ozone was found to have a removal efficiency of 50 % in comparison to a 43 % removal efficiency found through the use of UV radiation (Zarean et al., 2015). Ozone molecules are able to oxidise DEHP and the ozone dosage has been shown to have an effect

on the efficiency of the degradation of the DEHP compounds in water via ozonation (Zarean et al., 2017).

2.4.4.3 - Cypermethrin ozonation

Studies have researched the use of ozonated water to remove the pesticide cypermethrin from the surfaces of vegetables. A study has shown ozonated water at a concentration of 1.4 mg/L was effective at removing 60 – 99 % of CYM at a concentration of 0.1 mg/L (Wu et al., 2007). Whilst some conditions would have an effect on the suitability and efficiency of ozone to remove CYM, pH has been shown to not have an effect on the removal rate (Lin et al., 2012). The effectiveness of CYM removal via ozonated water being found to be highly dependable on the dissolved ozone levels in the solution, with the removal of CYM in water being shown to again be > 60 % at 0.4 ppm (Al-Dabbas et al., 2018).

2.4.5 - Hybrid processes

When combining a variety of different oxidants, an advanced oxidation process (AOP) can increase the oxidative capacity. This could be because of an increase in reactive oxygen species being produced or certain reactions occurring along individual processes that have a positive effect on the reaction scheme (Dewil et al., 2017).

Some examples of hybrid processes include:

- UV / H₂O₂
- Ozone / H₂O₂
- Ozone / UV
- Ozone / Activated Carbon

2.4.5.1 - UV/H₂O₂

Hydrogen peroxide can be photolysed at wavelengths of 200 nm to 300 nm. The formation of the hydroxyl radicals occurs from the homolytic fission of the O – O bond. It has been found in reactions with UV/H₂O₂, generation of free radicals occur faster at alkaline pH, strong concentrations of hydrogen peroxide are also required for the efficient degradation (Kurian, 2021).

UV/H₂O₂ is an advanced oxidation process that has potential for treatment processes. Existing studies show the degradation of some pesticides by this combined advanced oxidation process, as well as the use of this combination for disinfectant (Chelme-Ayala et al., 2010). UV/H₂O₂ works to remove organic pollutants by UV photolysis and the reaction of hydroxyl radical reactions. As an AOP, UV/H₂O₂ could completely mineralise the organic matter into CO₂. This reduces the amount of organic matter within the water, in turn, resulting in less chemically contaminated water (Toor & Mohseni, 2007). However, in water, there are other contaminants that can compete with the photons and radicals, to interfere with the desired reaction (Yao et al., 2013).

The combination of UV/H₂O₂ as an advanced oxidation process can degrade certain compounds that would not be degraded by UV alone. The compounds contain electron withdrawing groups that have an effect on the oxidation processes. These groups, such as halogens, reduce the rate constants below the diffusion limit, which in turn decreases the use of UV/H₂O₂ as an oxidative process.

2.4.5.2 - Ozone/H₂O₂

Hydrogen peroxide in reactions coupled with ozone works by accelerating the decomposition of ozone, increasing the hydroxyl radical generation. This occurs through the reaction shown in Figure 12 (Bermúdez et al., 2021).

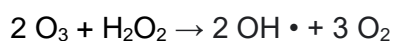


Figure 12: Equation showing the degradation of ozone with hydrogen peroxide to produce hydroxyl radicals

The direct mineralisation of the contaminants does not occur, instead resulting in the oxidation of organic contaminants. This can affect the number of hydroxyl radicals able to oxidise the organic contaminants of interest (Covinich et al., 2014). When using H₂O₂ as an oxidising agent, it is sometimes low and ineffective. When combined with another oxidation process, for example ozone, the increase in productivity can be seen. A further problem seen when working as an individual oxidiser is that high dosages are required, which can be expensive (Rostam & Taghizadeh, 2020).

2.4.5.3 - Ozone/UV

Ultraviolet radiation works as an advanced oxidation process in multiple ways. This can involve the immediate absorption of light by chemicals, which can break the chemical bonds and the overall contaminant. Some compounds do not degrade this easily with UV radiation, therefore, additional additives are required in the solution (Rosenfeldt et al., 2006). This process again works effectively by exploiting the production of hydroxyl radicals and the reactivity these radicals have in the oxidation process. Ozone can produce hydroxyl radicals effectively when absorbing UV light at 254 nm (Hachemi et al., 2013).

When using the combination of the advanced oxidation processes, the production of hydroxyl radicals is increased, meaning the combination of techniques is favourable, this therefore increases the radical concentration and hence the degradation rate (Boczkaj & Fernandes, 2017). With this certain combination, the oxidative process occurs through the production of hydroxyl radicals generated by the photolysis of ozone (Bermúdez et al., 2021).

2.4.5.4- Fenton's reaction

Fenton's reaction involves a photochemically excited Fenton reagent. This reagent consists of a mixture of hydrogen peroxide and iron (II) salt (Bossmann et al., 1998). Fenton's reaction works by generating hydroxyl radicals, however, the best way to generate these radicals is through the addition of the hydrogen peroxide as a bulk quantity. Due to environmental considerations, this is not a favourable approach and affects the overall efficiency over time, as the hydrogen peroxide gets consumed quickly (Liu et al., 2017). Specifically, the redox cycle of iron (II) and iron (III) produce the hydroxyl radicals in this reaction scheme. Recent years have used heterogenous iron catalysts within the reaction mixture in place of iron salts (Zhang et al., 2020).

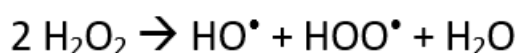


Figure 13: The chemical reactions that occur within the Fenton's reaction process

Within the Fenton reaction, the hydroperoxyl radical is produced, which also enhances the oxidation power of the system. This reaction is popular for use as an advanced oxidation process due to the low toxicity and lower costs, as well as a simple operating process. The main limitation of the process is it needs to be conducted at an acidic pH to avoid oxidation of iron (II) (Salgado et al., 2017). Large doses of iron (II) ions are required within the reaction scheme, which can lead to corrosive leaching into the solution, which will interfere with the reaction. The precipitation of the iron on a solid surface can also affect the reaction, as it limits the surface area for adsorption (Roy & Moholkar, 2020). The environmental benefits associated with this method make it favourable, however, there are some negative elements counteracting the favourability of this process (Hakika et al., 2019). These include the use of hydrogen peroxide and many radical species which are toxic to living organisms (Buyuksonmez et al., 1998).

2.4.6 - Adsorption

Adsorption is a scientific technique that is widely used for pollutant removal. With adsorption experimentation it is important to determine the thermodynamic and kinetic properties to better understand the mechanisms and rate of adsorption (Qiu et al., 2009).

Adsorption shows great promise for the removal of some organic contaminants. The contaminants are adsorbed into the adsorbent and the adsorbent can be removed and the regeneration of the organic contaminants can occur (Breitbach & Bathen, 2001).

One of the main adsorbents used for the removal of organic contaminants is activated carbon.

2.4.6.1 - Activated carbon

In the past, a variety of carbon based compounds have been used as adsorbents in the treatment of water, including wood char or coal char. The adaptation over time of these carbon based structures have led to the development of the compounds, such as activated carbon, which are better adapted for organic pollutant removal (González-García, 2018).

Activated carbon is a very popular adsorbent used to treat wastewater. The term activated carbon describes carbon based materials that have a well-developed pore structure that can maximise the surface area of the compound (Bhatnagar et al., 2013). The uses of activated carbon are extensive and include applications such as separation of compounds, removal of compounds and the modification of compounds, which can either be in the liquid or gas phase (Heidarinejad et al., 2020). The adsorption ability of activated carbon can be altered by the functionalisation of the carbon. The chemical properties of the carbon depend on the presence of additional heteroatoms within the carbon structure. These additional heteroatoms can be introduced into the carbon either from the starting material or from additional functionalisation that occurs, either through activation processes or by treating the carbon once it has been activated (Shafeeyan et al., 2010).

The ability of the activated carbon to assist in the removal of organic contaminants from wastewater is due to high porosity and high surface area of carbon, as well as the ability to functionalise carbon, leading to the presence of different heteroatoms. This makes activated carbon more susceptible to reactants being adsorbed and therefore, removed from wastewater (Karnib et al., 2014).

2.4.6.2 - Ozone/activated carbon

The combination of both technologies involving activated carbon and ozone have been investigated due to the promise that these applications have individually. The combination of ozone and activated carbon combines the high oxidation potential of ozone with the high adsorption properties of activated carbon. This results in the elimination of many organic pollutants, as well as the prevention of many pollutants' mutagenic potential (Valdes et al., 2002). The coupling of these techniques also provides a cost benefit, as neither the activated carbon or ozone need to be used and incorporated at such high concentrations than they do when used individually for the treatment of wastewater (Schollée et al., 2021). The oxidation potential of many oxidants can be shown in Table 1 below.

Table 1: Oxidation Potentials (Leusink, 2014).

Oxidant	Electrochemical Potential (V)
Free hydroxyl radical	2.8
Ozone atom	2.42
Ozone	2.07
Oxygen	1.23

The use of ozone individually requires large dosages to either directly oxidise the compounds or produce enough hydroxyl radicals, when combined with a porous material. For example, with activated carbon, the mineralisation rate is increased, as well as the efficiency of the reaction. This also shows a dramatic decrease in operational costs, as the production of large volumes of ozone is an expensive procedure (Xiong et al., 2020). When combining the two technologies, different pathways can be exploited to remove the organic pollutants.

Therefore, the combination can mean more pollutants are removed from wastewater by the varying reactions with ozone and activated carbon (Sun et al., 2018).

Whilst the processes of both ozonation and adsorption with activated carbon can be used as separate techniques, they can be also be used consecutively to maximise the degradation and removal of contaminants within the solution. For example, wastewater can be treated first with ozone, followed by the addition of activated carbon. With a breakdown of the compounds occurring first via oxidation of ozone, the smaller chemical compounds generated can then be adsorbed and removed by the activated carbon. Certain compounds will have a higher affinity to be adsorbed, so by initially oxidising the compounds, this process could be enhanced (Si et al., 2019).

2.4.6.3 - BET Isotherm

BET is an isotherm used for determining the adsorption of a solute on a surface. It takes into consideration the multi-layer adsorption that can occur, incorporating this into an equation used to determine the relative adsorptions. The method of BET can be used to determine the surface area, as well as the pore size distribution of many adsorbents and catalysts (Ebadi et al., 2009). BET is derived from the Langmuir isotherm, which works on the analysis of a single layer. The BET isotherm takes this single layer equation for surface area calculation and incorporates the ability of different layers within the surface to also adsorb reactants. Therefore, producing an equation which can be used to calculate the total surface area of an adsorbent or catalyst (Toth, 2000). Experimentally, BET works to measure the overall adsorption of a surface using nitrogen adsorption. The use of nitrogen is used primarily on porous materials and powders, and has proven very effective as it does not participate in alternative reactions as it is an inert gas (Van et al., 2011).

The BET isotherm model uses an equation which considers the adsorption onto the surface. This will vary depending on which layer is being studied. As the isotherm is developed for multilayer systems, differing assumptions are used when calculating the isotherm mathematically (Aguerre et al., 1989).

The model BET isotherm equation can be seen below.

Equation 1

$$\theta = \frac{cp}{\left(1 - \frac{p}{p_0}\right)(p_0 + p(c-1))}$$

Eq. 1: BET Isotherm

Where:

c is the BET constant,

p₀ is the vapour pressure of the bulk phase (Pa),

p is the vapour pressure (Pa),

θ is the surface coverage, defined below,

Equation 2

$$\theta = \frac{n_{ads}}{n_m}$$

Eq.2: Defining feta

n_{ads} is the amount of adsorbate (moles),

n_m is the monolayer equivalent.

2.4.6.4 – TOC

Total organic carbon (TOC) is a useful indicator within the environment, given the carbon comes from natural and anthropic sources. The presence of TOC in water is not harmful to human health, however, as the TOC varies across water supplies it is useful to understand differences in TOC content (Visco et al., 2005). A TOC compound is any compound containing any carbon atoms, except for CO₂ and related substances. TOC is present in water through many different courses, such as natural and man-made activities (Mook et al., 2012). Carbon can be found in solids, liquids and in extracts or leachates, as the carbon is found in a variety of different phases, the overall TOC value can be difficult to obtain (Bisutti et al., 2004).

2.4.6.5 - Iodine Number

Iodine number is an analytical technique used to characterise the activity of carbon materials. The iodine number relates to the amount of iodine adsorbed by 1 g of a carbon sample (Du et al., 2021). The amount of iodine adsorbed is measured in milligrams, and is measured when the concentration of the iodine in the filtrate is equal to 0.02 N. The experimental method is based on a three point isotherm (Nunes & Guerreiro, 2011). The iodine number is used to investigate the porosity of a sample of activated carbon by monitoring the amount of iodine adsorbed onto the surface of AC and therefore the surface area can be obtained; this can in turn give the porosity of the activated carbon.

To calculate the iodine number, the following calculations are required, these are expanded on in Appendix 1.

Equation 3

$$A = (\text{Iodine}, N)(12693.0)$$

Eq. 3: Used to calculate the iodine number.

Equation 4

$$B = (\text{Sodium Thiosulfate}, N)(126.93)$$

Eq. 4: Used to calculate the iodine number.

Equation 5

$$\frac{X}{M} = \frac{[A-(DF)(B)(S)]}{M}$$

Eq. 5: Used to calculate the iodine number of a sample of activated carbon.

Where:

$\frac{X}{M}$ is the iodine absorbed per gram of carbon (mg/g),

S is sodium thiosulfate used (mL),

M is the mass of carbon used (g),

DF is the dilution factor,

B calculated by Equation 4, and

A calculated by Equation 3.

2.4.7 - Isotherms

Analytical isotherms are a variety of techniques used for modelling adsorption data (Jeppu & Clement, 2012). It is important to be able to characterise different reactions in chemical processes and one of the easiest ways to do this is through the application of an isotherm. These isotherms allow better understanding of chemical reactions (LeVan & Vermeulen, 1981). An adsorption isotherm is used to predict how much solute can be adsorbed onto the surface of a solid like activated carbon, and the isotherms represent the amount adsorbed by a unit weight adsorbent (Desta, 2013). Isotherms are often describing the process of adsorption at a constant temperature and pH (Chen, 2015). The two most common isotherms are Langmuir Isotherm and Freundlich Isotherm, which are discussed in more detail below.

2.4.7.1 - Langmuir Isotherm

The Langmuir isotherm can be obtained when making some fundamental assumptions and the isotherm is applied to fit adsorption data obtained at equilibrium (Liu, 2006). The Langmuir isotherm was originally derived to describe the adsorption of a gas onto a solid phase adsorbent. There are several assumptions of the isotherm model, and these are (i) the monolayer surface coverage, (ii) identical and equivalent surface sites with equal sorption activation energy of each molecule resulting in homogenous adsorption, and (iii) no transmigration or interaction between the adsorbed species in the plane of the surface (Ghosal & Gupta, 2017). The Langmuir isotherm can be adapted to describe different interactions, most notably a liquid to solid adsorbate interaction (Sohn & Kim, 2005).

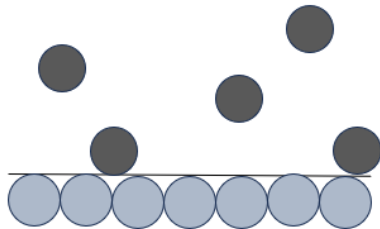


Figure 14: an equilibrium between the gas phase and the adsorbate phase

The equation for the Langmuir adsorption theorem is shown below, as well as the first two equations of the Langmuir adsorption theorem, once linearised, also being shown.

Equation 6

$$q_e = \frac{Q_m b C_e}{1 + b C_e}$$

Eq. 6: Langmuir Adsorption Theorem

Equation 7

$$\frac{C_e}{q_e} = \left(\frac{1}{Q_m}\right) \frac{1}{C_e} + \frac{1}{Q_m b}$$

Eq. 7: Langmuir - 1

Equation 8

$$\frac{1}{q_e} = \left(\frac{1}{bQ_m}\right)\frac{1}{C_e} + \frac{1}{Q_m}$$

Eq. 8: Langmuir - 2

The constants for both Langmuir equations are defined below.

q_e is the value of q at equilibrium (mg/g),

Q_m is the maximum adsorption capacity of adsorbent (mg/g),

b is the Langmuir constant (L/mg),

C_e is the concentration at equilibrium (mg/L).

2.4.7.2 - Freundlich isotherm

The Freundlich isotherm is derived from the Langmuir isotherm, with assumptions surrounding the energetic surface heterogeneity. The empirical derivation of the Freundlich isotherm applies to both monolayer and multilayer adsorption, however, it is more commonly applied to monolayer adsorption (Yang, 1998). Within the Freundlich isotherm shown in Equation 9, there are many constants, for example n , and it has been proven through the applied equation that the parameter n should be inversely dependent on the temperature of the reaction (Skopp, 2009). When the adsorption process is not directly linear, the Freundlich isotherm can be used instead. This is sometimes preferable, as the Freundlich isotherm contains two parameters. This isotherm often describes adsorption behaviour better than that of the linear adsorption isotherm due to the two parameters that can be altered independently of one another (Coles & Yong, 2006).

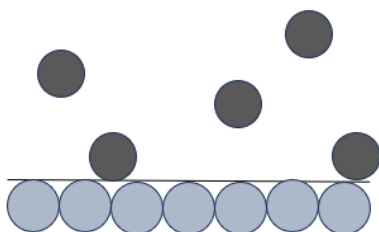


Figure 15: within the Freundlich isotherm, there is variety in the amount of gas adsorbed depending on the temperature and pressure.

The equation for the Freundlich Isotherm can be seen below, as well as the equation for the linearised form of the isotherm, used for analysis.

Equation 9

$$q_e = K_f C_e^{\frac{1}{n}}$$

Eq. 9: Freundlich Isotherm

Equation 10

$$\log(q_e) = \log(K_f) + \frac{1}{n} \log(C_e)$$

Eq. 10: Freundlich Isotherm Linearised

The constants for the Freundlich isotherm are highlighted below.

q_e is the value of q at equilibrium (mg/g),

C_e is the concentration at equilibrium (mg/L),

n is the Freundlich constant known as the sorption capacity,

$\frac{1}{n}$ is the heterogeneity factor,

K_f is the Freundlich constant, sorption capacity (L/mg).

2.5 - Rate theory

Transition state theory is a theory derived to allow quick estimates for reaction rates of specific reactions. This means that even when computational models were not yet developed for rate analysis, approximations could be made for a variety of processes (Pollak & Talkner, 2005). The probability that atoms are able to transition from an initial state to an end state can be expressed as the rate constant, as long as this transition occurs only one unit at a time (Horiuti, 1973).

The majority of kinetic systems will conform typically to one of the following orders of reaction; zero order, first order, second order, square root of time and cubic root. These orders express the delivery rate within the reaction system, as well as being combined with the design geometry and composition (Yang, 1998).

Zero order reactions are less commonly found within reaction systems than the alternative orders of reaction, however, they do have some unique and interesting qualities. A zero order reaction is constant and independent of concentrations of any reactants within the reaction system. Because of this, zero order reactions are quite rare, as it is surprising that a reaction system would not be at all impacted by the prevalence of any reactant material (Bain et al., 2018).

A first order reaction is more common, where the rate of reaction is directly proportional to the concentration of the reactant present. A first order reaction is expressed graphically as an exponential decay over time, representing decay is at the same rate depending on the concentration dose (Sunta et al., 2001). First order reaction curves are often described as single exponential decay graphs and this is a characteristic of a first order reaction which can help to identify the order of the reaction from the shape of the graph (Srividhya & Schnell, 2006).

2.5.2 - Arrhenius equation

The influence of temperature on the rate of chemical reactions can be described by the Arrhenius equation (Laidler, 1984). According to the Arrhenius equation, the reaction rates at very low temperatures are very small, but non-zero. This is shown through the curved Arrhenius plot that is obtained, representing that reaction rate approaches, but never reaches, zero (Kohout, 2021). The equation contains one constant, which is the gas constant and also two unknown parameters. These are k_0 , a pre-exponential factor and the activation energy, E_A . These can both be derived from experimental data (Rodionova & Pomerantsev, 2005).

Equation 11

$$k = Ae^{\frac{-Ea}{RT}}$$

Eq. 11: Arrhenius equation

Where:

k is the rate constant,

A is the Arrhenius factor,

Ea is the activation energy,

R is the universal gas constant, and

T is the absolute temperature in K.

2.6 - Analytical techniques

2.6.1.1 - Indigo Method

The indigo method is used to assist in the analysis of ozone concentrations within a liquid sample. The use of visible light enables low concentrations of ozone to be measured, by minute reactions occurring between ozone and the indigo solution. This results in a colour alteration that can be easily determined via absorption of light in the visible region (Garcia et al., 2014). The indigo sulphonate aqueous solution absorbs light at a wavelength of 600 nm. Within the indigo solution, ozone reacts with the olefinic bond, and the ozonation of this bond can result in the formation of two separate compounds, both colourless. This affects the colour intensity of the indigo solution, as well as the ozone present within the solution. The colour change can subsequently be determined accurately through UV-Vis spectroscopy (Felix et al., 2006).

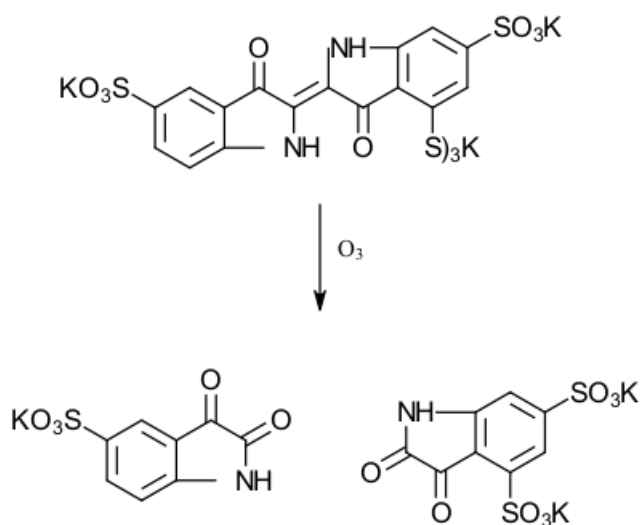


Figure 16: mechanism for the reaction of indigo sulphonate solution with ozone

The absorbance of the indigo sulphonate solution before and after the reaction with ozone can be compared, and resulting in a calculation for the ozone concentration in the sample being analysed using Equation 12 (Nobbs & Tizaoui, 2014).

Equation 12

$$C_s = \frac{\rho_s}{\rho_{ind}} \frac{m_{ind}}{m_s} \frac{M_{O_3}}{\varepsilon_{ind}L} [(Abs_{600})_0 - (Abs_{600})_f]$$

Eq.12: Calculating ozone concentration from indigo

Where:

C_s is phase sample ozone concentration (mg/L),

ρ_s and ρ_{ind} are densities of phase solvent and indigo reagent solution (g/L),

m_{ind} and m_s are respective masses of indigo reagent solution and phase solvent added to syringe (g),

M_{O_3} is the molecular mass of ozone (48,000 mg/mol),

ε_{ind} the extinction coefficient of indigo (20,069 L/mol cm),

L path length of the cell (1 cm),

$(Abs_{600})_0$ is the absorbance at 600 nm of the indigo reagent solution, and

$(Abs_{600})_f$ is the absorbance at 600 nm of the discoloured indigo reagent solution sample

2.6.1.2 - Beer Lambert Law

The Beer Lambert Law is used to equate absorbance to concentration of a substance. This relationship is established using the equation shown below in Equation 13 (Hardesty & Attili, 2010).

Equation 13

$$A = c \varepsilon l$$

Eq. 13: Beer-Lambert Law

Where:

A is absorbance,

c is concentration (mol dm^{-3}),

l is length of light path (m), and

ε is the molar absorptivity.

2.6.2 – Sample preparation

There are a variety of different extraction techniques that can be used to prepare samples for analysis. Some of these techniques are discussed below.

Solid phase extraction is used as a technique for sample preparation when separating the analyte from the aqueous solution. In this process, the analyte, initially found in large volumes of the aqueous solution, is extracted to a solid phase for analysis, before being obtained through elution in small solvent volume (Poole, 2003). Solid phase extraction is a very versatile technique, which means it can be used for a variety of different purposes, including purification and fractionation. Depending on the reaction mechanism, the sorbent (solid phase) can be selected. However, it needs to be an appropriate sorbent to ensure that the analyte is contained within the solid and the mobile phase does not have a high affinity (Zwir-Ferenc & Biziuk, 2015). The main advantage of solid phase extraction is the need for small volumes of organic solvents. This makes the process cheaper and more environmentally friendly (Rodriguez et al., 2000).

Liquid-liquid extraction is a commonly used sample pre-treatment process. The main purpose of this technique is to increase the concentration of the analyte and increase the selectivity, by removing interfering species from the analysis and further treatment (Silvestre et al., 2009). Liquid-liquid extraction is used for clean-up and sample enrichment, making it a very useful technique (Anthemidis & Ioannou, 2009). However, this extraction process requires an organic solvent and an inorganic solvent. These solvents are costly, as well as the organic solvents commonly being toxic and flammable. Due to this, liquid-liquid extraction is not as favourable a technique, especially with green chemistry guidelines in mind (Huddleston et al., 1998).

Solid supported liquid extraction is able to immobilise a liquid in an inert atmosphere. This means that the liquid can be analysed by being pumped through a column (Nave et al., 2007). This technique is compatible with a wide variety of solvents, making it preferable (Breitenbucher et al., 2001). Hydrophobic molecules are removed through the process, giving a clean extract for analysis (Owen & Keevil, 2013).

Chapter 3 – Materials and Methods

3.1 – Materials

3.1.1 - Emerging contaminants of interest:

- Fluoranthene was supplied by Thermo Fisher Scientific at a purity of 98 %. The CAS number is: 206-44-0.
- Di (2- ethyl hexyl) phthalate was supplied from Sigma Aldrich at a purity of > 98 %. The CAS number is: 117-81-7.
- Cypermethrin was supplied from Thermo Fisher Scientific at a purity of 96 %. The CAS number is: 52315-07-8.

3.1.2 - Contaminant Solution Preparation

Due to the low solubility of the compounds of interest, solutions of a higher concentration were prepared in methanol. The solutions in methanol were made to a concentration of 1 g/L. These solutions were diluted to 1 mg/L in water, by extracting 1 mL of solution in methanol. The solution was made up to 1 L with DI water. These solutions were then used for experimentation.

FLT was made to be 4.9 $\mu\text{mol/L}$.

DEHP was made to be 2.5 $\mu\text{mol/L}$.

CYM was made to be 2.4 $\mu\text{mol/L}$.

3.2 - Analytical

3.2.1 - UV-Vis Analysis

UV-Vis analysis was performed using Agilent Cary 60 UV-Vis. The chemicals were made up in solutions of DI water and these samples were used to run analysis. A background scan using DI water was run, and then the samples were analysed in a glass cuvette. The scan was run from 190 nm to 800 nm and the peaks were analysed.

3.2.2 - Fluorescence Analysis

Fluorescence analysis was performed using the Agilent Cary Eclipse Fluorescence Spectrophotometer. Samples were made up in DI water. A quartz cuvette was used, which was clear on all sides. A sample of DI water was first run to zero the machine and then the samples were run by analysing corresponding emission and excitation wavelengths of the compounds. The wavelengths of the scan varied depending on the wavelength of the emission and excitation pairs.

3.2.3 - High Performance Liquid Chromatography Analysis

An Agilent High Performance Liquid Chromatography (HPLC) was used to analyse the concentrations of chemical contaminants in solution. Samples were collected in HPLC vials from the reaction mixture at regular time intervals. Air was immediately bubbled into the solution to quickly remove any residual ozone in the sample to stop the reaction. A method was determined using the HPLC to have the best separation of components within solution, as well as clear peaks registering from either the FLD or DAD, to give a clear and easy determination of the concentration of the peak and the contaminant. The peak area was equated to the concentration of the contaminants using a calibration curve. The table below (Table 2) summarises the HPLC conditions used for each EC. All analysis was performed using a C18 Ascentis column, with an isocratic elution phase of 85 % acetonitrile and 15 % water, and with a sample injection volume of 5 μ L.

Table 2: HPLC conditions used for analysis

	% ACN	% Water	FLD wavelength (nm)	DAD wavelength (nm)	Retention Time (min)
FLT	85	15	486, 285		4.5
CYM	85	15		250	2.5
DEHP	85	15	456, 245		4

3.3 - Ozonation Experiments

Ozone was generated from pure oxygen using Ozonia Lab2B generator, BMT 964 analyser. The conditions varied throughout experimentation and are shown below in Table 3. The ozone was diffused into liquid solution (500 mL). This solution was stirred using a magnetic bar stirrer and samples were taken at regular time intervals to analyse the concentration of the emerging chemical contaminants and ozone, using the indigo method and HPLC respectively. The analysis of the chemical contaminants was performed on an Agilent 1200 series HPLC system using a Supelco Ascentis Express C18 column. The conditions for the injection volume and mobile phase for each EC are highlighted above in Table 2.

3.4 - Mass transfer of ozone in DI water

The absorption of ozone into DI water was measured via UV-Vis spectroscopy, using a pump to allow a constant flow of ozonated water through the UV-Vis spectrometer. Measurements were taken every minute for thirty minutes in the wavelength range from 190 nm to 350 nm. The ozone concentration was measured at the maximum absorbance wavelength of 260 nm. This was plotted against time to monitor the absorption of ozone over time. The Beer-Lambert law (Equation 11) was used to calculate ozone concentration at 260 nm.

Different variables were investigated to maximise the absorption of ozone into DI water.

These were:

- Effect of ozone gas concentration,
- Effect of pH,
- Effect of temperature,
- Effect of flow rate,
- Effect of radical scavengers

The reaction conditions for each experiment can be seen below in Table 3.

Table 3: conditions used for each experiment investigating ozone mass transfer into 500 mL DI water

Ozone gas concentration (g/m ³ NTP)	pH	Temperature (°C)	Flow rate (L/min)	Radical scavenger present
Standard experiment used for comparison				
50	6	18.9	0.50	No
Effect of ozone gas concentration				
30	6	19.1	0.48	No
70	6	19.1	0.50	No
Effect of pH				
50	2	18.9	0.50	No
50	9	19.3	0.49	No
Effect of temperature				
50	6	6.5	0.5	No
50	6	32.5	0.5	No
Effect of oxygen flow rate				
50	6	19.3	0.25	No
50	6	19.3	0.75	No
Effect of radical scavengers				
50	6	19.7	0.5	0.316 g sodium carbonate
50	6	19.6	0.5	100 µL tert-butanol

3.4.1 - Ozonation of chemical contaminants

Different conditions were tested to identify the optimum degradation for the three chemical contaminants in solution.

The conditions investigated are shown below:

- Effect of oxygenating the solution,
- Effect of ozonating the solution,
- Effect of pH on the degradation of the contaminant,
- Effect of temperature on the degradation of the contaminant,
- Effect of a radical scavenger on the degradation of the contaminant, and
- A stoichiometric analysis on the relationship between the chemical contaminant and ozone.

The effects of temperature were investigated using a chiller, to push water at a specified temperature around the jacket surrounding the reactor, to alter the temperature of the water solution within the reactor. The chiller temperature was set and the water circulated until the temperature of the water in the reactor stabilised.

The pH of solution was altered by spiking the solutions with hydrochloric acid or sodium hydroxide solution until the pH probe (Mettler Toledo) read the desired pH. Standardisation of the pH probe was conducted using pH buffers at pH 4 and pH 7.

Solutions for all the following experiments were made up of 475 mL DI water and 25 mL of the chemical contaminant in 1 mg/L solution.

All samples were taken from the reactor and bubbled with air to ensure there was no ozone remaining in the samples.

3.4.1.1 - Fluoranthene

Fluoranthene samples were taken at regular time intervals of 0 seconds, 30 seconds, 60 seconds, 90 seconds, and 120 seconds.

Table 4: Reaction conditions used when analysing the effect of different conditions on the ozonation of Fluoranthene.

Ozone gas concentration (g/m ³ NTP)	pH	Temperature (°C)	Flow rate (L/min)	Radical scavenger present
Oxygenating FLT solution				
0	6	19.7	0.5	No
Ozonating FLT solution at different ozone gas concentrations				
50	6	19.9	0.5	No
20	6	20.4	0.5	No
Effect of pH				
20	2	19.7	0.5	No
20	9	19.7	0.5	No
Effect of temperature				
20	6	29.8	0.5	No
20	6	14.8	0.5	No
20	6	5.1	0.5	No
Effect of radical scavenger				
20	6	20.1	0.5	100 µL tert-butanol

3.4.1.2 - Di (2- ethyl hexyl) phthalate

Di (2- ethyl hexyl) phthalate samples were taken at regular time intervals of 0 minutes, 1 minute, 2 minutes, 3 minutes, and 4 minutes.

Table 5: Reaction conditions used when analysing the effect of different conditions on the ozonation of Di (2- ethyl hexyl) phthalate.

Ozone gas concentration (g/m ³ NTP)	pH	Temperature (°C)	Flow rate (L/min)	Radical scavenger present
Oxygenating a solution of DEHP				
0	6	24.0	0.5	No
Ozonation of a solution of DEHP				
50	6	21.8	0.5	No
20	6	19.7	0.5	No
Effect of pH				
20	2	24.3	0.5	No
20	9	24.0	0.5	No
Effect of temperature				
20	6	15.3	0.5	No
20	6	24.7	0.5	No
20	6	29.3	0.5	No
Effect of a radical scavenger				
20	6	22.2	0.5	100 µL tert-butanol

3.4.1.3 - Cypermethrin

Cypermethrin samples were taken at regular time intervals of 0 minutes, 1 minute, 2 minutes, 3 minutes, 4 minutes, 5 minutes, and 10 minutes.

Table 6: Reaction conditions used when analysing the effect of different conditions on the ozonation of Cypermethrin.

Ozone gas concentration (g/m ³ NTP)	pH	Temperature (°C)	Flow rate (L/min)	Radical scavenger present
Oxygenating a solution of CYM				
0	6	19.7	0.5	No
Ozonation of a solution of CYM				
20	6	24.4	0.5	No
Effect of pH				
20	2	25.0	0.5	No
20	9	24.3	0.5	No
Effect of temperature				
20	6	21.7	0.5	No
20	6	15.2	0.5	No
20	6	29.6	0.5	No
Effect of a radical scavenger				
20	6	24.6	0.5	100 µL tert-butanol

3.4.1.4 - Stoichiometric Analysis

A stoichiometric analysis of all chemical contaminants was also performed. A solution of DI water was ozonated until saturation at 20 g/m³ NTP. This was mixed with the chemical contaminant solution made for experimentation (475 mL DI water and 25 mL chemical contaminant). The resulting solution was mixed with potassium indigo trisulphonate solution and the absorbance was measured using UV-Vis. The volumes used for all chemical contaminants were the same and can be seen below in Table 7.

Table 7: Volumes used to analyse the stoichiometric relationship of the chemical contaminants and ozone.

Contaminant volume (mL)	Ozone volume (mL)	Indigo volume (mL)
1	0.5	2
1	1	2
1	1.5	2
1	2	2

3.4.2 - Indigo Method

The indigo method was used to measure the concentration of ozone in solution. The reaction scheme is shown below in Figure 17.

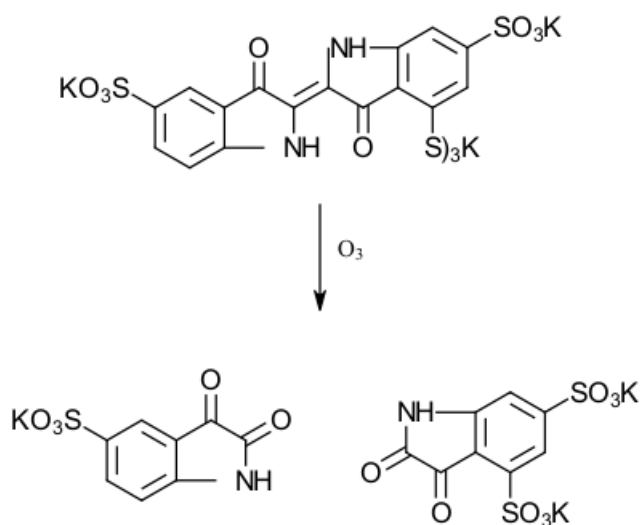


Figure 17: reaction scheme for the reaction with indigo trisulphonate

The indigo solution was prepared using 500 mL DI water and 1 mL concentrated phosphoric acid added whilst stirring to a 1 L volumetric flask. 77 mg of potassium indigo trisulfonate added whilst stirring and then made up to the mark. This solution was used to determine the concentration of ozone in water. A known volume of the indigo solution was extracted into a syringe and weighed. A smaller volume of the ozone solution was withdrawn from the reactor and the syringe weighed again. The UV-Vis spectrum of the pure indigo solution and the indigo and ozone solution were measured and the absorbances compared. This allowed the concentration of the ozone to be more accurately determined using the Beer Lambert Law (Equation 11).

3.5 - Adsorption experimentation

3.5.1 - Iodine Number

The iodine number experiment was performed on a variety of different samples that had been cleaned and treated using a commercial acid solution and washed and rinsed three times with DI water, in different percentages. These different samples were analysed to determine the iodine number of every sample. The method followed for this analysis is detailed below from the following documentation (International, 2006).

3.5.1.1 - Preparation of solutions

A variety of solutions were prepared for the experiment.

A hydrochloric acid solution at a concentration of 5 % by weight was prepared by mixing 70 mL concentrated hydrochloric acid and 550 mL of DI water. This was mixed thoroughly and then used for the next steps.

A sodium thiosulfate solution was prepared at a concentration of 0.100 N. For this solution 24.820 g of sodium thiosulfate pentahydrate was dissolved in 75 mL of DI water. 0.01 g of sodium carbonate was added into the solution and the volume made up to 1 L.

A standard iodine solution was prepared to a concentration of 0.001 N. 12.7 g of iodine and 19.1 g of potassium iodide were mixed and 5 mL of water was added and stirred. 60 mL of DI water was added and left for 4 hours. The solution was transferred to a volumetric flask and made up to 1 L.

A solution of potassium iodide was made up to a concentration of 0.1 N. This solution was made by drying 4 g of potassium iodate at 110 °C for 2 hours. 3.57 g of this potassium iodate was taken and dissolved in 100 mL of distilled water. This was transferred to a volumetric flask and made up to 1 L.

3.5.1.2 - Standardisation of solutions

The sodium thiosulfate solution was standardised using potassium iodate titration in the burette. The flask below the burette contained 2 g of potassium iodide with 5 mL of hydrochloric acid. The equations for this standardisation can be found in Appendix 1.

The iodine solution was standardised with the iodine solution being titrated against the previously standardised sodium thiosulfate. The indicator used was a starch solution, which was added when the solution became a light yellow colour. The solution turned black on addition of the starch and was then titrated until no colour was apparent.

3.5.1.3 - Iodine number procedure

Granulated activated carbon was ground and passed through a mesh screen of 425 microns. The carbon was dried and cooled to room temperature. The weighed samples of carbon were transferred into Erlenmeyer flasks and 10 mL of the hydrochloric acid solution was added, shaken and heated to remove any sulphur. 100 mL of the iodine solution was added into the flasks and shaken vigorously. The solution was filtered to remove the carbon and 50 mL of the resulting filtrate was used to titrate against the sodium thiosulfate. Starch solution was added to ensure the correct end point was recorded.

Calculations were performed to calculate the iodine number, which can be found in Appendix 1.

3.5.1.4 - Adsorption with GAC

The adsorption of each chemical contaminant onto the surface of GAC was investigated in DI water.

Samples of 1 mg/L of each contaminant were used (100 mL) and the mass of GAC used for experimentation varied. The masses used can be seen below in Table 8. The solutions were mixed using an Inku Shaker, set to a temperature of 20 °C and a speed rate of 200 rpm.

Table 8: Reaction conditions used for the analysis of adsorption rates of the chemical contaminants onto different masses of GAC.

Solution used	Mass of GAC used (g)
FLT analysis	
100 mL 1 mg/L Fluoranthene solution in DI water	0.021
100 mL 1 mg/L Fluoranthene solution in DI water	0.015
100 mL 1 mg/L Fluoranthene solution in DI water	0.010
100 mL 1 mg/L Fluoranthene solution in DI water	0.020
100 mL 1 mg/L Fluoranthene solution in DI water	0.015
100 mL 1 mg/L Fluoranthene solution in DI water	0.010
DEHP analysis	
100 mL 1 mg/L Di (2- ethyl hexyl) phthalate solution in DI water	0.020
100 mL 1 mg/L Di (2- ethyl hexyl) phthalate solution in DI water	0.015
100 mL 1 mg/L Di (2- ethyl hexyl) phthalate solution in DI water	0.010
100 mL 1 mg/L Di (2- ethyl hexyl) phthalate solution in DI water	0.020
100 mL 1 mg/L Di (2- ethyl hexyl) phthalate solution in DI water	0.015
100 mL 1 mg/L Di (2- ethyl hexyl) phthalate solution in DI water	0.010
CYM analysis	
100 mL 1 mg/L Cypermethrin solution in DI water	0.020
100 mL 1 mg/L Cypermethrin solution in DI water	0.016
100 mL 1 mg/L Cypermethrin solution in DI water	0.010
100 mL 1 mg/L Cypermethrin solution in DI water	0.005
100 mL 1 mg/L Cypermethrin solution in DI water	0.012
100 mL 1 mg/L Cypermethrin solution in DI water	0.017

Samples were taken at regular time intervals and analysed using HPLC to determine the concentration of the contaminants remaining in solution.

3.6 - Wastewater Analysis

Samples of final treated wastewater effluent were collected from Gowerton wastewater treatment plant. Samples were collected by Welsh Water and the water was analysed. The samples taken for experimentation were stored in the fridge and filtered through PVDF membrane filters 0.45 μm , to ensure there were no particulates in the solution to block the HPLC column.

Ozonation of the wastewater was investigated. The wastewater effluent was spiked with solutions of the chemical contaminants so the concentrations could be determined. All solutions were prepared using 475 mL filtered wastewater and 25 mL of 1 mg/L solutions of the contaminants. The conditions used for the experiments are shown below in Table 9.

Samples were collected at regular time intervals of 0 minutes, 0.5 minutes, 1 minute, 1.5 minutes, 2 minutes, 3 minutes, 4 minutes, 5 minutes, and 10 minutes. When the samples were collected, air was bubbled into the solutions to ensure no ozone was present.

These samples were then analysed using HPLC.

Table 9: Reaction conditions used for each experiment when investigating the ozonation of the chemical contaminants in wastewater.

Chemical	Ozone gas concentration (g/m^3 NTP)	pH	Temperature ($^{\circ}\text{C}$)	Oxygen gas flow rate (L/min)
FLT	20	7.1	13.2	0.5
DEHP	20	7.1	13.6	0.5
CYM	20	7.1	14.1	0.5

The wastewater was also investigated for the effects of adsorption onto GAC. Solutions of 1 mg/L were prepared in wastewater and 100 mL added and mixed with 0.015 g GAC each. This was mixed in the Inku Shaker, with the temperature set to 20 °C and the speed of mixing set to 200 rpm as before. Samples were taken at regular time intervals to monitor the concentration decrease. These were 0 minutes, 5 minutes, 10 minutes, 20 minutes, 30 minutes, 40 minutes, 60 minutes, 80 minutes, 100 minutes and 120 minutes. Samples were analysed using HPLC.

Chapter 4 – Ozone Mass Transfer Analysis

Different reaction conditions were used to determine the effects they would have on the overall reaction composition. These conditions involved ozone concentration, temperature, flow rate of oxygen and pH.

4.1 - Indigo Method

Differing ozone concentrations were investigated using the indigo method. The differing ozone concentrations investigated were 20 g/m³ NTP (normal temperature and pressure), 50 g/m³ NTP and 70 g/m³ NTP. The DI water was ozonated until maximum concentration reached and then the indigo method was performed and the absorbance at 260 nm measured.

4.2 - Ozone mass transfer

Using the ozone generator coupled with an ozone analyser, the different concentrations of ozone applied to the reaction system can be determined. For these reactions, the volume of DI water in the reactor was kept constant at 500 mL, as well as the pH of the water being kept constant and the rate of stirring and temperature. This enabled the results to depict only the relationship between the effects of ozone concentration on the mass transfer coefficient ($k_{L,a}$) values and the rate of absorption. Figure 18 shows the change of ozone concentration in the liquid phase (C_{AL}), as a function of time under different ozone gas concentrations. The values for C_{AL} were determined using the Beer-Lambert law with an extinction coefficient of 3000 M⁻¹cm⁻¹ for ozone.

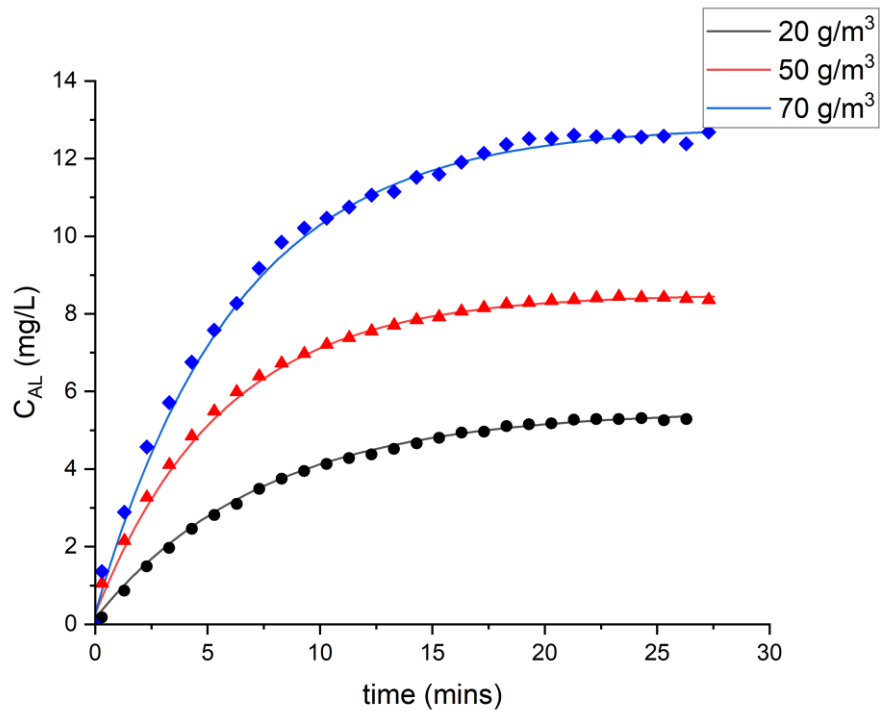


Figure 18: effect of gas ozone concentration on absorption into solution ($pH = 6$, temperature $\sim 20^\circ C$, oxygen gas flow = 0.5 L/min)

From looking at the relationships shown in the graph, the ozone liquid concentration increases with time until it reaches a plateau as the bubbling time becomes high. The higher the ozone gas concentration, the higher the final ozone liquid concentration. The experimental results were modelled using Equation 12 and Equation 13. The model parameters were determined using the Solver tool in MS Excel and their values summarised in Table 10.

Equation 14

$$C_{AL} = \frac{Abs_{260}}{\epsilon L}$$

Eq. 15: Equation to calculate CAL from the absorbance

Where:

C_{AL} is the aqueous ozone concentration (mg/L),

Abs_{260} is the measured absorbance for ozone at 260 nm,

ϵ is the ozone extinction coefficient and,

L is the path length of the cell (cm).

Equation 15

$$C_{AL} = C_{AL_0} \exp(-k_L a t)$$

Eq. 16: Equation to model the absorption of ozone into the liquid phase

Where:

C_{AL} is the aqueous ozone concentration (mg/L),

C_{AL_0} is the initial aqueous ozone concentration (mg/L),

k_L is the specific interfacial area,

a is the equilibrium concentration of ozone in the water and,

t is time (s).

From this equation, a graph of $\ln\left(\frac{C_{AL}}{C_{AL0}}\right)$ vs t can be plotted to model the absorption.

Table 10: k_{La} values and C_{AL}^* values for each experiment comparing ozone gas concentration

	30 g/m ³ NTP	50 g/m ³ NTP	70 g/m ³ NTP
C_{AL}^* (mg/L)	5.51	8.51	12.85
k_{La} (min ⁻¹)	0.14	0.18	0.16

As would be expected, the values of C_{AL}^* increases in relation to the concentration of ozone.

The values shown above are C_{AL}^* , which is the end concentration of ozone within the liquid phase, and k_{La} is the mass transfer coefficient, which determines the rate that ozone is transferred between the gas and the liquid phase during the reaction. Values for k_{La} are obtained to compare the rate of mass transfer within the solution. From looking at the values shown in Table 10, the ozone concentration of 50 g/m³ NTP offers the best rate of mass transfer of ozone into water within the reactor.

The value for k_{La} is calculated by comparing the values of C_{AL} obtained experimentally and comparing these values to ones of C_{AL} obtained through the model calculation using Beer-Lambert Law, shown in Equation 11. These values are compared until the difference is negligible and then used to determine the value of k_{La} through the calculations expanded on in Appendix 2.

As the values shown for k_{La} are all within a small range, it is not certain that this describes a significant change within the different reactions and could instead be due to error within the experiments.

4.2.1 - Effects of pH on ozone mass transfer

The ozonation of water was performed under different pH values. For these experiments the flow rate was maintained at 0.5 L/min, the volume of the solution was 500 mL, and the ozone concentration was 50 g/m³ NTP. Hydrochloric acid and sodium hydroxide solutions were used to set the pH of the working solutions.

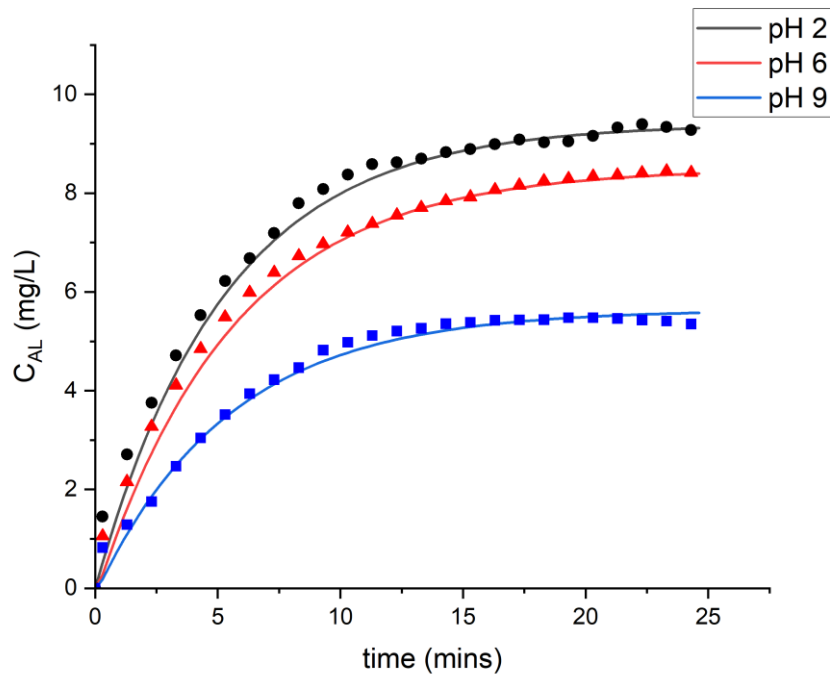


Figure 19: effect of pH on absorption of ozone into solution (ozone gas concentration = 50 g/m³ NTP, temp = ~ 20 °C, oxygen flow rate = 0.5 L/min)

Figure 19 shows the change of aqueous ozone concentration as a function of time at different pHs. It can be seen that as the pH increased, the curves plateau at a lower liquid concentration. As the pH is increased, the rate of degradation of ozone increases, this is due to the production of hydroxyl radicals increasing at a more alkaline pH (Mandavgane & Yenkie, 2011). At alkaline pH levels, the presence of hydroxyl radicals results in rapid decomposition of ozone, which in turns results in a lower half-life of the gas (Galdeano et al., 2018).

To evaluate the effect of pH on mass transfer, the experimental data was fitted with the equation and the parameters were determined, their values are given in Table 11. According to Table 11, the highest value of C_{AL}^* was obtained at pH 2. This is because at low pH, ozone is more stable which implies that higher concentrations of molecular ozone are obtained in the liquid phase. At a higher pH, for example pH 9, ozone decomposes rapidly due to the presence of the hydroxide ions which reduces its concentration in the liquid phase. The results obtained in this study are consistent with those reported in literature, as discussed below.

Table 11: Effect of pH on mass transfer parameters C_{AL}^* and k_{La}

pH	2	5	9
C_{AL}^* (mg/L)	9.41	8.51	5.64
k_{La} (min^{-1})	0.19	0.18	0.18

In the ozonation of dyes, the molecular ozonation reaction is preferable, this supports the findings outlined previously, as an increase in the removal percentage from 50 % to 90 % was found when the pH was altered from pH 10 to pH 3. Therefore, this supports the finding that pH does have an effect on ozone decomposition, which is accelerated at higher pH levels (Tizaoui & Grima, 2011). In a study looking at the ozonation of phenol, different rate constants for the decomposition of ozone into hydroxyl radicals were calculated. These results showed a rate of ozone decomposition at pH 2 of $8.3 \times 10^{-5} \text{ s}^{-1}$ while at pH 12 a rate of ozone decomposition at 2.1 s^{-1} . This shows that there is increased ozone decomposition at higher pH levels, supporting the findings that there is more molecular ozone present in a lower pH (Wu et al., 2000).

4.2.2 - Effect of temperature

The effect of temperature on ozone absorption in water was evaluated and the results are shown in Figure 20. The figure clearly shows that temperature plays an important role in assisting in the absorption of ozone into the water solution. It can be seen that the cold solution provides a much better basis for the absorption of ozone, with a significantly higher plateau for the C_{AL} at longer absorption times. At higher temperatures, the vibrational and rotational movements of the ozone molecule could have an effect on the absorption of ozone, resulting in lower concentrations of ozone being absorbed at higher temperatures (Molina & Molina, 1986).

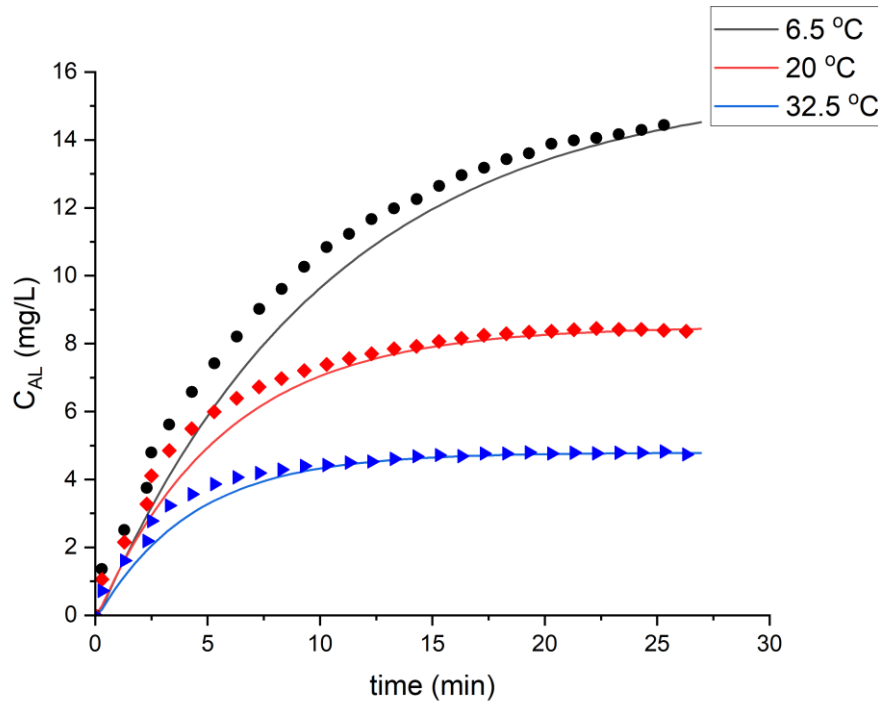


Figure 20: effect of temperature on absorption of ozone into the liquid phase (ozone gas concentration = $50 \text{ g/m}^3 \text{ NTP}$, $\text{pH} = 6$, oxygen flow rate = 0.5 L/min)

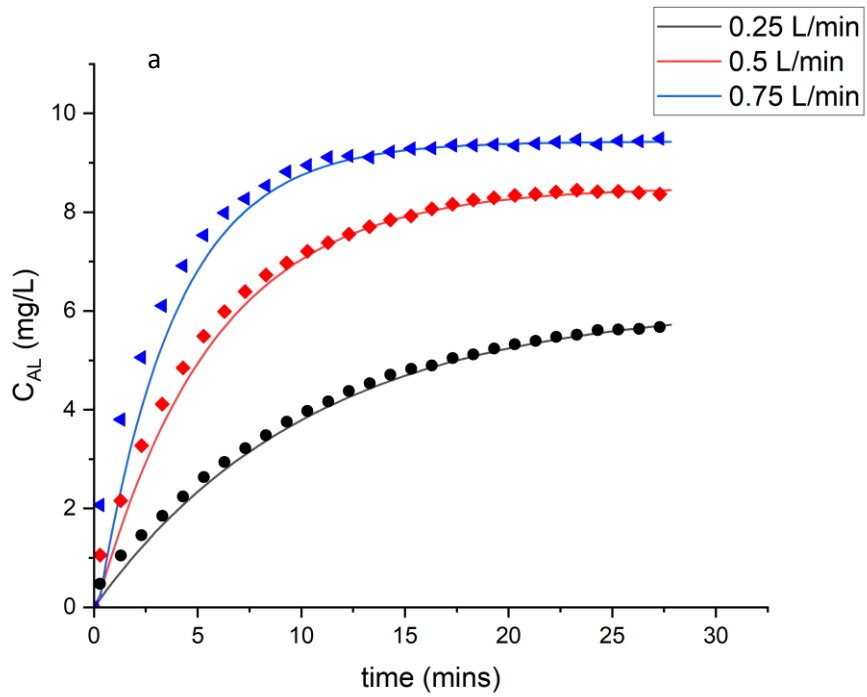
From looking at the values in the table above it can be seen that the cooler temperature has a higher C_{AL}^* value, paired with a lower value for k_{La} . This shows that the higher k_{La} value is also associated with a lower ozone concentration in the liquid phase. If the ozone is more soluble at lower temperatures, then a higher mass transfer coefficient from the gas to liquid phase would be expected (Galdeano et al., 2018).

Table 12: comparison of C_{AL}^* and k_{La} values from the effect of temperature

T (°C)	6.5	18.9	32.5
C_{AL}^* (mg/L)	15.7	8.51	4.79
k_{La} (min^{-1})	0.10	0.18	0.24

4.2.3 - Effect of flow rate

The effects of oxygen flow rate on ozone mass transfer were also investigated, ($T = 20\text{ }^{\circ}\text{C}$, $\text{pH} = 6$, ozone gas concentration = $50\text{ g/m}^3\text{ NTP}$).



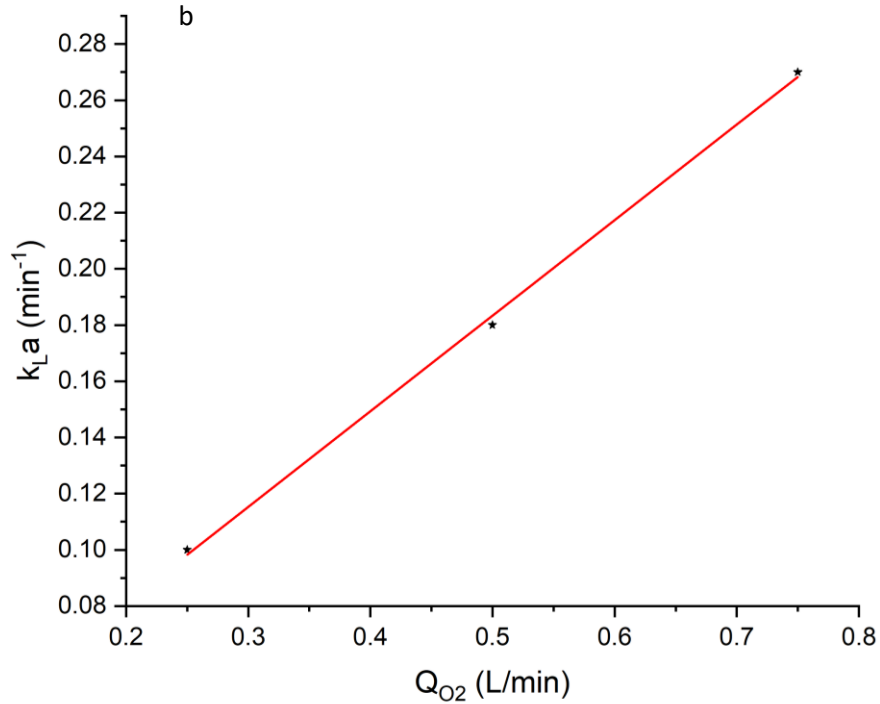


Figure 21: (a) effect of flow rate on absorption of ozone into solution; (b) effect of flow rate on k_La , (ozone gas concentration = $50 \text{ g/m}^3 \text{ NTP}$, $\text{pH} = 6$, $\text{temp} = \sim 20 \text{ }^\circ\text{C}$)

From looking at the graph above in Figure 21, it can be seen that the flow rate of oxygen has an effect on ozone absorption into water. This would be expected because the flow rate of gas passing through the reactor would affect the mass transfer. As the flow of gas increases, the distribution of the gas within the liquid increases, as well as mixing, resulting in an increased mass transfer (Kapoor et al., 2021). The flow rate of 0.25 L/min has the lowest C_{AL} model values, with the absorption of ozone plateauing at a much lower value than the others. Both the absorption rates of 0.5 L/min and 0.75 L/min plateau at a similar time, just at different values of C_{AL} model. This would be expected with a higher flow rate of oxygen, as the concentration gradient of ozone increases at a faster rate than with a lower oxygen flow rate. Thus, the effect of oxygen gas flow rate on the saturation concentration is not evident, since the inlet ozone gas concentration was the same for all flow rates. This discrepancy as observed on Figure 21 could be due to changes in the gas pressure as the flow rate changes, which affects the amount of ozone dissolved in water. The higher the flow rate, the higher the pressure resulting in a higher C_{AL}^* as depicted in Table 13. Table 13 also shows the enhanced mass transfer coefficient, k_La , as the flow rate increased. This effect can be predicted by a linear function within the range of flow rates used in this study (Figure 21).

Table 13: comparison of C_{AL}^* and k_La values looking at the effect of flow rate

Q_{O_2} (L/min)	0.25	0.5	0.75
C_{AL}^* (mg/L)	6.15	8.51	9.43
k_La (min^{-1})	0.10	0.18	0.27

To determine how the effects on the equilibrium gas concentration were determined, an additional experiment to investigate the change in pressure for the different flow rates was performed. Three variations were conducted in the experimental set up. The first was using oxygen as the gas, with no liquid in the reactor. The second was using oxygen as the gas, with 500 mL DI water in the reactor and the third was using ozone as the gas, with 500 mL DI water in the reactor. When the flow rate was altered, the change in the distance of DI water was measured equating to a change in pressure.

The results can be seen summarised in Table 14 below.

Table 14: Pressure change with gas flow change

Values obtained for the change in pressure for oxygen gas flow with no liquid in the reactor					
Flow (L/min)	0.1	0.25	0.5	0.75	0.93
Δp (mm H₂O)	6	19	42	68	88
Values obtained for the change in pressure for oxygen gas flow with 500 mL DI water in the reactor					
Flow (L/min)	0.09	0.25	0.5	0.76	0.92
Δp (mm H₂O)	137	142	162	179	193
Values obtained for the change in pressure for ozone gas flow with 500 mL DI water in the reactor					
Flow (L/min)	0.26	0.5	0.75	1.02	
Δp (mm H₂O)	159	171	182	202	

The values in the Table 14 show that the change in gas flow results in a change in pressure through the reaction system. This would have an effect on the end concentration of ozone absorbed into the system, as a higher pressure would result in more mass transfer of ozone into the water (Lau et al., 2004).

Through looking at the ideal gas law, shown in Equation 17, the relationship for pressure of the gas can be determined.

Equation 16

$$PV = nRT$$

Eq.17: Ideal gas equation

Where:

P is the pressure of the gas, Pa,

V is the volume of the gas, m³,

n is the number of moles of the gas

R is the ideal gas constant, 8.31 J K⁻¹ mol⁻¹

T is the temperature, K.

There are some assumptions made to ensure that the ideal gas law can be used (Pan et al., 1998). These assumptions are:

- The gas consists of a large number of molecules, that are in random motion and obey Newton's laws of motion.
- The volume of the molecules is negligible in comparison to the volume occupied by the gas.
- There is no force acting on the molecules, except the forces that occur during any collisions of the molecules.

As the ideal gas equation relates the number of particles to the pressure, the lower the pressure, the lower the number of particles in the gas phase that are available for absorption into the liquid phase (Kim et al., 2019).

4.2.4 - Effect of scavengers

The effect of scavengers on ozone absorption was investigated, using sodium carbonate and tert-butanol. These experiments were performed at room temperature and at an ozone concentration of 50 g/m³ NTP. Figure 22 shows that ozone absorption in DI water and in the presence of t-butanol increased up to a near-saturation (> 8 mg/L) but in the presence of carbonate, ozone concentration in the liquid phase obtained after 30 minutes gas bubbling was less than 1 mg/L. This indicated that in the presence of carbonate, ozone quickly reacts to form other products.

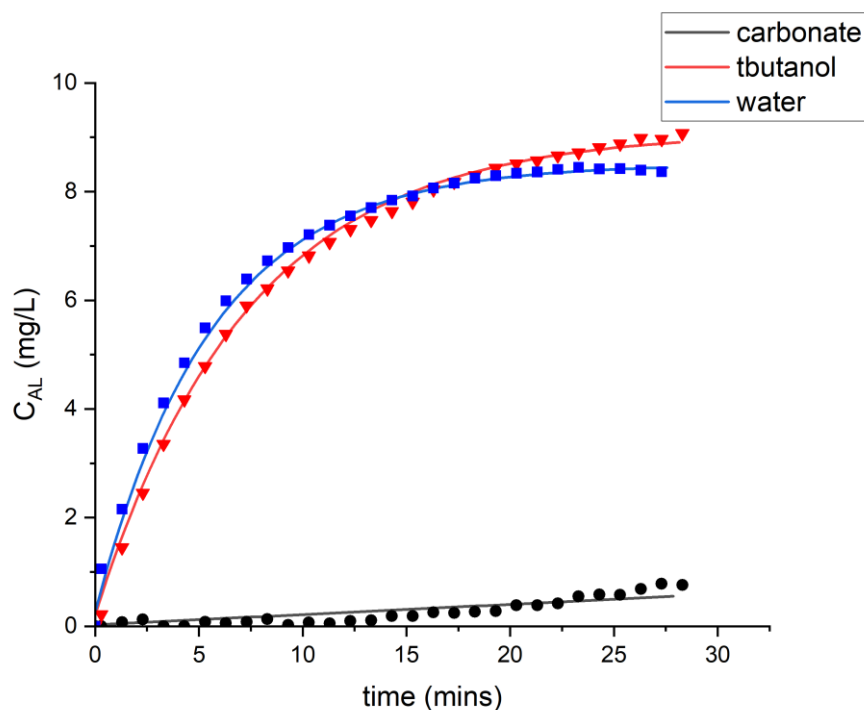


Figure 22: effect of radical scavengers on absorption of ozone into solution (ozone gas concentration = 50 g/m³ NTP, pH = 6, temp = ~ 20 oC, oxygen flow rate = 0.5 L/min)

The reaction of carbonate with ozone can disrupt the chain reaction of the hydroxyl radical formation and reform ozone within the solution. If this reaction had been left to run for longer, it could be seen as to whether the ozone concentration does begin to increase which would present the reforming of ozone. The reaction for how carbonate scavenges the hydroxyl radicals and converts them into ozone is shown in Figure 23 (Eriksson, 2005). At pH 6, the carbonate in solution would have dissociated to form HCO₃⁻ and CO₃²⁻ which would also assist in the acceleration of the production of hydroxyl radicals.

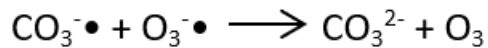
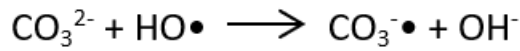


Figure 23: Chemical reactions for the conversion of radicals to ozone by carbonate

The reaction of tert-butanol appears to have little impact on the absorption of ozone into the water. This is because the addition of tert-butanol, although affecting the hydroxyl radicals, has the added benefit of altering the bubble size of the ozone being diffused into the solution. The smaller bubbles mean that the ozone mass transfer is increased. As can be seen in the data presented in Table 15, the mass transfer coefficient, k_La , for DI water and tert-butanol is 0.14 min^{-1} , while for DI water it is 0.18 min^{-1} . The coefficient, k_La , is in fact the sum of the mass transfer coefficient and the rate constant of ozone decomposition. This value is reduced because of the elimination of radicals by the scavenger, thus, the experimental value of k_La can be ignored and the calculated k_La can be taken as the true mass transfer coefficient.

Table 15: comparison of C_{AL}^* and k_La values from different scavengers

	Sodium carbonate	Pure water	Tert-butanol
C_{AL}^* (mg/L)	Negligible	8.51	9.10
k_La (min^{-1})	N/A	0.18	0.14

Chapter 5 - Ozone Degradation of Chemical Contaminants

Throughout this sub section of the thesis, the effect of different conditions on the degradation of three chemical contaminants were investigated to decipher the best set of reaction conditions for the fastest and most efficient rate of degradation within wastewater.

The chemicals that were investigated are:

- Fluoranthene
- Di (2- ethyl hexyl) phthalate
- Cypermethrin

The following conditions and variables were investigated:

- Effect of oxygenating solution
- Effect of pH
- Effect of temperature
- Effect of a radical scavenger

The findings are all outlined in this chapter.

5.1 - FLT analysis

5.1.1 - UV-Vis Analysis

Fluoranthene (FLT) is a solid with very low water solubility which makes the production of an aqueous solution difficult. The solubility of fluoranthene has been found to be 265 µg/L (Agency & 1980). The analysis of the solution of this concentration with UV-Vis resulted in no changes in the spectrum being observed, highlighting that the concentration would be too low for appropriate absorption. This meant that the analysis of the concentration of FLT within the water samples had to be analysed by another, more appropriate technique, which would allow the concentration change over time to be adequately analysed.

As a clear identification of FLT could not be made through UV-Vis analysis, alternative methods of analysis needed to be found.

5.1.2 - Fluorescence Analysis

The analysis of FLT presence in aqueous solution was trialled using the fluorimeter. This included the sample of FLT in water being placed in the fluorimeter and excited at a certain wavelength of light. Through the investigations using fluorescence, it was seen that a spectrum was obtained for the presence of FLT within solution. This enabled the excitation and emission wavelength values to be obtained and used for further analysis.

The pairs were obtained through investigating the highest peak obtained for the emission and then comparing this by exciting the solution at this peak emission wavelength. The peak wavelengths were found to be 285 nm and 466 nm.

These wavelengths were then incorporated into the HPLC analysis method, which means that throughout the analysis, the samples and separated fractions were excited and emitted at the specified wavelengths to give a clear peak for analysis.

5.1.3 - HPLC Analysis

HPLC Analysis was performed following the method outlined in the methodology section.

5.1.3.1 - Calibration Curve

To equate the peak areas obtained from the HPLC analysis to concentration, a calibration curve needed to be produced using samples of known concentrations of FLT. As the concentration of the FLT solutions used for the analysis were a maximum concentration of 0.05 mg/L, a maximum concentration of 0.1 mg/L was chosen as the highest concentration for the calibration curve production to ensure that the values obtained fell well within the calibration curve. The minimum value was a sample of pure water, with the FLT concentration being 0 mg/L. Three samples were chosen in the middle, with concentrations of 0.025 mg/L, 0.0125 mg/L and 0.00625 mg/L. These samples were all prepared from the FLT solution and pure water. The samples were all analysed using FLD analysis within the HPLC, and a graph was plotted comparing the peak area obtained with a retention time of approximately 1.7 minutes and the known concentration of the samples.

In using the HPLC, a guard for the column was installed to ensure the integrity of the column performance was maintained throughout the extensive analysis performed. However, the installation of this guard meant that the retention time for FLT was altered, as well as the peak areas relating to the concentration of the sample. Another calibration curve needed to be obtained to ensure that the accurate comparison of peak area to FLT concentration could be determined to enhance the analysis of the concentration degradation of FLT for future experimentation. The graph shown below in Figure 24 shows the alternative calibration curve obtained, which was then used for analysis of all experiments performed once the guards had been installed.

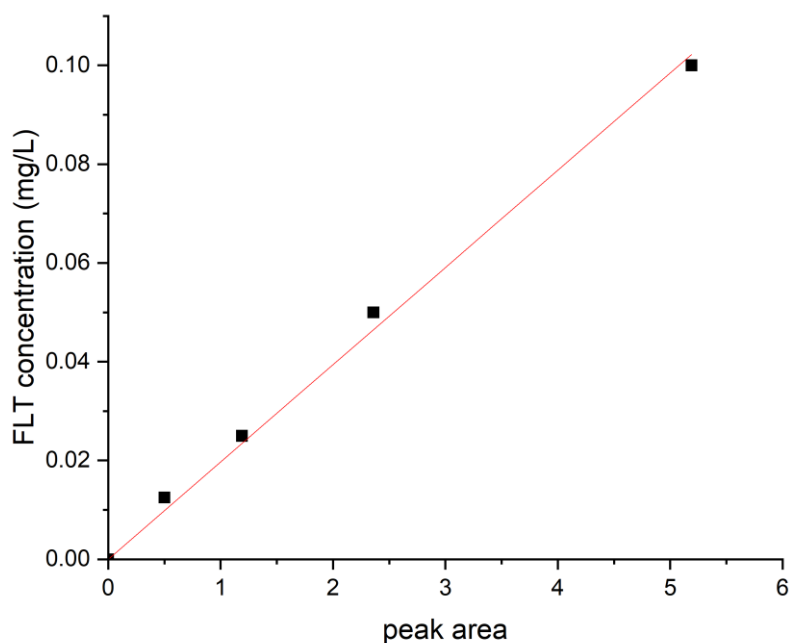


Figure 24: Calibration curve obtained for FLT once guards were installed on the column

From the graph in Figure 24, an alternative equation can be found that equates both the FLT concentration and the peak area. The equation used can be seen below in Equation 18.

Equation 17

$$y = 0.0197x$$

Eq. 18: equation obtained from the calibration curve

5.1.4 - Effect of oxygenating solution

To ensure that the degradation of FLT investigated occurred via oxidation from ozone as opposed to a reaction using pure oxygen, a reaction where the gas flowing into the reactor was pure oxygen was trialled. If degradation of FLT could still be seen from this reaction, then the FLT would be very volatile and so merely the flow of a gas into the solution would cause the FLT to degrade and evaporate. The graph shown below in Figure 25 shows that this was not the case and the concentration of FLT within the solution remained constant and no degradation occurred. This means that for all future experimentation it can be said with some certainty that the degradation of FLT does occur via ozonation and can then be investigated as the treatment technique for the FLT removal from wastewater.

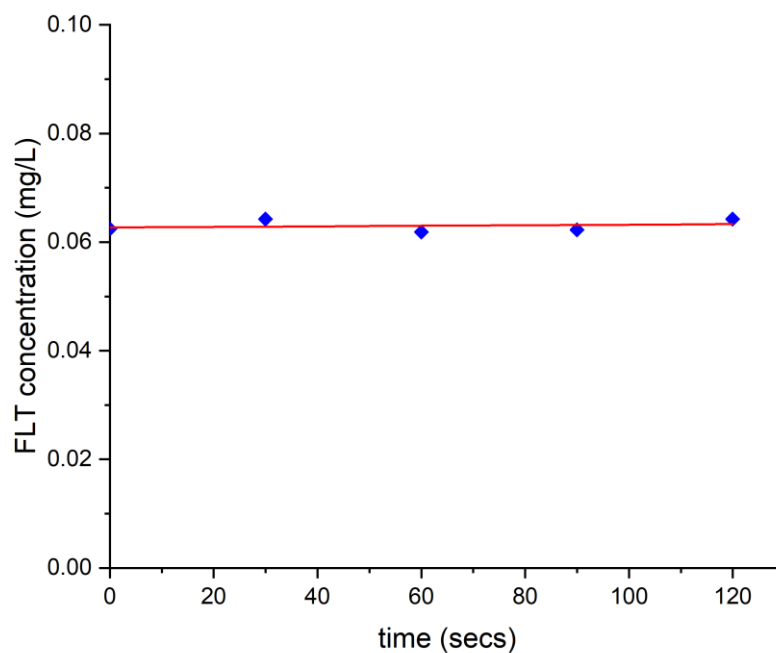


Figure 25: Graph depicting the effect of flowing oxygen into solution on FLT degradation (oxygen flow rate = 0.5 L/min, pH = 6, temp = ~ 20 °C)

5.1.5 - Effect of ozone concentration

The effects of ozone concentration were investigated by performing a reaction at 50 g/m³ NTP. However, the reaction was too fast meaning that no monitoring of the FLT concentration could effectively occur. Therefore, the effect of ozone concentration was not investigated further, instead all experiments were performed at 20 g/m³ NTP to allow for appropriate monitoring for the degradation of FLT with ozonation. The rate of degradation seen was positive, showing that large amounts of FLT in solution were degraded within 2 minutes of ozonation.

5.1.6 - Effect of pH

When looking at the effects that the pH of the solution has on the degradation of fluoranthene, a solution of FLT begins at the same concentration to ensure that the comparison is fair. The flow of oxygen and concentration of ozone produced is also kept constant. Temperature also remained constant.

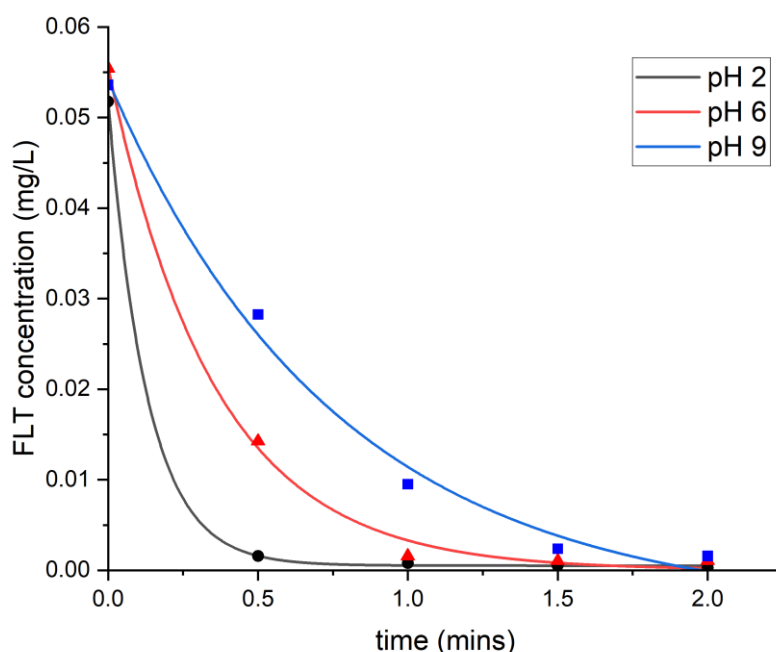


Figure 26: Graph comparing the effects of pH on FLT degradation (ozone gas concentration = 20 g/m³ NTP, temp = ~ 20 oC, oxygen flow rate = 0.5 L/min)

In Figure 26, it shows that the pH of the solution does have an effect on the rate of degradation of the fluoroanthene. The speed of degradation was significantly increased with a pH of 2 than it was with the pH of 9. This is represented through the significant gradient difference shown between the pH 2 and pH 9 model lines. The gradient for pH 2 is much steeper, showing that the degradation of fluoroanthene occurred more rapidly. However, with the reaction at pH 2 being so fast, it meant that monitoring the reaction was difficult, as more samples could not be taken within the time frame to have a better understanding of the reaction kinetics. Within 30 seconds, most of the fluoroanthene had been degraded, which resulted in the very steep curve. Although this reaction mixture pH appears to be the most efficient way to degrade FLT rapidly, there could be more errors associated with this line due to the speed of degradation being faster than the speed that samples can be taken.

The data collected for pH 9 was significantly slower in comparison to both pH 2 and pH 6. This is shown through it having the shallowest gradient on the graph. This follows the relationship discussed previously for the absorption of ozone into solution at different pH

levels, with the lowest pH showing an increased absorption of ozone in comparison to a high, alkaline pH.

At solutions of a higher pH, the concentration of hydroxyl radicals within the solution would increase, whereas in a solution of a lower pH, the hydroxyl radicals would be less prevalent, meaning oxidation would occur primarily via molecular ozonation. When looking at the chemical of interest here, the oxidation process that would be most effective would be molecular ozone, this explains why the rate of degradation is so much faster at pH 2 for fluoranthene.

When looking at the structural formula for fluoranthene, there are three benzene rings within the structure, which would result in a high density of double bonds. This means that the reaction with ozone occurs via direct ozonation rather than indirect ozonation in this instance. Therefore, a lower pH would result in a better degradation of fluoranthene, as at a higher pH there would instead be more hydroxyl radicals present which would favour indirect ozonation. Due to this specific degradation being via direct ozonation, the increased number of hydroxyl radicals would decrease the ozone concentration resulting in a slower rate of degradation as shown in the graph (Khuntia et al., 2015).

pKa is a value that refers to the negative log value of the Ka, which is the acidity constant. The Ka value is obtained from the equilibrium equation of a weak acid and provides a value for the ionising potential of a compound within solution, typically water (Kutt et al., 2018). The value of pKa, allows compounds to be compared by their relative acidity. (Seybold & Sheilds, 2015).

The pKa value of fluoranthene is recorded in literature as being higher than 15 (Christensen et al., 1975). This is a high pKa value and would infer that FLT is not a strongly acidic compound. The higher the pKa value, the tighter that a proton can be held to the compound, so the high pKa value for fluoranthene would suggest that protons would have a high affinity to the compound structure. This would be expected due to the pi bonding orbitals surrounding the benzene ring, which would mean that the ring is surrounded by a 'cloud' of negative charge (Hilbert et al., 1995). There are many techniques that can be used to protonate the molecule.

Despite pH 2 having the fastest rate of FLT degradation, pH 6 would be taken forward for further investigation. This is because the rate of degradation can be monitored slightly more effectively than the degradation with pH 2 due to the reaction speed, as well as a more neutral pH being more environmentally friendly and more appropriate for treating wastewater. This is due to the fact that if solutions of varying pH were used, additional treatment could be required to ensure the wastewater obtained after treatment is at a pH suitable for the use of the water once treatment has been completed.

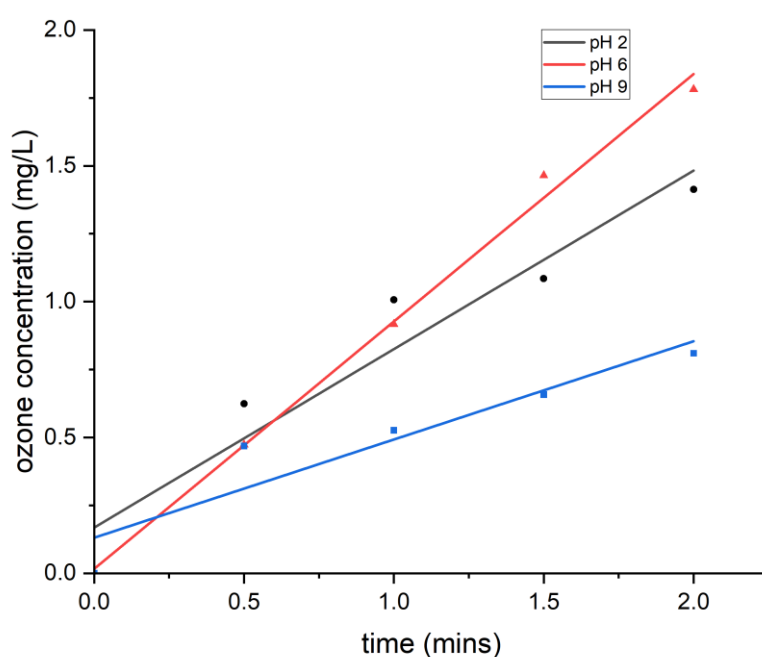


Figure 27: Effect of pH on ozone concentration (ozone gas concentration = 20 g/m³ NTP, temp = ~ 20 oC, oxygen flow rate = 0.5 L/min)

Figure 27 shows the effect of pH on the concentration of ozone absorbed into the solution. The indigo method is not 100% accurate to determine the concentration of ozone within solution, this is because the reaction between the indigo solution and ozone may not have gone to completion. Also, the sample of ozonated water taken may not have been thoroughly mixed meaning an accurate value cannot be obtained. This explains why the lines shown in Figure 27 do not all pass through the origin, as the calculated values for concentration rely on the experimental absorption values obtained.

These values were obtained using the indigo method and measuring the absorption differences of these samples in indigo reacted with ozone and pure indigo solution. When comparing the ozone concentration of a solution at pH 2 and pH 9, it can be seen that there are vast differences in the ozone concentration obtained. This supports the conclusion made previously that ozonation occurs directly via molecular ozone at low pH levels and that the ozone is converted into hydroxyl radicals at higher pH values. The ozone decomposition is increased at higher pH values, which supports the decrease in ozone concentration seen. The indigo method would only detect the molecular ozone within the solution, and the higher concentration of this would support the faster rate of reaction that occurs in the lower pH levels.

5.1.7 - Effects of temperature

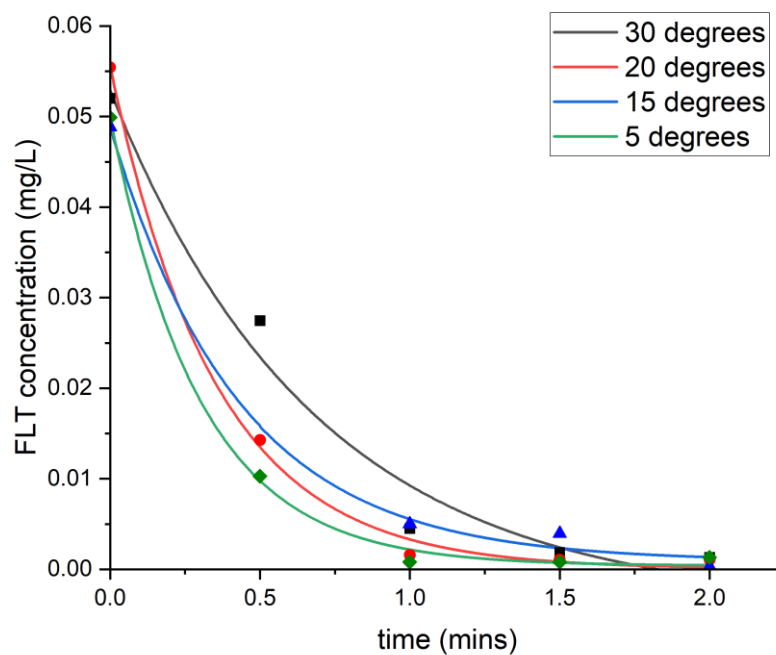


Figure 28: Effect of temperature on FLT degradation (ozone gas concentration = 20 g/m³ NTP, pH = 6, oxygen flow rate = 0.5 L/min)

When looking at the temperature comparison of the degradation of FLT by ozone, there are two main factors to consider which can act as competing factors. As temperature increases, the rate of the reaction should increase, (Barrow, 1992), which can be seen by comparing the data obtained for 20 degrees and 15 degrees. The data at 20 degrees shows a slightly steeper slope of degradation initially in comparison. The second factor that can have a large impact on the rate of degradation of FLT in solution is the ozone absorption into the liquid phase. The more ozone that is absorbed into the liquid phase, the more ozone that is available to then oxidise the FLT and result in the degradation. It is shown that ozone absorbs significantly better into water and solution at cooler temperatures in comparison to warmer temperatures (Molina & Molina, 1986). This can be seen in the significant difference in the data obtained for 5 degrees and 30 degrees. The more ozone absorbed into the solution at 5 degrees would then mean the concentration of ozone in the liquid phase would be significantly higher. This would then increase the oxidation of FLT by molecular ozone in the solution which results in the much faster rate of degradation.

There will be a point where these two factors are competing. The rate of reaction would be more favourable at a certain temperature, which would be less favourable for the absorption of ozone. A balance between these is shown with the 15 degrees and 20 degrees data sets, where 20 degrees has a faster rate of reaction than 15 degrees, despite the fact that 15 degrees is a cooler temperature and would therefore favour an increase of molecular ozone absorption into solution.

It can be assumed that the reaction of FLT and ozone occurs via a 1st order rate of reaction. Therefore, following data analysis, the values for the rate constant can be determined for the reaction rate for each temperature investigated. These values are shown below in Table 16.

Table 16: temperature effects on rate constants

Temperature (°C)	Rate constant (k) (min ⁻¹)
5	2.74
15	1.23
20	2.82
30	1.71

From taking these values obtained from the assumption of the 1st order reaction, further data analysis can be carried out to calculate the activation energy of the reaction system.

A graph plotting the natural log of the rate constants and 1 over the temperature in kelvin can be plotted and the gradient can then be used to determine the activation energy of the reaction using the Arrhenius equation, as shown in Equation 19.

Equation 18

$$k = A e^{-\frac{E_a}{RT}}$$

Eq. 19: Arrhenius Equation

The gradient of this graph will be equal to $-\frac{E_a}{R}$, which will allow the activation energy for the reaction to be determined. The graph below shows the gradient when the values of $\ln k$ and $1/T$ are plotted against each other.

As the data points were very varied, resulting in the values for the rate constant following no trend, it can be assumed that due to the low solubility of the fluoranthene in water, the values obtained at 5 degrees would be unreliable and the concentrations calculated not necessarily a fair reflection of the solution due to this solubility issue. The most reliable data points would be 15 degrees and 20 degrees, due to these both being in the region where ozone solubility would be at an acceptable threshold, whilst the contaminant would also be soluble enough in the solution. From this observation, a graph of $1/T$ in kelvin and $\ln(k)$ can be plotted from the Arrhenius equation. From this graph, the activation energy for the oxidation of fluoranthene via ozonation can be determined.

This gradient of this relationship can then be used to calculate the activation energy of the reaction using the Arrhenius equation (Equation 17). The activation energy of this reaction is calculated to be 12 kJ (Laidler, 1984). This would be beneficial within the wastewater treatment industry as an energy source would not be required to stimulate the reaction which would reduce the costs of treatment.

5.1.8 - Effect of tert-butanol

The effect of tert-butanol in the solution was investigated to observe the effects that a radical scavenger has on the ozonation and therefore degradation of FLT within the solution.

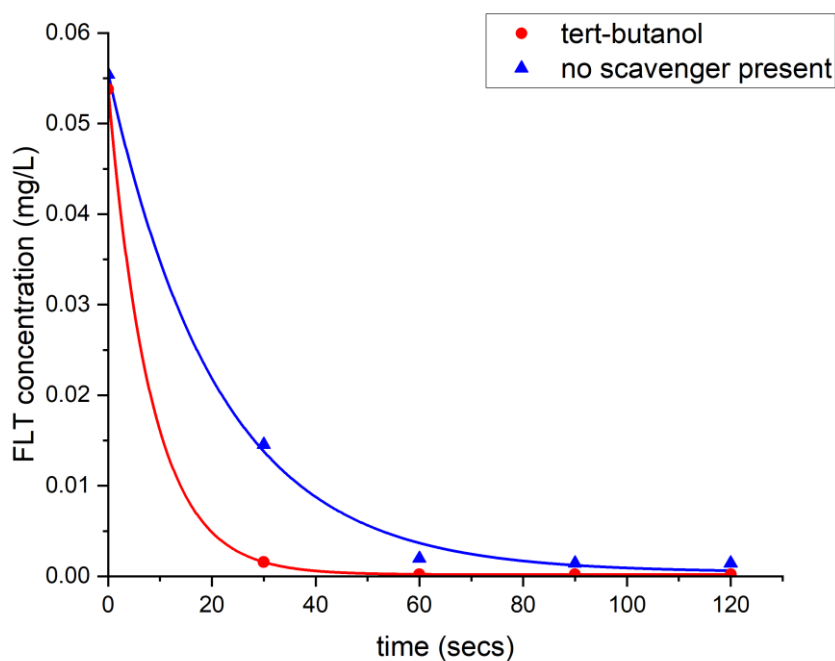


Figure 29: Effect of tert-butanol on FLT degradation (ozone gas concentration = 20 g/m³ NTP, temp = ~ 20 °C, oxygen flow rate = 0.5 L/min, pH = 6)

The reaction with tert-butanol within the solution was conducted under the same conditions as previously used, to allow a comparison to be made between the addition of a scavenger and no additive into the solution. As stated previously, the presence of the scavenger in solution means that the number of hydroxyl radicals in solution resulting from the ozone decomposition decreases.

Due to the structure of FLT, oxidation is more likely to occur effectively via molecular ozonation, therefore, by having a scavenger in solution to decrease the amount of hydroxyl radicals and increase the amount of molecular ozone in solution, the reaction should be more effective. From looking at the graph in Figure 29, it can be seen that this was true. When tert-butanol was added into solution, the rate of FLT degradation was increased, shown by the steeper gradient of the line within the first 20 seconds. This supports the fact that FLT degradation would be more efficient via molecular ozonation than with hydroxyl radicals and suggests that while oxidation of FLT does occur with a combination of hydroxyl radicals and ozone molecules, it is a more efficient method when hydroxyl radicals are taken out of the equation. Tert-butanol also has an effect on the size of the bubbles of ozone that diffused into solution. This could have an effect on the reaction kinetics as the smaller bubbles can increase the mass transfer of ozone into the solution (Tizaoui et al., 2009). This would then increase the rate of reaction and therefore, the degradation rate of FLT in solution.

5.1.9 - Stoichiometric Effects

The stoichiometric relationship between ozone and FLT was investigated with a standard concentration solution of ozonated water and this being reacted at different volumes with a standard concentration solution of FLT. The relationship can be seen in Figure 30. The graph represents the change in volume of the ozonated water used, in comparison to the ratio of the change in moles of ozone before and after the reaction, as well as the change in moles of the FLT before and after the reaction.

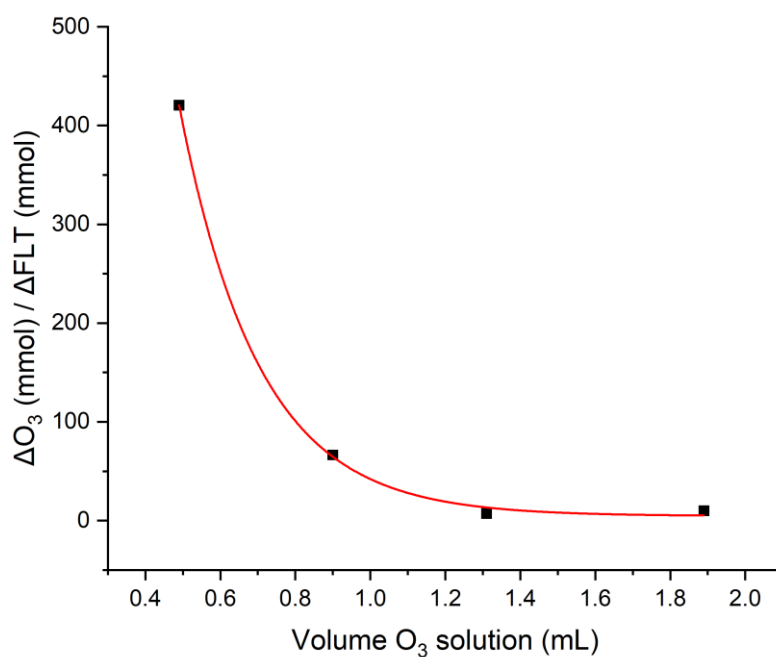


Figure 30: Relationship between the volume of ozonated water used in the reaction and the ratio of change of moles of ozone throughout the reaction and change of moles of FLT throughout the reaction

The graph in Figure 30 shows an exponential relationship between volume of ozonated water and the stoichiometric ratio, which proves that there is a point within the reaction where the amount of ozone does not alter the stoichiometric relationship, and this causes the plot to plateau. This suggests that the optimum stoichiometric ratio for FLT and ozone has a ratio of around 7 mmol at a volume of 1.3 mL of ozonated water at a concentration of ~ 4 mg/L.

5.1.10 - Summary of findings

To conclude this section of findings for the analysis of the reaction conditions, the following results and conditions were found to be most favourable for the increased rate of degradation of FLT by ozone.

- Ozone was found to degrade FLT within the solution.
- Oxygen did not cause the concentration of FLT within solution to decrease.
- A lower, more acidic pH was found to preferable for the degradation of FLT.
- A lower temperature was shown to have a faster rate of degradation, however there is the problem of solubility being decreased at a lower temperature.
- The addition of a radical scavenger into solution increased the rate of degradation of FLT.

5.2 - DEHP analysis

5.2.1 - UV-Vis Analysis

The solubility of di (2- ethyl hexyl) phthalate is very low, found to be 0.041 µg/L (Leyder & Boulanger, 1983) in water, but showing higher levels of solubility in organic solvents. When analysing a solution of DEHP in water with UV-Vis, no signal was obtained. This highlighted that the concentration of DEHP present within the solution was too low for appropriate analysis to be conducted. Due to the low solubility, the concentration in solution could not be increased to improve UV detection, therefore, an alternative method of analysis needed to be used.

5.2.2 - Fluorescence Analysis

As the analysis of DEHP with UV-Vis did not result in any clear peaks, another form of analysis to determine the presence of DEHP needed to be determined. The fluorescence of the compound was investigated to see if this could be an appropriate technique. Due to the low solubility of DEHP in water, a solution of a low concentration of DEHP in water was created and the fluorescence pairs analysed. The emission and excitation pairs were determined to be used in further analysis. For DEHP, the combination of emission and excitation wavelengths that had the highest peak values and therefore could be noted down for further analysis were found to be 285 nm and 466 nm, respectively.

This pair of wavelengths could then be incorporated into further analysis for determination of how the concentration varies over time with DEHP degradation. This was performed by solutions of 0.05 mg/L of DEHP in water being prepared and ozonated over time, with samples being taken at regular intervals to monitor the degradation of DEHP via ozonation. Through using this technique, an exponential decay could be seen for DEHP degradation once ozone was applied into the solution.

5.2.3 - HPLC Analysis

HPLC Analysis was performed following the method outlined in the methodology section.

5.2.3.1 - Calibration Curve

Samples of varying concentrations were prepared to allow a calibration curve to be created, equating peak area to concentration values. The original attempts of the calibration curve caused some issues, with higher concentrations of DEHP in the solutions causing contamination within the HPLC system and the column within it. The structure of DEHP meant that the arms of the compound could get stuck on the column, resulting in the concentration readings being too high or invalid. This was solved by using more dilutions of DEHP in solution, so the concentration of DEHP in the injections into the machine was lower. This resulted in more reliable results from the HPLC for use with the calibration curve, but also meant that the concentration range was adjusted for the experiments, meaning that reliable data was produced.

The calibration curve obtained can be seen below in Figure 31. This equates the peak areas obtained from the HPLC with the known concentration of DEHP contained within the samples injected. This can be used to equate the peak areas obtained from different experimentation samples to the real known concentrations, to allow proper analysis to be performed. For HPLC analysis, an isocratic solvent phase was used consisting of 85 % acetonitrile and 15 % water. To obtain high enough concentrations to complete the calibration curve, partial methanol solutions were prepared.

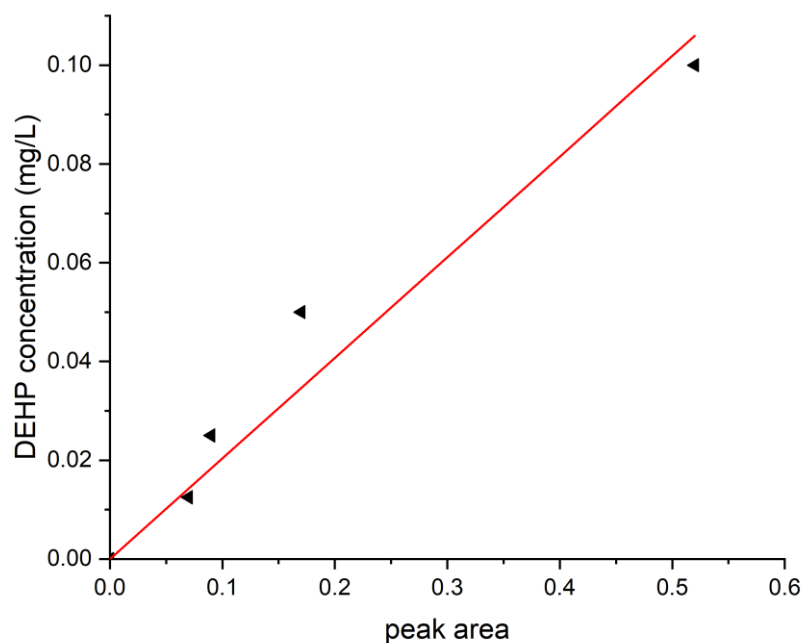


Figure 31: calibration curve for the first peak shown in the HPLC analysis for DEHP concentration

In the graph shown above in Figure 31, the calibration curve for the DEHP peak can be seen. From equating a line of best fit within the data points, an equation for the line to generate the DEHP concentration from peak area can be generated and then used for further calculations of the concentrations. The equation for this graph can be seen below in Equation 20.

Equation 19

$$y = 0.0485 x$$

Eq. 20: Equation for the calibration curve

5.2.4 - Oxygenation of DEHP

To confirm whether the addition of ozone into solution was actually the result of the decrease of concentration within the experiments, it first needed to be proven whether the concentration of DEHP was decreased solely from the addition of a gas flow into the solution. If the substance within the solution was particularly volatile, then the addition of a gas flow into the solution would result in the concentration of DEHP decreasing. Therefore, it could not be said that ozone provides degradation of this compound within solution.

When conducting this experiment, it was seen that there was no change in the concentration of DEHP in any of the samples taken over time, therefore, it can be said that merely by the flow of oxygen into the solution, the concentration of DEHP does not decrease. This proves that any data and results that are obtained from the ozonation experiments are only due to the process of removal or degradation of the compound by the addition of ozone and the subsequent oxidation that occurs.

5.2.5 - Ozonation of DEHP

The ozonation of DEHP was investigated and the conditions for the experimentation were determined. For DEHP, an ozone gas concentration of 20 g/m³ NTP was used, and samples were extracted every minute for four minutes of ozonation. The DEHP was shown to degrade under the presence of ozone, which would be expected due to the structure of DEHP having long hydrocarbon chains attached to the central benzene ring. This would make the benzene ring very susceptible to the oxidation of ozone and would be easily attacked within the solution.

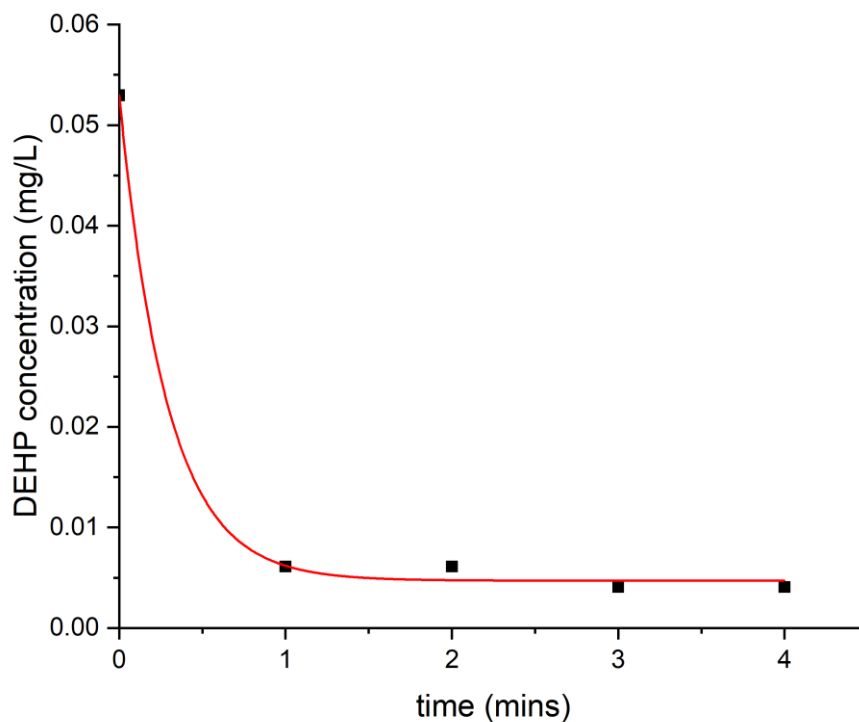


Figure 32: ozonation of DEHP (ozone gas concentration = $20 \text{ g/m}^3 \text{ NTP}$, temp = $\sim 20^\circ\text{C}$, oxygen flow rate = 0.5 L/min , pH = 6)

The optimum conditions for ozone concentration were taken forward for the rest of the experiments looking at the degradation of DEHP in solution via ozonation. The ozonation and degradation of DEHP occurred in a similar time frame to that of FLT which is at a fast rate of reaction, which would be beneficial within industry.

5.2.6 - Effect of pH

The effect of pH was investigated by spiking solutions of DEHP to certain pH levels. The reactions were then carried out as stated previously, with an ozone concentration of $20 \text{ g/m}^3 \text{ NTP}$ and the change in concentration of DEHP monitored over 4 minutes.

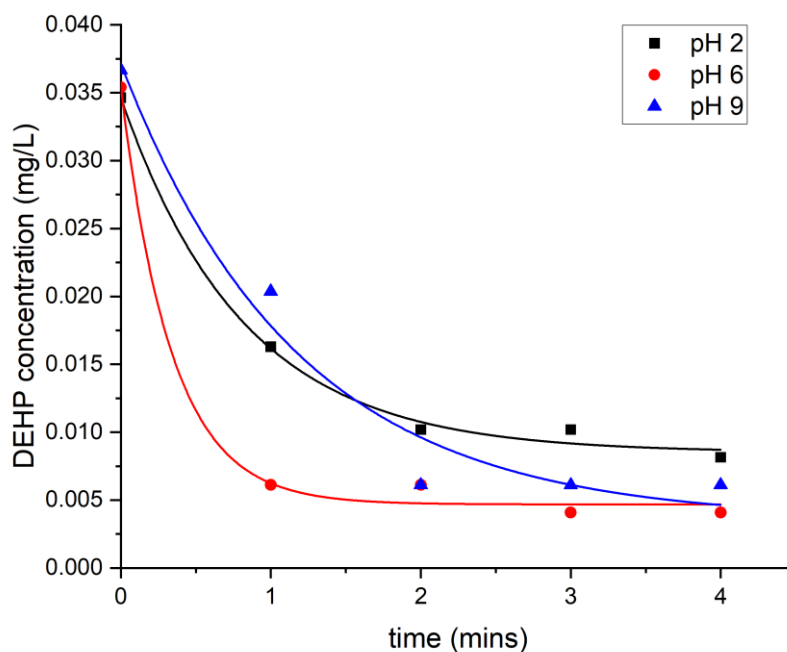


Figure 33: effect of pH (ozone gas concentration = 20 g/m³ NTP, temp = ~ 20 oC, oxygen flow rate = 0.5 L/min)

The graph above in Figure 33 shows the effect that the change in pH had on the degradation of DEHP by ozonation. The pH was altered by spiking the solution of DI water and DEHP with hydrochloric acid and sodium hydroxide until the pH was recorded as pH 2, pH 6 and pH 9, respectively. The pH was measured with a pH probe in the solution until the pH stabilised at the desired pH for the experiment. The experiments were all performed at room temperature (20 °C), with an ozone gas concentration of 20 g/m³ NTP and a pure oxygen flow rate of 0.5 L/min.

When looking at the graph shown above in Figure 33, no clear trend about the effect of pH can be seen. pH 6 is shown as the most favourable pH of the solution to maximise the degradation of DEHP in solution.

When looking at the effect of pH on chemical degradation, the most effective pH to maximise the degradation will depend on the reaction mechanism that occurs in the solution. With a lower pH the mechanism would be more likely to proceed via a molecular ozone mechanism for oxidation, whereas, with a higher pH, the degradation is more likely to occur via the generation and presence of hydroxyl radicals within the solution. As pH 6 is shown as the most favourable pH for the rate of degradation by a significant margin, there could be no clear mechanism of oxidation that occurs within the solution, and instead a combination of both molecular ozone and the generation of radicals is preferable. When looking at the chemical structure of DEHP this could be explained with the oxidation of the benzene ring being more likely to occur via the oxidation of molecular ozone. Whereas, when looking at the long chain hydrocarbon arms on the benzene ring, these may be more likely to be degraded with hydroxyl radicals, due to how easy they are to attack. The pH of the solution will affect the structure of the DEHP compound, meaning that pH will result in the molecules not all having the same molecular configuration. This would explain why trends were not easily identifiable within the pH analysis.

From looking at the graph, the degradation rates of pH 2 and pH 9 are very similar, this could again be due to the fact that neither mechanism is greatly favourable to the degradation of DEHP. Therefore, at a lower pH only certain aspects of the molecule are being degraded and vice versa at a higher pH.

The pKa value of DEHP is found in literature to be around ~ 6.7 (The-Metabolomics-Innovation-Centre). This pKa value would suggest that the compound would readily dissociate. Below the pKa value of 6.7 it would be protonated at the oxygen, whereas above this value of 6.7, there would not be protonation at the oxygen.

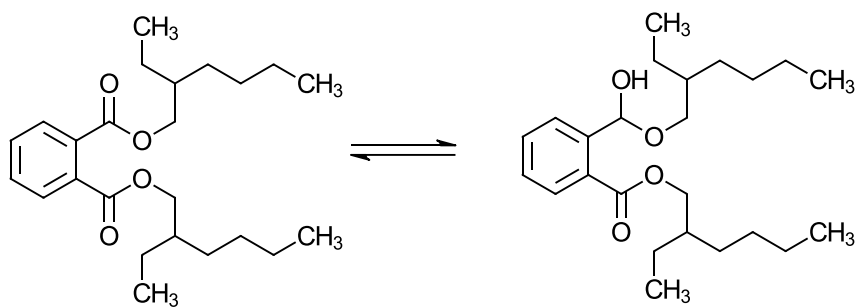


Figure 34: Protonation of DEHP molecule

5.2.7 - Effect of temperature

Temperature effects on the degradation of DEHP were investigated.

The graph to compare the degradation rates of DEHP, can be seen below in Figure 35. However, when looking for trends within the graph, there is no clear trend visible.

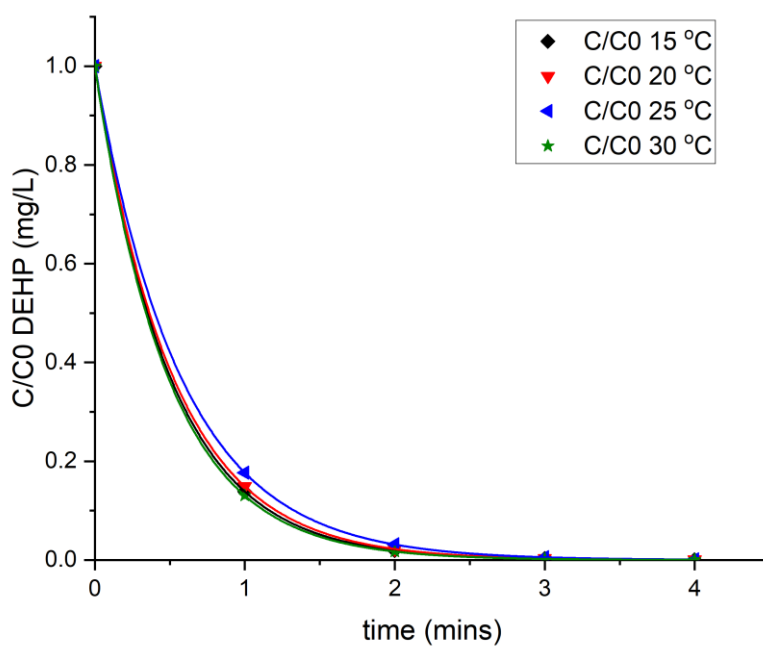


Figure 35: effect of temperature on DEHP degradation (ozone gas concentration = 20 g/m³ NTP, pH = 6, oxygen flow rate = 0.5 L/min)

There is a little difference in the degradation rates when comparing the rate at 25 °C and other temperatures. This could be expected because at a higher temperature the rate of reaction would be faster, and the ozone solubility would be better at the lower temperatures. The rate constants can be obtained from looking at the data points, and if the rate would conform to a first order reaction system. The rate constants can be seen highlighted below in Table 17. There is not much variation in the rate constants obtained from this temperature analysis, this could be due to the small variation in temperature values used. There is a slight increase in the rate constant for 30 degrees which supports that the rate of reaction increases as the temperature increases.

Table 17: rate constants calculated for the different temperatures used to investigate the degradation of DEHP

Temperature (°C)	Rate constant, k (min ⁻¹)
15	1.98
20	1.90
25	1.73
30	2.04

The rate constants can then be used to calculate the activation energy of the reaction system and determine the effectiveness of ozone to oxidise the DEHP contaminant within the water. These rate constants can be plotted as the natural log of the values against the inverse of the temperature values in Kelvin. The gradient of the line would then be equal to the activation energy divided by the gas constant.

The gradient can be calculated, which was found to be 1129.2. From this, the activation energy of the reaction is calculated to be 9 kJ. This suggests that although the reaction would occur naturally when ozone is applied into the solution, energy supplied into the solution would assist in the speed of the reaction, hence increasing the effectiveness of the ozonation on the oxidation of DEHP.

5.2.8 - Effect of scavengers

The effect of a hydroxyl scavenger within solution on the degradation of DEHP can be seen in the graph below in Figure 36. A concentration of 100 mM of tert-butanol was added into the solution, that was kept at 20 °C, a pure oxygen flow rate of 0.5 L/min and an ozone gas concentration of 20 g/m³ NTP was used. Samples were taken at the same time intervals as before (one sample taken every minute, for 4 minutes) to analyse the effect of a scavenger on the degradation of DEHP. The data obtained from the tert-butanol effect experiment was then combined with the data from the ozonation of DEHP with the same conditions, but without tert-butanol, to understand the effect of a scavenger on the degradation.

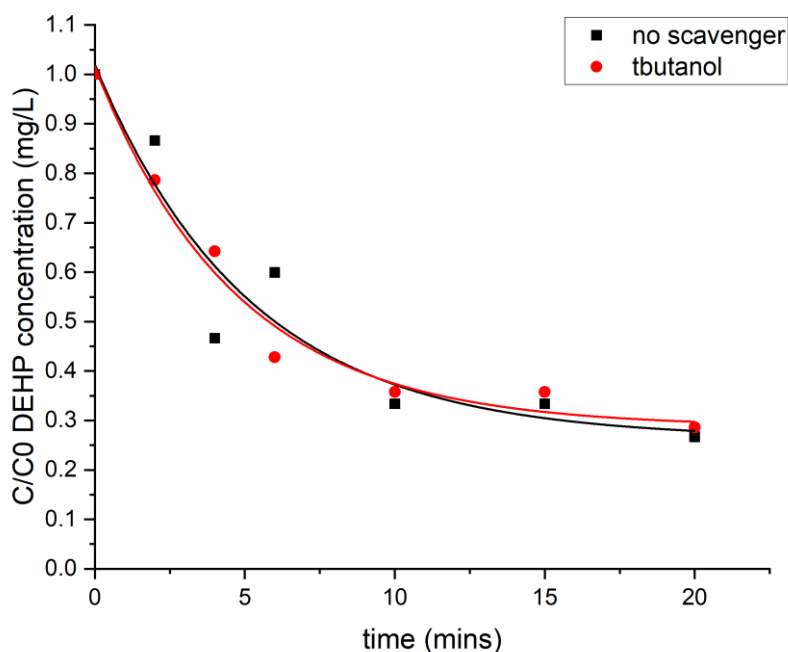


Figure 36: effect of the presence of a radical scavenger (ozone gas concentration = 20 g/m³ NTP, temp = ~ 20 °C, oxygen flow rate = 0.5 L/min, pH = 6)

The graph above in Figure 36 shows the effect of adding a radical scavenger into the reaction mixture. Tert-butanol was chosen to be the radical scavenger. From looking at the trends in the graph, the addition of a scavenger does not affect the rate of degradation of DEHP in solution. This again supports the discussion that the whole molecule is not oxidised by a singular oxidation mechanism. The removal of the hydroxyl radicals has little effect on the rate of degradation, which could mean that when there are no radicals, the oxidation occurs via molecular ozonation. However, when the radicals are present in the solution, it is no more favourable, so the addition of a radical scavenger into solution does not seem to hinder or enhance the degradation process.

5.2.9 - Stoichiometric Analysis

The stoichiometric analysis of the relationship between DEHP and ozone was investigated. For this experimentation, a standard solution of ozonated water was prepared, and different volumes of solutions were mixed as outlined in the methodology.

For the analytical representation of the data, the volume of ozonated water added to the solution was plotted against a relationship. The relationship compared the change in moles of ozone both before and after the reaction, to a change in the number of moles of DEHP, measured both before and after the reaction. The results can be seen plotted on the graph below in Figure 37.

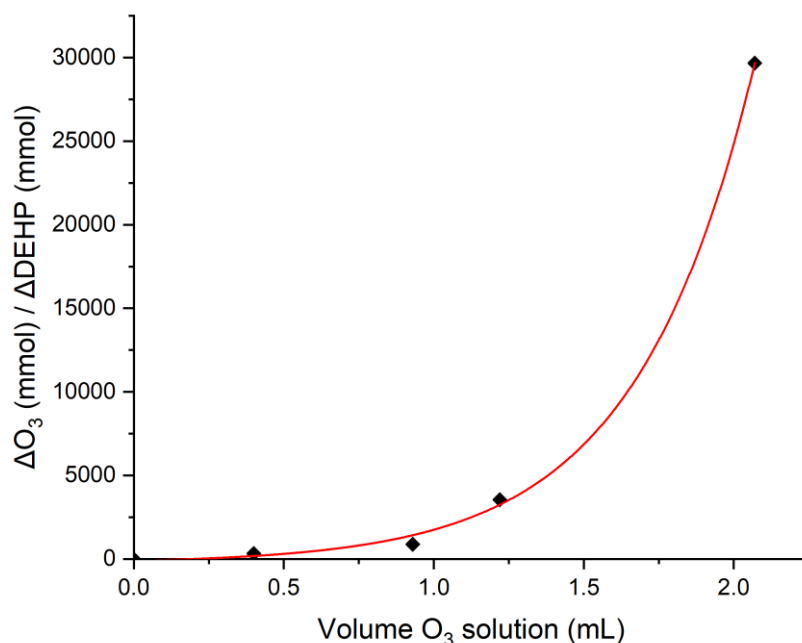


Figure 37: stoichiometric relationship between DEHP concentration and ozone concentration

The graph in Figure 37 shows the relationship obtained. From this, the stoichiometric relationship can be determined. The y axis shows the ratio between the change on moles of ozone throughout the reaction compared to the change in moles of DEHP. Throughout the reaction, the amount of moles of both ozone and DHEP decrease, due to the ozone reacting with the DEHP to oxidise it to other molecules and the ozone concentration decreasing as it is oxidising the molecules in the solution or being decomposed into hydroxyl radicals.

From this analysis, an observation can be made regarding the best volume of ozone required to reduce the relationship of DEHP and ozone to a suitable level for the experimentation.

Through analysing the data, a specific ratio for DEHP can be determined, and this relationship will change depending on the chemical of interest being oxidised from ozone. The large ratio found here suggests that a large volume of ozone is required to fully oxidise the DEHP in comparison to FLT. This implies that the DEHP molecule was harder to oxidise, which follows the other results highlighted in this section.

5.2.10 - Summary of findings

In summary, ozone can be used to oxidise DEHP in solution and reduce the concentration of the contaminants in the solution. The conditions that were found to be preferable in speeding up the reaction process can be seen highlighted below.

- Ozone was able to degrade DEHP effectively to minimal concentrations within the solution.
- When the solution was oxygenated, there was no degradation of DEHP, highlighting that the degradation was in fact due to ozonation.
- pH 6 was preferable for the degradation of DEHP.
- A temperature of 15°C / 20°C would be preferable to maximise the ozone solubility in the solution, enhancing the availability of ozone for oxidation.
- Scavengers did neither increase the reaction scheme nor decrease the reaction scheme.

5.3 - CYM Analysis

5.3.1 - UV-Vis Analysis

The solubility of cypermethrin is very low in water, at 0.01 mg/L, (Abramovitch et al., 1996). To determine the best process to analyse the change in concentration of CYM, UV-Vis analysis was tested on a solution of CYM in water to identify if the UV Vis spectrum is easily obtained and whether CYM is actually visible on the UV-Vis spectrum. The CYM was observed on the UV-Vis spectrum as shown in Figure 38 below, this meant that a peak could be seen at 214 nm and 220 nm, which allowed these peak wavelength values to be used for further analysis of the concentration of CYM in solutions of water.

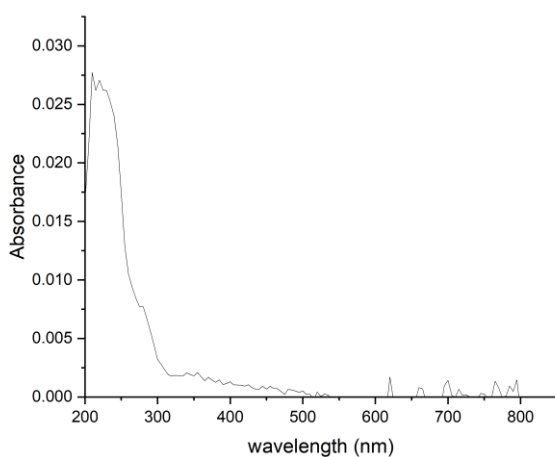


Figure 38: UV-Vis spectrum

5.3.2 - Fluorescence Analysis

The fluorescence of CYM was also investigated to see if this provided clearer results than the UV-Vis for analysis of CYM in solutions of water. Again, due to the low solubility of CYM in water solutions, a solution of low concentration was prepared and then used for analysis in the fluorimeter. The emission and excitation pairs were analysed. However, in this case the pairs were not very clear and therefore it was determined that CYM was not a very fluorescent compound, and that future analysis for the concentration would be determined using DAD and the UV-Vis peaks that had been seen.

5.3.3 - HPLC Analysis

HPLC Analysis was performed with the method outlined in the methodology section.

5.3.3.1 - Calibration Curve

To allow a comparison to be made between the peak areas given by the DAD and the HPLC and the concentration of the CYM in the solution, a calibration curve needed to be constructed. The calibration curve was constructed by samples being made of a specific known concentration of CYM in water and running these samples through the HPLC to give the corresponding peak area. As the concentration of CYM was known, a graph could be plotted comparing the concentration of CYM in solution and the peak area given by the DAD analysis. The graph can be seen below in Figure 39. To allow the solutions to be prepared at concentrations suitable to construct a calibration curve, the solutions were prepared in partial methanol solutions.

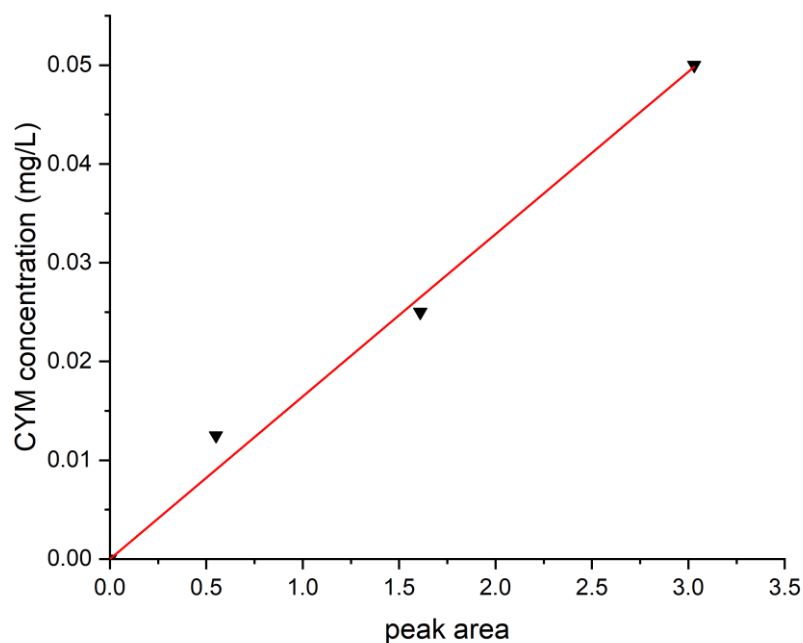


Figure 39: calibration curve for the HPLC analysis of CYM

From looking at the calibration curve, a line of best fit can be plotted and then an equation of this line can be determined. This gives the equation to be used to equate the peak area given from the HPLC analysis to equate it to the concentration of CYM in that solution. This was necessary to observe the degradation of CYM in solution and to be able to determine the limits there were within the reaction system, also allowing it to be determined if the use of ozonation provided appropriate levels of degradation of the contaminant.

The equation for the graph can be seen below in Equation 21, which was then used throughout the rest of the analysis.

Equation 20

$$y = 0.0164 x$$

Eq. 21: equation determined from the calibration curve

5.3.4 - Oxygenation of CYM

When analysing the effect of ozonation on the degradation of CYM in solution, it is important to determine if the degradation and decrease in the concentration of CYM was definitely from the addition of ozone into the solution and not just from the addition of a gas bubbling into the solution, which would result in the contaminant in the water being extremely volatile and being displaced from the solution due to this.

To determine this, pure oxygen was bubbled into the solution and samples taken over time. These samples were then analysed for the concentration of CYM in the samples and the concentration compared. Following this, it could be seen that the addition of oxygen into the solution had no effect on the concentration of CYM and therefore, all conclusions drawn from the further analysis can be confidently due to the effect of ozone within the solutions and not because of the mere addition of a gas into the solution.

5.3.5 - Ozonation of CYM

The ozonation of CYM was investigated to identify if it was an appropriate method for the degradation for CYM in solution and whether ozone did in fact have any oxidative potential for the oxidation of CYM. An ozone gas concentration of 20 g/m³ NTP was used and a temperature of 20 °C. Also, a pure oxygen gas flow rate of 0.5 L/min was used with a solution of pH 6. Samples were taken at regular intervals over 10 minutes throughout the experiment and once the samples had been extracted, oxygen was bubbled into the samples to remove the ozone from the solution. This ensured the ozonation reaction had stopped. This would otherwise have affected the trends seen, as ozone could have continued to degrade the samples once they had been extracted.

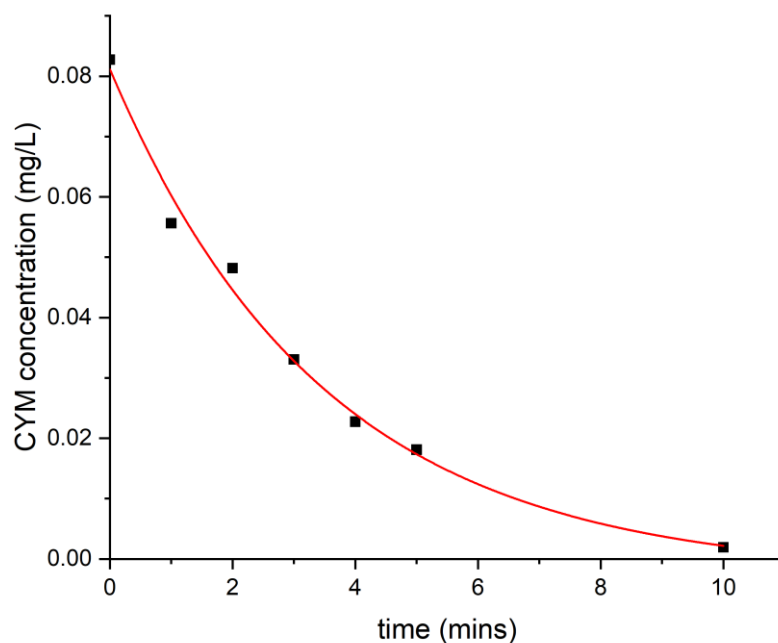


Figure 40: ozonation of CYM (ozone gas concentration = $20 \text{ g/m}^3 \text{ NTP}$, temp = $\sim 20 \text{ }^\circ\text{C}$, oxygen flow rate = 0.5 L/min , pH = 6)

From looking at the graph in Figure 40, it can be seen that ozonation did in fact cause the degradation of CYM in solution, and therefore further analysis will be performed to find the optimum conditions for the most efficient rate of degradation of CYM in solution. The ozone gas concentration of $20 \text{ g/m}^3 \text{ NTP}$ provided sufficient degradation of CYM in water over 10 minutes, providing concentrations within solutions that were easy to monitor throughout the process of the reaction.

5.3.6 - Effect of pH

The effect of pH was investigated.

As the concentration of the CYM samples were analysed with DAD, once the solutions had been spiked to alter the pH, there was no longer a signal for the concentration of CYM in solution. Therefore, the effects of pH could not be analysed appropriately to give any results.

When looking in literature at the dissociation of cypermethrin at different pH levels, it can be found that there is no dissociation of this compound in different pH solutions (Database, 2023). This would mean that no pH level would have a clear increase on the degradation rate of cypermethrin. Therefore, a neutral pH of pH 6 / 7 would be preferable for this reaction, as the pH would have no effect on the degradation rate of cypermethrin and due to this a neutral solution would not provide any adverse effects to the environment, especially when looking at the treatment of wastewater. A study has shown degradation of CYM in solution at pH 9, however, the degradation took 30 minutes which is longer than the degradation speed found previously. (Wu, 2007)

5.3.7 - Effect of temperature

The effect of temperature on the degradation of CYM was monitored at four temperatures: 15 °C, 20 °C, 25 °C, and 30 °C. Samples were taken at regular time intervals and concentrations were calculated from the peak areas from the HPLC.

The graph below in Figure 41 shows the gradients and relationship with the degradation of CYM by ozonation in solution.

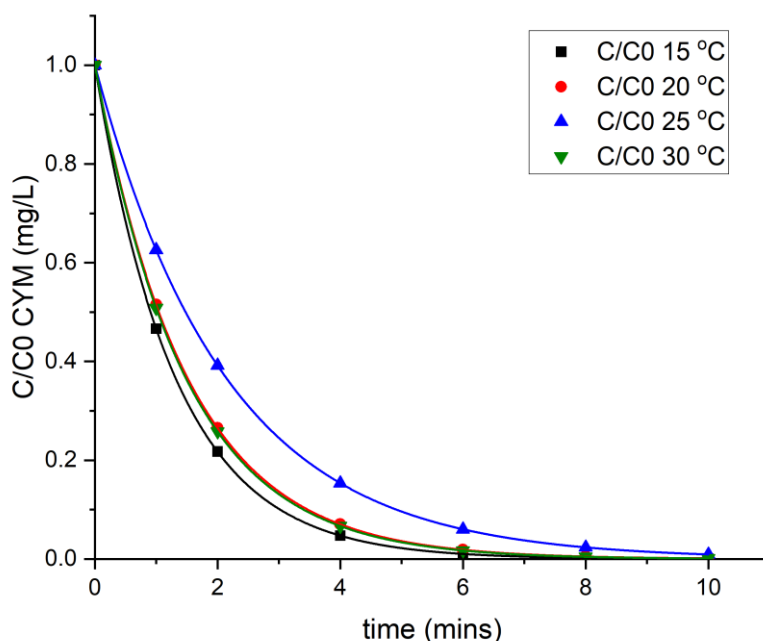


Figure 41: degradation of CYM by ozonation at different temperatures (ozone gas concentration = 20 g/m^3 NTP, oxygen flow rate = 0.5 L/min , $\text{pH} = 6$)

From looking at the trends appearing on the graph above in Figure 41, a trend can be seen where the most preferable temperature was found to be $15 \text{ }^\circ\text{C}$. This would be expected as the ozone solubility in water is increased at lower temperatures, and the more ozone absorbed within the solution, which would then increase the ozone present within the solution to ozonate the CYM (Molina & Molina, 1986). A similar trend can be seen with the highest temperature, with this also being a favourable temperature, which could be due to the higher rate of reaction associated with more energy being within the reaction. The temperature experiment conducted at $25 \text{ }^\circ\text{C}$ was the least effective due to the ozone solubility being decreased and the increase in temperature not providing enough energy to succumb this effect. It would be important to find a temperature where the ozone solubility is increased while the solubility of the chemical contaminant is not disrupted which would be detrimental to the experiment. Therefore, temperatures below $15 \text{ }^\circ\text{C}$ were considered but not experimented, as although the ozone solubility would be increased, the solubility of the chemical contaminant would be decreased. Therefore, an accurate determination of the degradation would not be effective.

From the data obtained, the rate constants can be determined for each temperature, these are highlighted below in Table 18.

Table 18: rate constants determined from the different temperatures used to affect the rate of degradation

Temperature (°C)	Rate constant, k (min ⁻¹)
15	0.763
20	0.663
25	0.468
30	0.219

The rate constants can be plotted against temperature to determine the activation energy of the reaction system. Values of the natural log of k were plotted against the inverse of the temperature in kelvin..

The gradient of the relationship was determined and used to calculate the activation energy of the reaction system. The activation energy can then be calculated from the graph, and these values can be used to work out whether an additional input of energy into the reaction would enhance the reaction process. For CYM it was found that, while energy was not required for the ozonation of CYM it would enhance the overall reaction scheme.

5.3.8 - Effect of scavengers

Samples were taken at the same time intervals as before to analyse the effect of a scavenger on the degradation of CYM in solution. This data was then compared to the reaction performed in the exact same reaction conditions, but with no radical scavenger present, to determine whether the presence of a radical scavenger was more favourable for the rate of degradation or not.

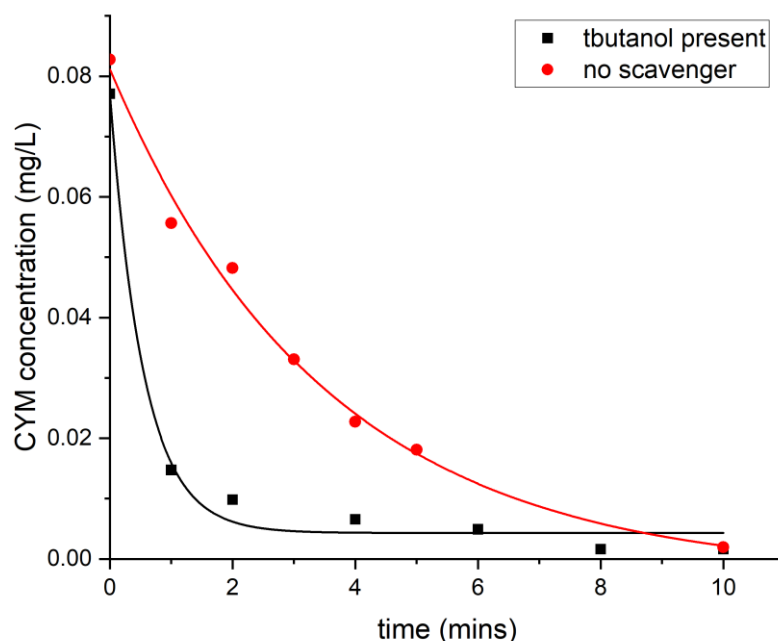


Figure 42: ozonation of CYM comparing the reaction with the presence of tert-butanol as a radical scavenger and with no scavenger present (ozone gas concentration = $20 \text{ g/m}^3 \text{ NTP}$, temp = $\sim 20 \text{ }^\circ\text{C}$, oxygen flow rate = 0.5 L/min , pH = 6)

From looking at the graph above in Figure 42, it can be seen that when a radical scavenger, in this case tert-butanol, was added to the solution a more favourable rate of CYM degradation occurred. This is seen through the much steeper rate of degradation once the radical scavenger was added. Through analysing this outcome, it could be said that the oxidation of CYM occurs mainly via a molecular ozone mechanism, as opposed to with the presence of radical scavengers. This could be because once the scavengers are removed from the reaction mix, the degradation speeds up rapidly. It may also be due to the fact that the addition of tert-butanol also affects the size of the bubbles being diffused into the reaction system from the diffuser, making them smaller.

The bubble size being decreased could have positive effects on the rate of degradation, as the smaller bubbles could result in a faster rate of mass transfer of the ozone in the gas phase into the liquid phase. Therefore, increasing the concentration of ozone within the liquid phase and increasing the rate of degradation of CYM in the solution.

5.3.9 - Stoichiometric Analysis

The stoichiometric analysis for the relationship between ozone and CYM was investigated. Different volumes of a standard solution of ozonated water were reacted with CYM and indigo solution to determine the decrease in concentration of ozone and CYM throughout the process of the reaction.

The graph in Figure 43 shows the relationship between the volume of ozonated water used within the reaction and the ratio of the change in moles of ozone throughout the experiment and the change in moles of CYM throughout the experiment.

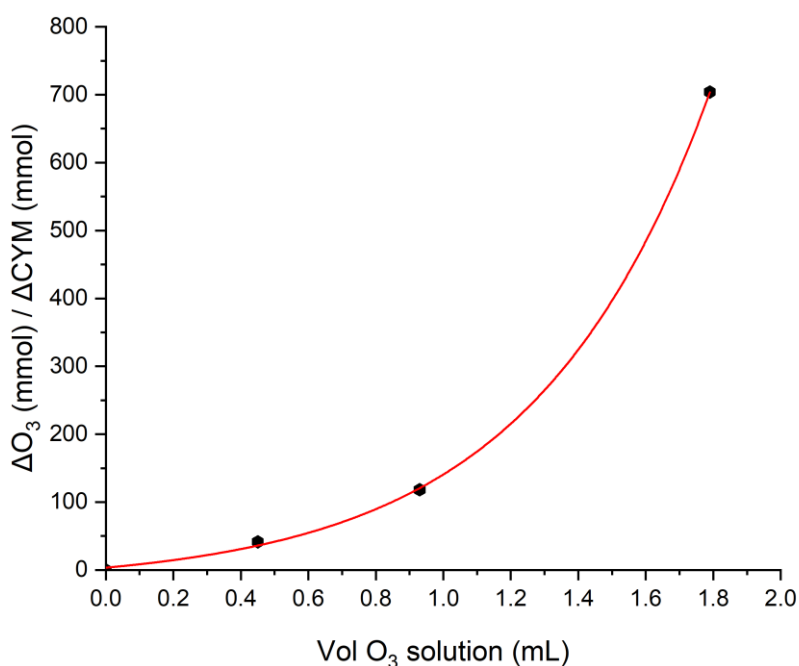


Figure 43: Relationship between the volume of ozonated water used within the reaction and the ratio of change of moles of ozone throughout the reaction compared to the change in moles of CYM throughout the reaction

The graph in Figure 43 shows the relationship obtained from this comparison. From this, the stoichiometric relationship can be determined. The y axis shows the ratio between the change on moles of ozone throughout the reaction compared to the change in moles of CYM. Throughout the reaction, the number of moles of both ozone and CYM decrease linearly.

5.3.10 - Summary of findings

To summarise, cypermethrin was found to degrade in solution with ozonation. The conclusions on the variables can be seen highlighted below.

- Cypermethrin was found to degrade with ozonation within 10 minutes.
- When the solution was oxygenated, there was no decrease in the CYM concentration, concluding the degradation was due to the presence of ozone.
- Temperatures at 15 °C and 30 °C were preferable, one would increase the ozone solubility and the higher temperature would increase the rate constant.
- When scavengers were added into the solution, the degradation of CYM increased.

5.4 - Combined Ozonation

While the effects of ozonation on the degradation of the chemical contaminants were investigated in solutions singularly in water, a combination of the contaminants were also investigated to determine whether the interactions between the chemicals had an effect on the rates of degradation and the behaviour of the ozone within the solution.

The degradation rates of the chemicals were monitored simultaneously, with one sample being analysed for all three contaminants. The data is shown below in Figure 44.

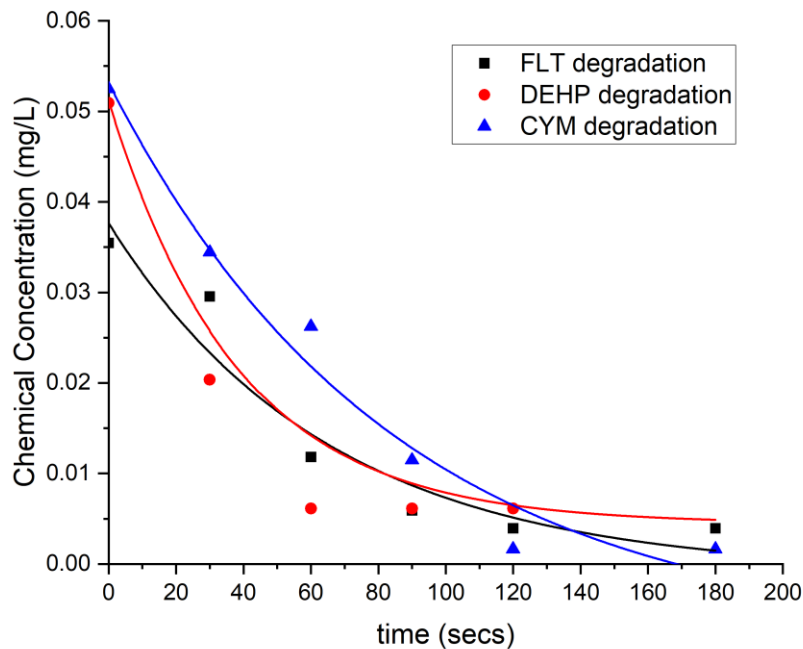


Figure 44: ozonation degradation rates of all contaminants when ozonated in a solution of DI water containing all three contaminants (ozone concentration = 20 g/m³ NTP, oxygen flow rate = 0.5 L/min, pH = 6, temperature = 20 oC)

The trends were slightly different when the contaminants were combined, which could be due to interactions within the chemicals, or due to ozone having a higher preferential interaction to different chemicals.

All the chemical contaminants degraded to a safe rate within three minutes.

When looking at the FLT degradation and comparing this to the data obtained previously, the reaction rate was significantly slower. Before, the FLT was reduced to negligible concentrations within a minute, whereas, when combined with the other contaminants this was extended to 3 minutes to reach the same levels. This could show that FLT does not compete as favourably as both DEHP and CYM in the combined solution for the ozone and hydroxyl radicals generated.

With DEHP, the reaction scheme was sped up significantly, with the DEHP concentration reaching minimal levels within 1 minute, whereas previously the reaction needed to be extended to 8 minutes to reach low levels. This could show that when competing in the solution, the DEHP was more preferable for the ozone to oxidise than the fluoranthene. It could also suggest that the hydroxyl radicals worked quicker to degrade the DEHP in the solution. When looking at the effects of scavengers previously, they were found to increase the rate of degradation of both fluoranthene and cypermethrin but had no impact on the degradation of DEHP. This could show that the hydroxyl radicals would degrade the DEHP in the solution efficiently, which would not happen to the other two contaminants. This could explain why DEHP degradation occurs quicker than the degradation of FLT and CYM in a combined solution.

The speed of degradation of CYM was also increased in this reaction mixture than when it was when investigated singularly, with the degradation occurring with 2 minutes, in comparison to the 10 minutes previously required. As the reaction was shown to previously increase speed upon the addition of scavengers, the relationship found here could suggest that FLT was acting as a scavenger in the solution, increasing the reaction rate for the oxidation of CYM. The solubility of the molecules in the solution could alter once they are combined in solution.

5.5 - Ozonation Summary

To summarise the investigations into the effect of ozonating the chemical contaminants in water, it can be seen that ozone works to effectively degrade the contaminants in the solution. This was investigated in solutions of DI water with individual contaminants, which were effective in the degradation rates. This was also investigated in DI water containing a combination of contaminants, while the degradation rates alter slightly with the interactions between the chemicals, degradation of all contaminants: fluoranthene, di (2- ethyl hexyl) phthalate and cypermethrin all degrade within three minutes.

Chapter 6 - Adsorption onto Activated Carbon

The adsorption of the chemical contaminants onto the surface of granulated activated carbon (GAC) were investigated. The kinetics were first determined to evaluate the time frame of the isotherm before the specific isotherms were investigated using different masses of carbon.

6.1 - FLT Adsorption

Different masses of GAC were used to investigate the adsorption of FLT onto GAC. Increasing the mass of GAC increases the availability of the surface area for adsorption of the chemical contaminants. The graph shown below in Figure 45 shows the decrease in concentration of FLT when different masses of GAC are used.

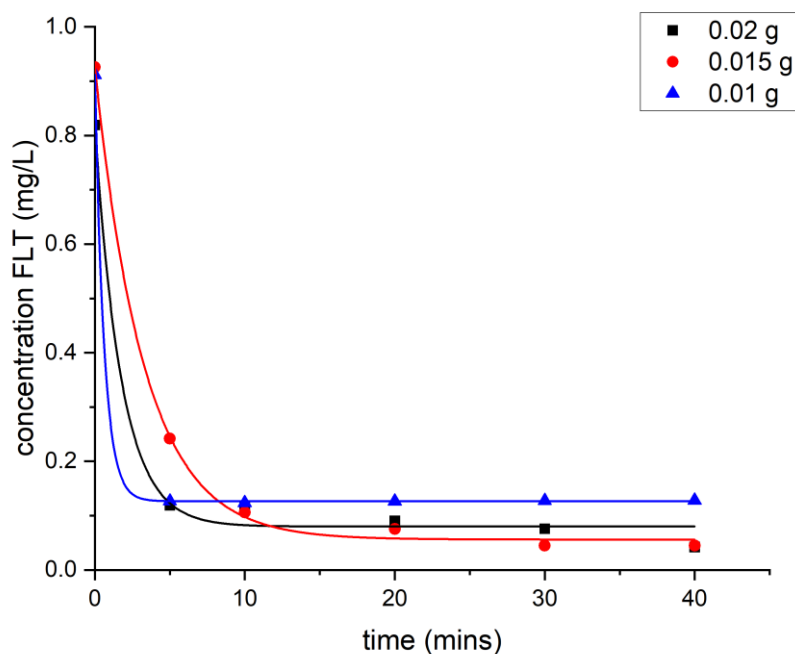


Figure 45: effect of different masses of GAC on adsorption of FLT onto the surface of GAC

In Figure 45 above, the decrease in concentration of FLT when varying masses are used can be seen. When 0.01 g of GAC are used in the solution, the end concentration is higher than that of when 0.015 g and 0.02 g are used. As the resultant concentration range is minimal, they would most likely all be within the error range. This suggests that the change in masses of GAC used were not effective enough to alter the surface area available or the adsorption of CYM.

The lower mass of GAC would be expected to have the highest end concentration due to the surface of the carbon becoming 'full' from the adsorption of FLT onto the surface. Therefore, it would not be possible for any more of the contaminant to be adsorbed onto the surface. This is because an equilibrium has been reached, where no more contaminants can leave the solution, causing the concentration to be maintained.

When comparing the rate of concentration decrease for 0.015 g and 0.02 g, it can be seen that there is a faster rate of concentration decrease with 0.02 g which would be expected due to the increased surface area of GAC available in the solution.

The q values can also be plotted against time. q is calculated from the equation shown in Equation 22.

Equation 21

$$q = V \times 0.001 \times \frac{(C_0 - C)}{mGAC}$$

Eq. 22: equation to calculate the value of q .

Where:

q is the adsorption capacity (mg/g),

V is the volume (L),

C_0 is the initial concentration (mg/L),

C is the final concentration (mg/L) and

$mGAC$ is the mass of GAC used (g).

The graph below in Figure 46 shows the relationship between q and time for the adsorption of FLT onto the surface of GAC at different GAC masses.

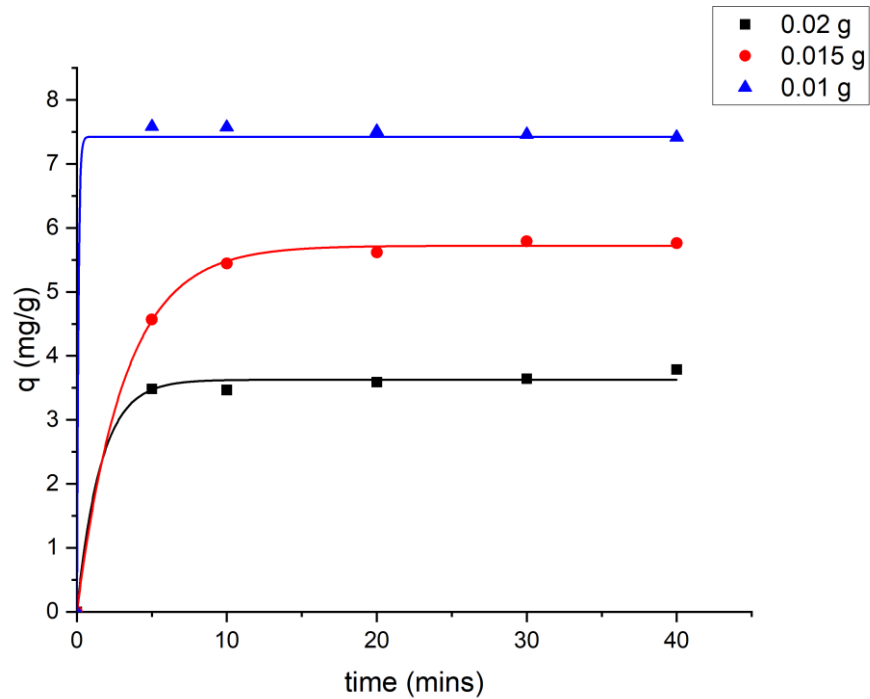


Figure 46: plot of Q against time for the adsorption of FLT onto GAC ($T = 20\text{ }^{\circ}\text{C}$)

As the calculation of q incorporates the mass of GAC used, a clear difference can be seen in the values for q on the graph. This makes it clear to see the equilibrium point reached within the solution and the time in which this happens.

The kinetics of the adsorption can be assumed to be first order and the rate constant can be calculated using Equation 23.

Equation 22

$$\ln(q_e - q_t) = \ln(q_e) - K_1 t \quad \text{Eq. 23: kinetics equation assuming 1st order reaction.}$$

Where:

q_e is the adsorption capacity at equilibrium (mg/g),

q_t is the adsorption capacity at a specific time (mg/g),

K_1 is the rate constant (min^{-1}) and

t is the time (mins)

From the kinetics equation shown in Equation 23, a graph can be plotted of $\ln(q_e - q_t)$ against time and the gradient will be equal to the rate constant. Rate constants were calculated for all three masses of GAC used and the results can be seen below in Table 19.

Table 19: values for the rate constant calculated for each mass of GAC

Mass of GAC (g)	Rate constant (min^{-1})	error	q max (mg/g)	error
0.02	0.25	22 %	4.18	0.66 %
0.015	0.24	16 %	5.77	0.19 %
0.01	0.25	23 %	7.41	0.26 %

The results obtained in this study agree with other studies conducted on the adsorption of FLT on GAC. For example, (Liu et al., 2014) reported first order rate constants for the adsorption of FLT on GAC in the range of 0.14 and 0.30 min^{-1} . As shown in Table 19, the rate constants obtained in this study fall within the range reported by (Liu et al., 2014).

6.2 - CYM Adsorption

Different masses of GAC were investigated in solutions of CYM to determine the adsorption relationship onto the surface of GAC. The graph below in Figure 47 shows the relationship between the concentration and time with the differing masses of GAC in solution.

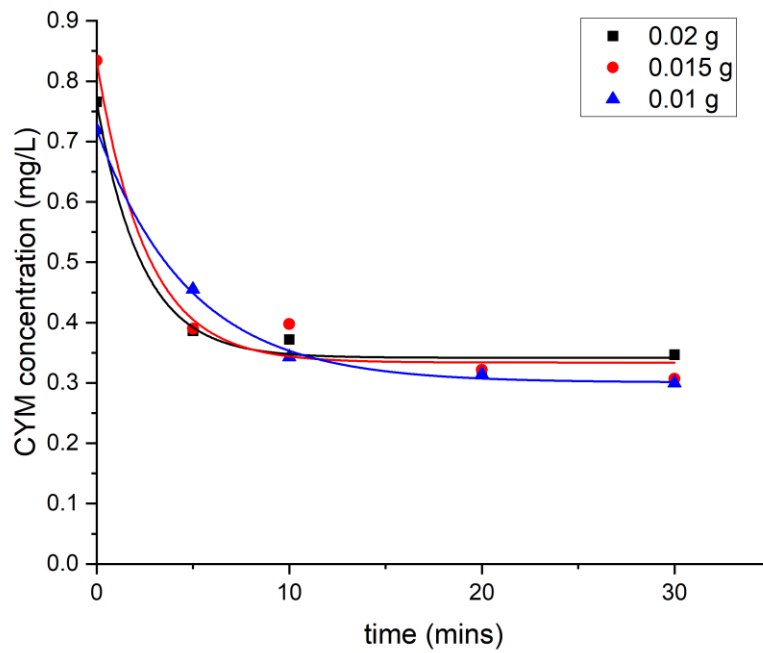


Figure 47: change in concentration of CYM over time due to adsorption onto GAC

The graph in Figure 47 shows that the adsorption of CYM onto the surface of the GAC was effective at removing 65 % of the CYM from within the solution. The kinetics of the reaction were very rapid, with the equilibrium concentration being reached after 10 minutes. There is little difference seen with the change in masses of GAC used, however, all the masses show evidence of the adsorption of CYM onto the surface of the GAC.

The relationship between q and time can also be plotted using the equation shown previously in Equation 20. The result of this relationship can be seen below in Figure 48.

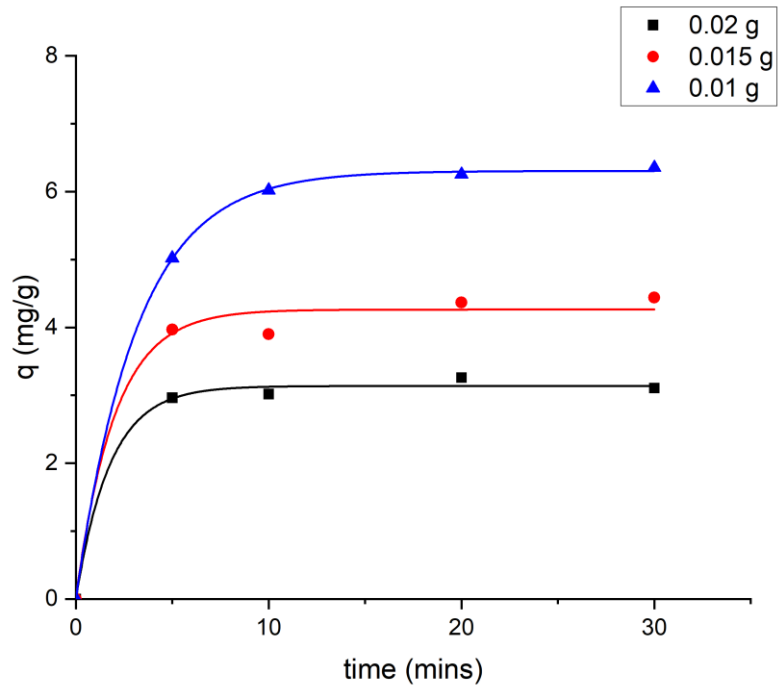


Figure 48: plot of Q against time for the adsorption of CYM onto GAC

The relationship between q and the time can show the adsorption capacity of the reaction system with different masses of carbon. Using values of q , the kinetics of the reaction system can also be determined. The rate constants of the reaction schemes can be obtained through using Equation 21 shown previously. The values for q obtained for the GAC sample at 0.005 g did not follow the trend line too closely. This could be due to the surface area being quickly filled with the contaminant, resulting in the contaminant having to adsorb onto small areas. This could follow a monolayer Freundlich isotherm. The rate constants can be seen below in Table 20.

Table 20: rate constants for the different masses of GAC used.

Mass of GAC (g)	Rate constant (min ⁻¹)	q max (mg/g)
0.02	0.45	2.02
0.015	0.41	3.21
0.01	0.21	3.80
0.0175	0.43	2.34
0.0125	0.31	3.81
0.005	0.25	10.97

For the adsorption of cypermethrin onto GAC, a study was found in literature that also looked at this reaction. For this experiment, a value for the rate constant was found to be around 3 L/ μ g. This suggests that less energy would be required for the reaction within the literature. This could be due to the reactions being conducted at 25 °C as opposed to 20 °C (Domingues et al., 2007).

6.3 - DEHP Adsorption

Different masses of GAC were investigated in solutions of DEHP at 1 mg/L. These different reaction mixtures were investigated to monitor the decrease in concentration of DEHP over time. The results can be shown below in Figure 49.

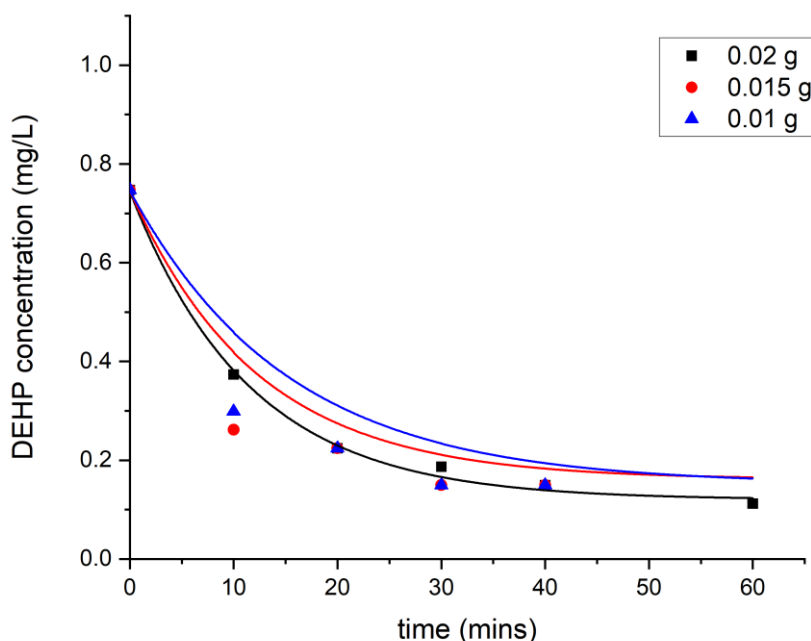


Figure 49: change in concentration of DEHP over time due to adsorption onto the surface of GAC

From looking at the results shown in Figure 49 a clear trend can be seen. This trend shows that the higher the mass of GAC in solution, the faster the rate of decrease of the concentration of DEHP. There was also a slightly lower end concentration of DEHP in solution. This would be expected, as the surface area of GAC in the solution would be increased when there is more GAC in the solution. Therefore, it would be expected that the concentration would decrease more when there is a larger surface area available for the GAC to adsorb onto.

Figure 49 shows that the concentration of DEHP decreases significantly throughout the time of the experiment. This would be preferable, as a large decrease would mean that a further technique would not be necessarily required to rely upon. This shows that GAC would be a good technique for the removal of DEHP from the solution without the fear of creating toxic by-products within the solution from the use of alternative techniques.

The relationship between the adsorption capacity and the time can also be investigated and these results are shown in the graph below in Figure 50.

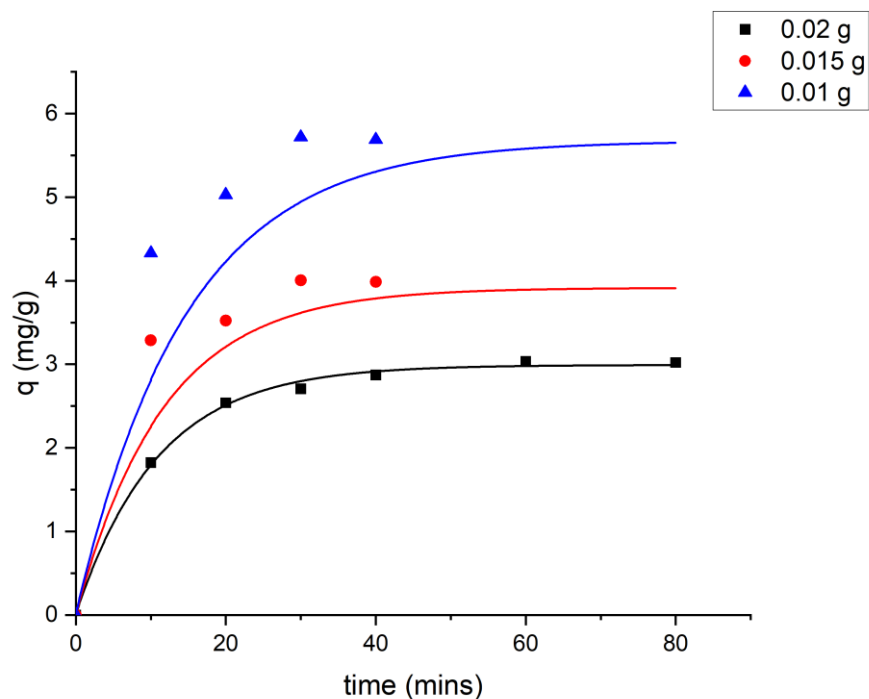


Figure 50: plot of Q against time for the adsorption of DEHP onto the surface of GAC

The relationship between q and time can be seen above in Figure 50. From this relationship the value for the rate constants were calculated using Equation 21. The results for the rate constants obtained can be seen below in Table 21.

Table 21: rate constants obtained for the kinetics of DEHP sorption onto GAC.

Mass of GAC (g)	Rate constant (min^{-1})	error	q max (mg/g)	error
0.02	0.06	86 %	2.72	9.4 %
0.015	0.14		3.70	
0.01	0.13	13 %	5.19	0 %

In literature, an experiment that carried out the adsorption of DEHP onto GAC in ethanol was found. The experiment was carried out in ethanol to increase the solubility of DEHP in the solution. This experiment was carried out at different temperatures, as well as using different percentages of ethanol. For the experiments at 20 °C, and with the percentages of ethanol ranging from 30 % up to 100 %, the values for the rate constant varied from 0.38 to 0.03. This would suggest that the rate constants obtained from the experiments would fit into the range, as the rate constants would likely be lower because of the low solubility of DEHP (Zhou et al., 2022). This could also be due to the DEHP having more affinity to the ethanol in solution as opposed to the GAC.

An iodine number analysis for samples of the granulated activated carbon was also investigated. This included different samples of granulated activated carbon being treated differently and analysed to determine the surface area available for chemical contaminant adsorption.

6.5 - Iodine Number

The iodine number for carbon is calculated to determine the absorption of contaminants onto the surface of the granulated activated carbon. This is to understand whether it would be effective at removing contaminants from the system through the process of adsorption onto the surface and pores of the granulated activated carbon.

Different samples of granulated activated carbon were treated and cleaned using a commercial acid solution and then being washed thoroughly and rinsed three times with DI water. By using three different carbon dosages or weights obtained from each activated carbon sample, a graph can be plotted showing the linear regression line. This allows the iodine number to be calculated. The iodine number is obtained from calculating the X/M value when C is equal to 0.02. The equations are shown in Appendix 1.

From plotting the individual graphs for each type of carbon sample, (cleaned and treated), the values for the iodine number can be calculated.

The iodine number experiment is important at determining how effective different carbon samples are at retaining chemical contaminants onto the surface, and therefore the effectiveness of using granulated activated carbon to assist in the treatment of water contaminants from wastewater.

Table 22: Iodine numbers calculated for different GAC samples.

Sample	Iodine Number
Not cleaned	691.94
Not cleaned, treated 50 %	563.05
Not cleaned, treated 25 %	1013.04
Not cleaned, treated 0 %	555.22
Cleaned	697.776
Cleaned, treated 50 %	674.60
Cleaned, treated 2 5%	723.642

The values shown in Table 22 above highlight the iodine number values obtained once the three values found were compared using the calculations found in Appendix 1. The lines obtained from the experimental data, which were used to calculate the values can be seen in the graph below in Figure 51.

From looking at previous studies, it can be seen that the typical range of iodine number values ranges from 500 – 1200 mg/g. Which correlates to a surface area between 900 and 1100 m²/g (Mopoung et al., 2015).

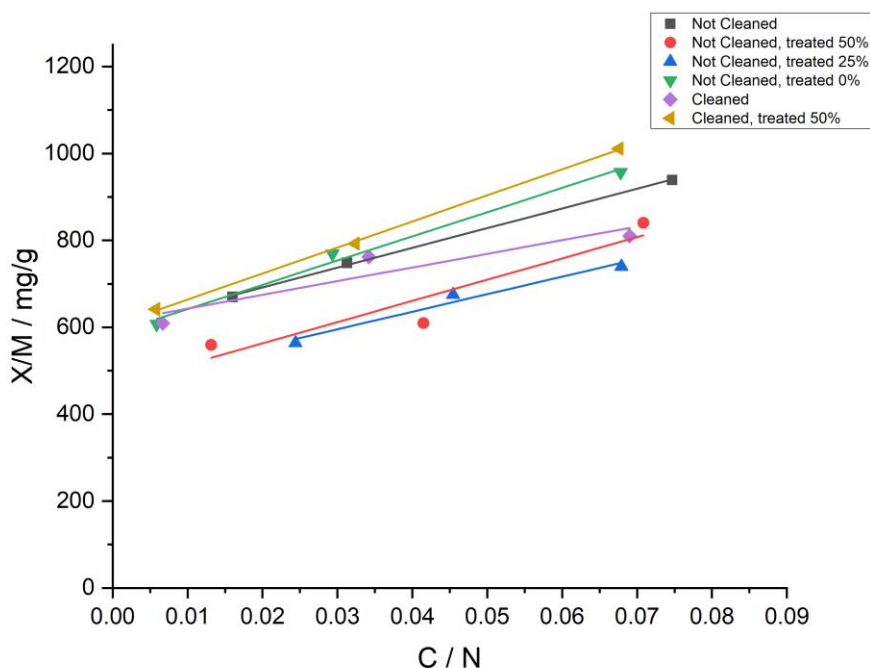


Figure 51: graph representing the iodine number of different samples of granulated activated carbon

Through comparing the different cleaned and treated samples of granulated activated carbon, patterns can be seen that emphasise the effects of cleaning and treating the granulated activated carbon.

Irregularities can be seen in the uncleaned carbon. A clear trend is not seen in the differing amount of iodine adsorbed onto the granulated activated carbon when the carbon is uncleaned and untreated. This would emphasise that the process of cleaning and treating the carbon is worthwhile, as it increases the adsorption of iodine into the carbon shown by the increase in the iodine number.

The cleaning of the carbon would remove any impurities within the carbon meaning the surface area of the granulated activated carbon would be maximised for the adsorption of iodine. This would in turn increase the iodine number of the granulated activated carbon sample. The removal of any contaminants on the surface of the activated carbon would allow more surface area for the chemical contaminants that are desired to be removed from the solution to adsorb to.

Once the carbon had been cleaned it showed an enhanced property for adsorption of iodine, showing an increased iodine number. This would be expected, which is supported experimentally by the data produced. When the carbon had been treated, you would expect the adsorption of iodine to also increase. This is because the carbon has been treated to enhance the adsorption potential. This can be seen with the carbon treated at 25 %, where a clear increase is shown, emphasising that the treatment process was effective in increasing the adsorption of iodine.

From studying the graph in Figure 51 above, it can be seen that the granulated activated carbon cleaned and treated to 25 % shows the largest iodine number. For future experimentation, this would be the preferred type of carbon due to the larger iodine number and enhanced adsorption rates.

6.6 - Summary of findings

From studying the behaviour of the chemical contaminants with GAC, relationships can be seen. These show that there is adsorption of all the chemical contaminants onto the surface of the GAC with all the different masses of GAC used in the solution. From the analysis and experimentation of GAC at varying masses in solutions of the different chemical contaminants, comparison to isotherms can be made. These isotherms can describe the behaviour of adsorption. This understanding will be beneficial when deciding on the optimum mass of GAC to use for the experimentation in wastewater. An optimum mass would be decided from the isotherms, and this would be used to determine the effect of adsorption in wastewater scenarios.

From observing the iodine number experiments, the specific surface area of different types of GACs were investigated. This showed that the GAC sample that was cleaned and treated to 25 % was preferable for the optimum adsorption. Therefore, this would maximise the adsorption of the chemical contaminants.

Chapter 7 – Wastewater Analysis

Wastewater samples of final treated effluent were collected from Gowerton wastewater treatment plant. Samples were taken and analysed, allowing for characterisation of the wastewater used for analysis. The characterisation results obtained are presented in Table 23.

The results in Table 23 highlight the presence of solids and metals that are present within the final effluent used. This means that when comparisons are made between the wastewater solutions and DI water solutions, reasoning can be obtained on whether the increased presence of dissolved substance in the water had an impact on the degradation rates of the chemical contaminants. From looking in the table below, there are many metals and solids present within the effluent, and this is vital to know when comparing the results.

Table 23: Results for the characterisation of the wastewater final treated effluent from Welsh Water

pH	7.1
Total COD	19 mg/L
Ammoniacal Nitrogen	0.4 mg/L
Suspended Solids	6 mg/L
Alkalinity	114 mg CaCO ₃ /L
Orthophosphate	0.12 mg/L
Phosphorous	0.2 mg/L
Soluble Copper	0.005 mg/L
Copper	0.005 mg/L
Soluble Zinc	0.02 mg/L
Zinc	0.02 mg/L
Lead	0.002 mg/L
Chromium	0.005 mg/L
Nickel	0.005 mg/L

7.1 - Ozonation of wastewater

The effect of ozonation on the emerging contaminants in wastewater was first investigated in a solution containing all three contaminants. However, when the analysis was conducted by HPLC, the retention times of the contaminants had changed due to the additives in wastewater interfering with the signal. The peaks for FLT and DEHP overlapped, therefore, no clear determination of the concentrations could be calculated, meaning that the concentration decrease over time could not be appropriately monitored.

Due to this occurrence, the ozonation of the ECs in wastewater were analysed individually to monitor the degradation of the contaminants within wastewater. The degradation of the compounds can be seen in Figure 52 below.

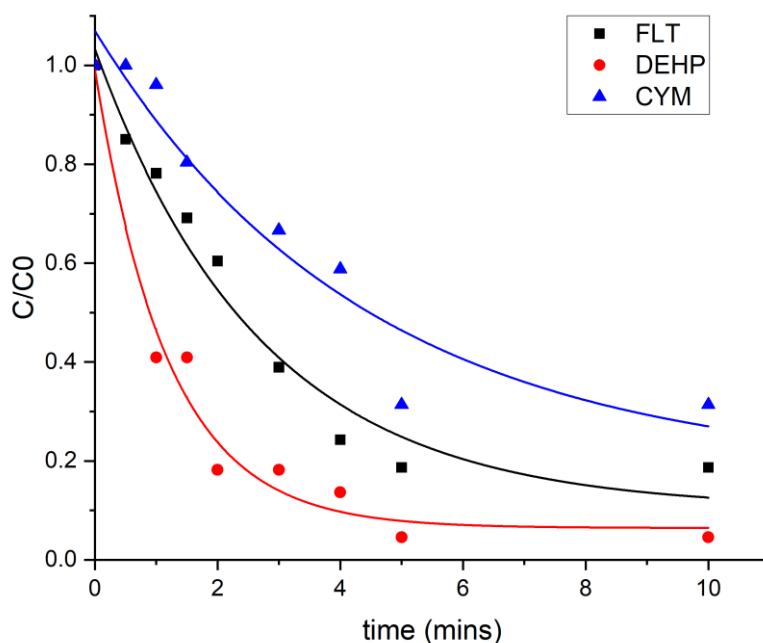


Figure 52: Degradation of the three emerging contaminants in final wastewater effluent by ozonation. ($T = 20\text{ }^{\circ}\text{C}$, $\text{pH} = 6$, ozone concentration = $20\text{ g/m}^3\text{ NTP}$, oxygen flow rate = 0.5 L/min)

Figure 52 shows that all the chemical contaminants within the treated final wastewater effluent degraded over time using oxidation via ozone.

Contaminant	Wastewater final effluent Percentage degradation	DI water Percentage degradation
FLT	80 % degradation within 6 minutes	75 % degradation within 1 minute
DEHP	90 % degradation within 4 minutes	90 % degradation within 5 minutes
CYM	50 % degradation within 10 minutes	90 % degradation within 4 minutes

7.2 - Adsorption onto GAC in wastewater

The adsorption of each chemical contaminant onto GAC was investigated in solutions of treated final wastewater effluent. The solutions were all made individually within the wastewater treated effluent and the adsorption was investigated over time.

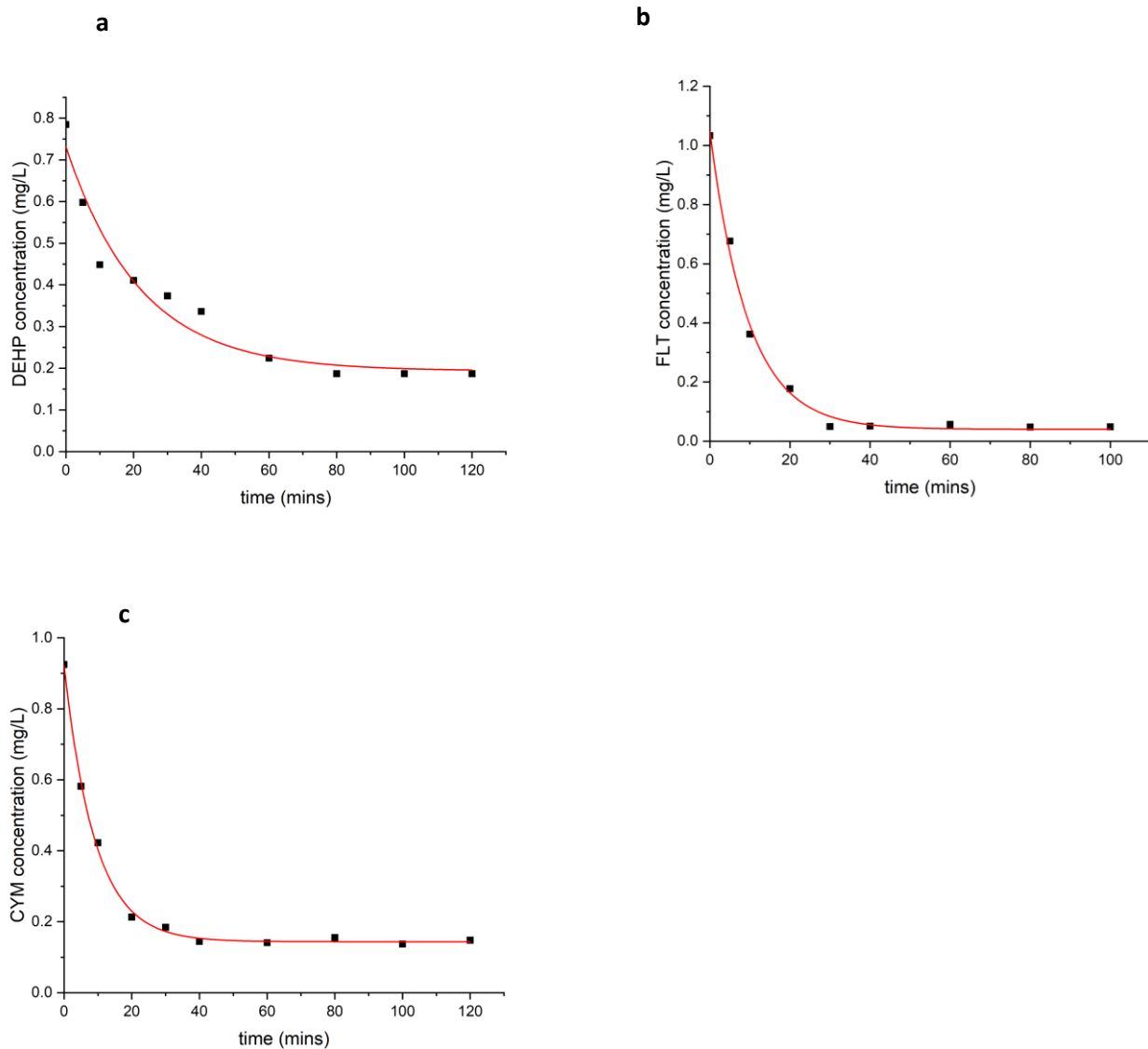


Figure 53: Rate of concentration decrease over time of (a) DEHP, (b) FLT, and (c) CYM from adsorption onto GAC (mass GAC = 0.015 g, T = 20 °C)

Contaminant	Wastewater final effluent Percentage decrease	DI water Percentage decrease
FLT	90 % decrease within 50 minutes	90 % decrease within 25 minutes
DEHP	75 % decrease within 80 minutes	80 % decrease within 80 minutes
CYM	85 % decrease within 40 minutes	75 % decrease within 40 minutes

Chapter 8 – Conclusion and Future Work

8.1 - Ozone Mass Transfer

A variety of different reaction conditions were analysed, and the findings studied for their effect on ozone mass transfer into DI water.

pH effects showed a higher ozone concentration being absorbed in a lower pH solution. At a lower pH there is less ozone decomposition, meaning that there is more ozone available to be absorbed. At higher pH levels, the decomposition increases, and the concentration of hydroxyl radicals increases, therefore, decreasing the concentration of ozone.

The effect of temperature showed that ozone is significantly more soluble in lower temperatures than in higher temperatures. This was shown by a much higher equilibrium concentration being reached in lower temperatures.

The increase in the flow rate of oxygen in L/min into the reactor increased the amount of ozone absorbed into DI water. This is due to the increase in pressure seen with an increase in flow rate, which would increase the mass transfer into water.

When studying the effect of radical scavengers in solution, two scavengers were investigated: (i) tert-butanol and (ii) carbonate. (i) Tert-butanol worked by decreasing the ozone decomposition into hydroxyl radicals, as well as the presence of tert-butanol in solution decreases the size of the ozone bubbles, increasing the mass transfer. (ii) With carbonate, no ozone was absorbed into DI water. Carbonate promotes the decomposition of ozone.

8.2 - Ozonation of emerging contaminants

8.2.1 - FLT

FLT was found to degrade when ozone was added into solution, and different reaction conditions were trialled to find the best scenario of reaction conditions to maximise the degradation of FLT in solutions of DI water.

When looking at the effect of pH on the degradation of FLT, a lower pH was found to be preferable. This would be due to the higher concentration of ozone found in lower pH, compared to the higher concentration of radicals found at higher pH values.

The effect of temperature involved the solubility of ozone being preferable at lower temperatures, but the reaction rate being more favourable at higher temperatures. A median temperature would be ideal to ensure that FLT is dissolved appropriately within solution, while maintaining a balance between the solubility of ozone and reaction kinetics.

When tert-butanol was added as a radical scavenger into solution, the rate of degradation of FLT was increased. This supports previous understanding that the degradation of FLT in DI water occurs via oxidation with molecular ozone as opposed to oxidation through indirect ozonation with hydroxyl radicals.

FLT can be degraded effectively within solutions of DI water. A lower pH, temperature and the presence of a scavenger has been shown to increase the rate of degradation.

8.2.2 - DEHP

DEHP in solutions of DI water can be degraded by the addition of ozone gas. The effect of pH, temperature and radical scavengers were investigated to maximise the rate of degradation.

A neutral pH was found to be the most favourable for the degradation of DEHP in DI water. This is due to the acidic pH favouring the direct ozonation, whilst the alkaline pH favoured the indirect ozonation via hydroxyl radicals. Due to the structure of DEHP containing a benzene ring, as well as long side chains, both types of ozonation were required to effectively degrade the DEHP.

For the effect of degradation at different temperatures, a temperature of 15 °C / 20 °C would be desirable as it would ensure that the DEHP is dissolved into the DI water. A lower temperature would again increase the solubility of ozone into water, whereas a higher temperature would favour the reaction kinetics. Therefore, a temperature around room temperature would ensure that there is a balance in the ozone solubility in comparison to the rate of reaction.

The addition of scavengers neither increased nor decreased the rate of degradation of DEHP in solution. This could be due to the benzene ring and the long side chain being oxidised by both molecular ozone and direct ozonation as well as hydroxyl radicals and indirect ozonation.

DEHP can be degraded effectively via ozone, a neutral pH and a temperature between 15 °C and 20 °C were shown to be best for the rate of degradation amongst the studied parameters. The presence of scavengers offered minimal effect and are of no benefit.

8.2.3 - CYM

When ozone is added to solutions of DI water containing CYM, the concentration of CYM is shown to decrease. This shows the feasibility of using ozone as a degradation technique for CYM in water.

The pH effect of ozonation in solution could not be analysed due to difficulties in the analysis of the solutions of CYM by UV Vis spectroscopy. When the solutions were dosed with the different pH levels, this affected the absorption peak of the solution, yielding unreliable results.

The effects of temperature were investigated, and again a middle temperature would be most effective for the degradation of CYM in solution. This is because the solubility of both CYM in solution and the ozone concentration would be at an appropriate level, as well as the reaction kinetics being sufficient.

The addition of tert-butanol into the solution increased the rate of degradation of CYM in solution. This suggests that the degradation of CYM by ozone would occur via direct ozonation from molecular ozone, as opposed to the indirect ozonation from hydroxyl radicals.

The degradation of CYM by ozone did occur effectively in solutions of DI water. A lower temperature was shown to be more favourable due to the ozone solubility, however, a temperature of 15 °C would be recommended for treatment; given the solubility of CYM and the reaction kinetics. The addition of a radical scavenger increased the rate of degradation.

When the contaminants were combined in a single solution, the rates of degradation altered, however, all three contaminants were degraded to negligible levels of concentration within 3 minutes of ozonation.

8.3 - Adsorption by Granulated Activated Carbon

GAC can adsorb all three of the emerging chemical contaminants being studied, but at different rates of adsorption and different end concentrations. Fluoranthene was adsorbed onto GAC and a concentration plateau was obtained within a maximum of 20 minutes, with 90 % of the fluoranthene in solution being adsorbed within this time. Cypermethrin had a concentration plateau of 10 minutes. However, the concentration depletion ranged from 50 % to 80 %. Di (2- ethyl hexyl) phthalate showed a much slower mechanism of adsorption onto GAC, with 80 % of the di (2- ethyl hexyl) phthalate being adsorbed within 50 minutes.

8.4 - Wastewater Analysis

8.4.1 - Ozonation of chemical contaminants in wastewater

All the chemical contaminants were degraded when in solutions of final treated wastewater effluent. However, a comparison between the rate of degradation by ozone in solutions of wastewater and DI water can be made. The results are summarised below in Table 24.

Table 24: Summary of results comparing the ozonation of the contaminants in solutions of DI water and wastewater effluent

Contaminant	Wastewater final effluent Percentage degradation	DI water Percentage degradation
FLT	80 % degradation within 6 minutes	75 % degradation within 1 minute
DEHP	90 % degradation within 4 minutes	90 % degradation within 5 minutes
CYM	50 % degradation within 10 minutes	90 % degradation within 4 minutes

8.4.2 - Adsorption of chemical contaminants in wastewater

The three emerging chemical contaminants all showed a decrease in concentration upon the addition of GAC for adsorption. The results obtained are summarised below in Table 25.

Table 25: Summary of results comparing the adsorption in solutions of DI water and solutions of final wastewater effluent

Contaminant	Wastewater final effluent Percentage decrease	DI water Percentage decrease
FLT	90 % decrease within 50 minutes	90 % decrease within 25 minutes
DEHP	75 % decrease within 80 minutes	80 % decrease within 80 minutes
CYM	85 % decrease within 40 minutes	75 % decrease within 40 minutes

In conclusion, this study has shown that ozone and activated carbon can be used to treat fluoranthene, cypermethrin and di (2- ethyl hexyl) phthalate in solutions of DI water, as well as in treated solutions of wastewater final effluent.

Further analysis needs to be conducted into the by-products generated from the oxidation of the contaminants with ozone and whether the by-products produced are toxic. This would allow a deeper understanding of the feasibility of using ozone as a treatment process of wastewater.

The feasibility of these techniques would also need to be investigated on a larger scale before being implemented into the wastewater treatment process, to ensure ozone can treat large volumes of effluent safely and effectively.

A cost analysis plan would also need to be constructed to understand whether these processes would be feasible and cost effective on a large scale.

References

- Abramovitch, A., LaRocca, G., & Jacoby, H. (1996). Environmental Fate and Ground Water Branch. *US-EPA*.
- Adams, C. D., & Gorg, S. (2002). Effect of pH and Gas-Phase Ozone Concentration on the Decolorization of Common Textile Dyes. *Journal of Environmental Engineering*, 128(3), 293-298. <https://doi.org/10.1061/ASCE0733-93722002128:3293>
- Affam, A. C., & Chaudhuri, M. (2013). Degradation of pesticides chlorpyrifos, cypermethrin and chlorothalonil in aqueous solution by TiO₂ photocatalysis. *Journal of Environmental Management*, 130, 160-165.
- Agency, U. E. P., & (1980). *AMBIENT WATER QUALITY CRITERIA FOR FLUORANTHENE*.
- Aguerre, R., Aguerre, R. J., Suarez, C., & Viollaz, P. E. (1989). New BET Type Multilayer Sorption Isotherms. Part I: Theoretical Derivation of the Model New BET Type Multilayer Sorption Isotherms. Part 1: Theoretical Derivation of the Model. *Lebensmittel-Wissenschaft and Technologie*, 22, 188-191.
- Ahmed, M. B., Zhou, J. L., Ngo, H. H., Guo, W., Thomaidis, N. S., & Xu, J. (2017). Progress in the biological and chemical treatment technologies for emerging contaminant removal from wastewater: A critical review. *Journal of Hazardous Materials*, 323, 274-298.
- Al-Dabbas, M. M., Shaderma, A. A., Al-Antary, T. M., Ghazzawi, H. A., & Hamad, H. J. (2018). EFFECT OF OZONATION ON CYPERMETHRIN AND CHLORPYRIFOS PESTICIDES RESIDUES DEGRADATION IN TOMATO FRUITS. *Fresenius Environmental Bulletin*, 27(10), 6628-6633.
- Alawneh, R., Ghazali, F. E. M., Ali, H., & Asif, M. (2018). Assessing the contribution of water and energy efficiency in green buildings to achieve United Nations Sustainable Development Goals in Jordan. *Building and Environment*, 146, 119-132. <https://doi.org/10.1016/j.buildenv.2018.09.043>
- Almomani, F. A., Shawaqfah, M., Bhosale, R. R., & Kumar, A. (2016). Removal of emerging pharmaceuticals from wastewater by ozone-based advanced oxidation processes. *Environmental Progress and Sustainable Energy*, 35(4), 982-995. <https://doi.org/10.1002/ep.12306>
- Amiri, M. C., & Dadkhah, A. A. (2006). On reduction in the surface tension of water due to magnetic treatment. *Colloids and Surfaces A: Physicochemical and Engineering Aspects*, 278(1-3), 252-255. <https://doi.org/10.1016/j.colsurfa.2005.12.046>
- Anthemidis, A. N., & Ioannou, K. I. G. (2009). Recent developments in homogeneous and dispersive liquid-liquid extraction for inorganic elements determination. A review. *Talanta*, 80(2), 413-421. <https://doi.org/10.1016/j.talanta.2009.09.005>
- Anthony, C. R., Kamat, P. M., Thete, S. S., Munro, J. P., Lister, J. R., Harris, M. T., & Basaran, O. A. (2017). Scaling laws and dynamics of bubble coalescence. *Physical Review Fluids*, 2(8). <https://doi.org/10.1103/PhysRevFluids.2.083601>
- Arora, N. K., & Mishra, I. (2019). United Nations Sustainable Development Goals 2030 and environmental sustainability: race against time. *Environmental Sustainability*, 2, 339-342. <https://doi.org/10.1007/s42398-019-00092-y>
- Ason, B., Armah, F. A., & Essumang, D. K. (2022). Characterization and quantification of endocrine disruptors in female menstrual blood samples. *Toxicology Reports*, 9, 1877-1882. <https://doi.org/10.1016/j.toxrep.2022.10.007>
- Avery, L., Jarvis, P., & Macadam, J. Review of literature to determine the uses for ozone in the treatment of water and wastewater: Executive Summary. *Centre of expertise for waters*.

- Bain, K., Rodriguez, J. G., & Towns, M. H. (2018). Zero-Order Chemical Kinetics as a Context To Investigate Student Understanding of Catalysts and Half-Life. *Journal of Chemical Education*, 95(5), 716-725.
- Barrow, N. J. (1992). A brief discussion on the effect of temperature on the reaction of inorganic ions with soil. *Journal of Soil Science*, 43, 37-45.
- Bataklijev, T., Georgiev, V., Anachkov, M., Rakovsky, S., & Zaikov, G. E. (2014). Ozone decomposition. *Interdisciplinary Toxicology*, 7(2), 47-59. <https://doi.org/10.2478/intox-2014-0008>
- Beattie, J. K., Djerdjev, A. M., Gray-Weale, A., Kallay, N., Lützenkirchen, J., Preočanin, T., & Selmani, A. (2014). PH and the surface tension of water. *Journal of Colloid and Interface Science*, 422, 54-57. <https://doi.org/10.1016/j.jcis.2014.02.003>
- Beckera, K., Seiwerta, M., Angerer, J., Hegera, W., Kochb, H. M., Nagorkaa, R., Roßkampa, E., Schlütera, C., Seiferta, B., & Ullricha, D. (2004). DEHP metabolites in urine of children and DEHP in house dust. *International Journal of Hygiene and Environmental Health*, 207(5). <http://www.elsevier.de/intjhyg>
- Beltrán, F. J., & Rey, A. (2018). Free Radical and Direct Ozone Reaction Competition to Remove Priority and Pharmaceutical Water Contaminants with Single and Hydrogen Peroxide Ozonation Systems. *Journal of the International Ozone Association*, 40(4), 251-265. <https://doi.org/10.1080/01919512.2018.1431521>
- Benitez, F. J., Acero, J. L., Garcia-Reyes, J. F., Real, F. J., Roldan, G., Rodriguez, E., & Molina-Díaz, A. (2013). Determination of the reaction rate constants and decomposition mechanisms of ozone with two model emerging contaminants: DEET and nortriptyline. *Industrial and Engineering Chemical Research*, 52(48), 17064-17073. <https://doi.org/10.1021/ie402916u>
- Bermúdez, L. A., Pascual, J. M., Martínez, M. D. M., & Capilla, J. M. P. (2021). Effectiveness of advanced oxidation processes in wastewater treatment: State of the art. *Water* 13(15). <https://doi.org/10.3390/w13152094>
- Bhatnagar, A., Hogland, W., Marques, M., & Sillanpää, M. (2013). An overview of the modification methods of activated carbon for its water treatment applications. *Chemical Engineering Journal*, 219, 499-511. <https://doi.org/10.1016/j.cej.2012.12.038>
- Biń, A. K., Duczmal, B., Machniewski, P., & (2001). Hydrodynamics and ozone mass transfer in a tall bubble column. *Chemical Engineering Science*, 56(11-22), 6233-6240. [https://doi.org/10.1016/S0009-2509\(01\)00213-5](https://doi.org/10.1016/S0009-2509(01)00213-5)
- Bin, A. K., & Roustan, M. (2000). Fundamental and Engineering Concepts for Ozone Reactor Engineering. International Specialised Symposium IOA, Toulouse.
- Bisutti, I., Hilke, I., & Raessler, M. (2004). Determination of total organic carbon – an overview of current methods. *Trends in Analytical Chemistry*, 23(10-11).
- Boczka, G., & Fernandes, A. (2017). Wastewater treatment by means of advanced oxidation processes at basic pH conditions: A review. *Chemical Engineering Journal*, 320, 608-633. <https://doi.org/10.1016/j.cej.2017.03.084>
- Bodzek, M., Dudziak, M., & Luks-Betlej, K. (2004). Application of membrane techniques to water purification. *Desalination*, 162, 121-128.
- Bolong, N., Ismail, A. F., Salim, M. R., & Matsuura, T. (2009). A review of the effects of emerging contaminants in wastewater and options for their removal. *Desalination*, 239(1-3), 229-246. <https://doi.org/10.1016/j.desal.2008.03.020>
- Borikar, D., Mohseni, M., & Jasim, S. (2015). Evaluations of conventional, ozone and Uv/H2O2 for removal of emerging contaminants and THM-FPS. *Water Quality Research Journal*, 50(2), 140-151. <https://doi.org/10.2166/wqrjc.2014.018>
- Bossmann, S. H., Oliveros, E., Go, S., Siegwart, S., Dahlen, E. P., Payawan, L., Straub, M., Wo, M., & Braun, A. M. (1998). New Evidence against Hydroxyl Radicals as Reactive

- Intermediates in the Thermal and Photochemically Enhanced Fenton Reactions. *The Journal of Physical Chemistry* 102(28). <https://pubs.acs.org/sharingguidelines>
- Breitbart, M., & Bathen, D. (2001). Influence of ultrasound on adsorption processes. *Ultrasonics Sonochemistry*, 8(3), 277-283. www.elsevier.nl/locate/ultsonch
- Breitenbucher, J., Arienti, K., & McClure, K. (2001). Scope and limitations of solid-supported liquid - Liquid extraction for the high-throughput purification of compound libraries. *Journal of Combinatorial Chemistry*, 3(6).
- Bromberga, P. A., & Korenb, H. S. (1995). Ozone-induced human respiratory dysfunction and disease. *Toxicology Letters*, 82183, 307-316.
- Buyuksonmez, F., Hess, T. F., Crawford, R. L., & Watts, R. J. (1998). Toxic Effects of Modified Fenton Reactions on *Xanthobacter flavus* FB71. *Applied Environmental Microbiology*, 64(10), 3759-3764.
- Caldwell, J. C. (2012). DEHP: Genotoxicity and potential carcinogenic mechanisms-A review. *Mutation Research*, 751(2), 82-157. <https://doi.org/10.1016/j.mrrev.2012.03.001>
- Cambridge Dictionary. In. (2023). *Cambridge Dictionary*
- Cébron, A., Faure, P., Lorgeoux, C., Ouvrard, S., & Leyval, C. (2013). Experimental increase in availability of a PAH complex organic contamination from an aged contaminated soil: Consequences on biodegradation. *Environmental Pollution*, 177, 98-105. <https://doi.org/10.1016/j.envpol.2013.01.043>
- Chelme-Ayala, P., El-Din, M. G., & Smith, D. W. (2010). Degradation of bromoxynil and trifluralin in natural water by direct photolysis and UV plus H₂O₂ advanced oxidation process. *Water Research*, 44, 2221-2228.
- Chen, C. Y., Wu, P. S., & Chung, Y. C. (2009). Coupled biological and photo-Fenton pretreatment system for the removal of di-(2-ethylhexyl) phthalate (DEHP) from water. *Bioresource Technology*, 100(19), 4531-4534. <https://doi.org/10.1016/j.biortech.2009.04.020>
- Chen, X. (2015). Modeling of Experimental Adsorption Isotherm Data *Information*, 6, 14-22.
- Christensen, L. R., Jorgenson, D. W., & Lau, L. J. (1975). Transcendental Logarithmic Utility Functions. *The American Economic Review*, 65(3), 367-383.
- Christenson, H. K., Bowen, R. E., Carlton, J. A., Denne, J. R. M., & Lu, Y. (2008). Electrolytes that show a transition to bubble coalescence inhibition at high concentrations. *The Journal of Physical Chemistry*, 112(3), 794-796. <https://doi.org/10.1021/jp075440s>
- Coles, C. A., & Yong, R. N. (2006). Use of equilibrium and initial metal concentrations in determining Freundlich isotherms for soils and sediments. *Engineering Geology*, 85, 19-25.
- Collins English Dictionary In. (2023). *Collins English Dictionary*
- Covinich, L. G., Bengoechea, D. I., Fenoglio, R. J., & Area, M. C. (2014). Advanced Oxidation Processes for Wastewater Treatment in the Pulp and Paper Industry: A Review. *American Journal of Environmental Engineering*, 4(3), 56-70. <https://doi.org/10.5923/j.ajee.20140403.03>
- Cretin, M., & Huong, T. X. (2015). •OH Radicals Production. *Encyclopedia of Membranes*, 1-2.
- Crincoli, K. R., & Huling, S. G. (2020). Hydroxyl radical scavenging by solid mineral surfaces in oxidative treatment systems: Rate constants and implications. *Water Research*, 169, 115240.
- Daiem, M. M. A., Rivera-Utrilla, J., Ocampo-Pérez, R., Méndez-Díaz, J. D., & M, S.-P. (2012). Environmental impact of phthalic acid esters and their removal from water and sediments by different technologies - A review. *Journal of Environmental Management*, 109, 164-178. <https://doi.org/10.1016/j.jenvman.2012.05.014>
- Das, K., & Roychoudhury, A. (2014). Reactive oxygen species (ROS) and response of antioxidants as ROS-scavengers during environmental stress in plants. *Frontiers Environmental Science*, 2. <https://doi.org/10.3389/fenvs.2014.00053>

- Database, P. P. (2023). Cypermethrin (Ref: OMS 2002). *PPDB*.
- David, G., Rana, M. S., Saxena, S., Sharma, S., Pant, D., & Prajapati, S. K. (2023). A review on design, operation, and maintenance of constructed wetlands for removal of nutrients and emerging contaminants. *International Journal of Environmental Science and Technology*, 20, 9249-9270.
- Desta, M. B. (2013). Batch Sorption Experiments: Langmuir and Freundlich Isotherm Studies for the Adsorption of Textile Metal Ions onto Teff Straw (*Eragrostis tef*) Agricultural Waste. *Journal of Thermodynamics*, 2013.
- Dewil, R., Mantzavinos, D., Poulis, I., & Rodrigo, M. A. (2017). New perspectives for Advanced Oxidation Processes. *Journal of Environmental Management*, 195, 93-99. <https://doi.org/10.1016/j.jenvman.2017.04.010>
- Domingues, V. F., Priolo, G., Alves, A. C., Cabral, M. F., & Delerue-Matos, C. (2007). Adsorption behavior of α -cypermethrin on cork and activated carbon. *Informa UK Limited*.
- Drozdova, M., Jablonka, R., Kucerova, R., & Kasakova, H. (2014). APPLICATION OF OZONATION TO INTENSIFY NITRIFICATION AND DENITRIFICATION PROCESSES. *GeoScience Engineering*, 3, 37-45.
- Du, C., Liu, B., Hu, J., & Li, H. (2021). Determination of iodine number of activated carbon by the method of ultraviolet–visible spectroscopy. *Materials Letters*, 285. <https://doi.org/10.1016/j.matlet.2020.129137>
- Ebadi, A., Mohammadzadeh, J. S. S., & Khudiev, A. (2009). What is the correct form of BET isotherm for modeling liquid phase adsorption? *Adsorption*, 15, 65-73. <https://doi.org/10.1007/s10450-009-9151-3>
- Edokpayi, J. N., Odiyo, J. O., Popoola, O. E., & Msagati, T. A. M. (2016). Determination and Distribution of Polycyclic Aromatic Hydrocarbons in Rivers, Sediments and Wastewater Effluents in Vhembe District, South Africa. *International Journal of Environmental Research and Public Health*, 13, 387.
- Elbetieha, A., Da'as, S. I., Khamas, W., & Darmani, H. (2001). Evaluation of the Toxic Potentials of Cypermethrin Pesticide on Some Reproductive and Fertility Parameters in the Male Rats. *Archives of Environmental Contamination and Toxicology*, 41, 522-528.
- Eriksson, M. (2005). *Ozone chemistry in aqueous solution -Ozone decomposition and stabilisation -Ozone decomposition and stabilisation* [Royal Institute of Technology]. Stockholm, Sweden.
- Erythropel, H. C., Maric, M., Nicell, J. A., Leask, R. L., & Yargeau, V. (2014). Leaching of the plasticizer di(2-ethylhexyl)phthalate (DEHP) from plastic containers and the question of human exposure. *Applied Microbiology and Biotechnology*, 98, 9967-9981. <https://doi.org/10.1007/s00253-014-6183-8>
- Felix, E. P., Souza, K. A. D. D., Dias, C. M., & Cardoso, A. A. (2006). Measurements of Ambient Ozone Using Indigo Blue-Coated Filters. *Journal of AOAC International*, 89(2). <https://academic.oup.com/jaoac/article/89/2/480/5657657>
- Fester, T., Giebler, J., Wick, L. Y., Schlosser, D., & Kästner, M. (2014). Plant-microbe interactions as drivers of ecosystem functions relevant for the biodegradation of organic contaminants. *Current Opinion in Biotechnology*, 27, 168-175. <https://doi.org/10.1016/j.copbio.2014.01.017>
- Galano, A. (2008). Carbon nanotubes as free-radical scavengers. *The Journal of Physical Chemistry*, 112(24), 8922-8927. <https://doi.org/10.1021/jp801379g>
- Galdeano, M. C., Wilhelm, A. E., Goulart, I. B., Tonon, R. V., Freitas-Silva, O., Germani, R., & Chavez, D. W. H. (2018). Effect of water temperature and pH on the concentration and time of ozone saturation. *Brazilian Journal of Food Technology*, 21.

- Garcia, G., Allen, A. G., & Cardoso, A. A. (2014). A new and simple visual technique based on indigo dye for determination of ozone in ambient air. *Water, Air and Soil Pollution*, 225. <https://doi.org/10.1007/s11270-013-1836-2>
- George, J. E., Chidangil, S., & George, S. D. (2017). A study on air bubble wetting: Role of surface wettability, surface tension, and ionic surfactants. *Applied Surface Science*, 410, 117-125. <https://doi.org/10.1016/j.apsusc.2017.03.071>
- Ghattas, A. K., Fischer, F., Wick, A., & Ternes, T. A. (2017). Anaerobic biodegradation of (emerging) organic contaminants in the aquatic environment. *Water Research*, 116, 268-295. <https://doi.org/10.1016/j.watres.2017.02.001>
- Ghosal, P. S., & Gupta, A. K. (2017). Determination of thermodynamic parameters from Langmuir isotherm constant-revisited. *Journal of Molecular Liquids*, 225, 137-146.
- Giraud, F., Guiraud, P., Kadri, M., Blake, G., & Steiman, R. (2001). BIODEGRADATION OF ANTHRACENE AND FLUORANTHENE BY FUNGI ISOLATED FROM AN EXPERIMENTAL CONSTRUCTED WETLAND FOR WASTEWATER TREATMENT. *Water Research*, 35(17), 4126-4136.
- Giray, B., Gurbay, A., & Hincal, F. (2001). Cypermethrin-induced oxidative stress in rat brain and liver is prevented by Vitamin E or allopurinol. *Toxicology Letters*, 118, 136-146.
- González-García, P. (2018). Activated carbon from lignocellulosics precursors: A review of the synthesis methods, characterization techniques and applications. *Renewable and Sustainable Energy Reviews*, 82, 1393-1414. <https://doi.org/10.1016/j.rser.2017.04.117>
- Gounden, A. N., & Jonnalagadda, S. B. (2019). Advances in treatment of brominated hydrocarbons by heterogeneous catalytic ozonation and bromate minimization. *Molecules*, 24(19). <https://doi.org/10.3390/molecules24193450>
- Grewal, K. K., Sandhu, G. S., Kaur, R., Brar, R. S., & Sandhu, H. S. (2010). Toxic Impacts of Cypermethrin on Behavior and Histology of Certain Tissues of Albino Rats. *Toxicology International*, 17(2).
- Guo, Y., Zhang, Y., Yu, G., & Wang, Y. (2021). Revisiting the role of reactive oxygen species for pollutant abatement during catalytic ozonation: The probe approach versus the scavenger approach. *Applied catalysis B: Environmental*, 280. <https://doi.org/10.1016/j.apcatb.2020.119418>
- Hachemi, M. E. E., Naffrechoux, E., Suptil, J., & Hausler, R. (2013). Bicarbonate Effect in the Ozone-UV Process in the Presence of Nitrate. *The Journal of the International Ozone Association*, 35(4), 302-307. <https://doi.org/10.1080/01919512.2013.794650>
- Hakika, D. C., Sarto, S., Mindaryani, A., & Hidayat, M. (2019). Decreasing COD in sugarcane vinasse using the fenton reaction: The effect of processing parameters. *Catalysts*, 9(11). <https://doi.org/10.3390/catal9110881>
- Hammad, K. M., & Jung, J. Y. (2008). Ozonation catalyzed by homogeneous and heterogeneous catalysts for degradation of DEHP in aqueous phase. *Chemosphere*, 72(4), 690-696. <https://doi.org/10.1016/j.chemosphere.2008.02.037>
- Hao, L., Huiping, D., & Jun, S. (2012). Activated carbon and cerium supported on activated carbon applied to the catalytic ozonation of polycyclic aromatic hydrocarbons. *Journal of Molecular Catalysis A: Chemical*, 363-364, 101-107. <https://doi.org/10.1016/j.molcata.2012.05.022>
- Hardesty, J. H., & Attili, B. (2010). Spectrophotometry and the Beer-Lambert Law: An Important Analytical Technique in Chemistry.
- Hasan, S. A., & Jabeen, S. (2015). Degradation kinetics and pathway of phenol by *Pseudomonas* and *Bacillus* species. *Biotechnology and Biotechnological Equipment* 29(1), 45-53.

- Hauner, I. M., Deblais, A., Beattie, J. K., Kellay, H., & Bonn, D. (2017). The Dynamic Surface Tension of Water. *Journal of Physical Chemistry Letters*, 8(7), 1599-1603. <https://doi.org/10.1021/acs.jpcllett.7b00267>
- Heidarinejad, Z., Dehghani, M. H., Heidari, M., Javedan, G., Ali, I., & Sillanpää, M. (2020). Methods for preparation and activation of activated carbon: a review. *Environmental Chemistry Letters*, 18, 393-415. <https://doi.org/10.1007/s10311-019-00955-0>
- Hickman, Z. A., & Reid, B. J. (2008). Earthworm assisted bioremediation of organic contaminants. *Environment International*, 34(7), 1072-1081. <https://doi.org/10.1016/j.envint.2008.02.013>
- Hilberty, P. C., Danovich, D., Shurki, A., & Shaik, S. (1995). Why Does Benzene Possess a Deh Symmetry? A Quasiclassical State Approach for Probing π -Bonding and Delocalization Energies. *Journal of the American Chemical Society*, 117, 7760-7768.
- Horiuti, J. (1973). THEORY OF REACTION RATES AS BASED ON THE STOICHIOMETRIC NUMBER CONCEPT. *Annals of the New York Academy of Sciences*, 213(1), 5-30.
- Huddleston, J. G., Willauer, H. D., Swatoski, R. P., Vlsser, A. E., & Rogers, R. D. (1998). Room temperature ionic liquids as novel media for 'clean' liquid-liquid extraction. *Chemistry Communications*, 1765-1766.
- Ibáñez, M., Gracia-Lor, E., Morales, E., Pastor, L., & Hernández, F. (2013). Removal of emerging contaminants in sewage water subjected to advanced oxidation with ozone. *Journal of Hazardous Materials*, 260, 389-398. <https://doi.org/10.1016/j.jhazmat.2013.05.023>
- International, A. (2006). D 4607: Standard Test Method for Determination of Iodine Number of Activated Carbon. In: ASTM International.
- Iwuozor, K. O. (2019). Prospects and Challenges of Using Coagulation-Flocculation method in the treatment of Effluents. *Advanced Journal of Chemistry: A*, 2(2), 105-127. <https://doi.org/10.29088/sami/ajca.2019.2.105127>
- Jeppu, G. P., & Clement, T. P. (2012). A modified Langmuir-Freundlich isotherm model for simulating pH-dependent adsorption effects. *Journal of Contaminant Hydrology*, 129-130, 46-53.
- Jilani, S. (2013). Comparative assessment of growth and biodegradation potential of soil isolate in the presence of pesticides. *Saudi Journal of Biological Sciences* 20, 257-264.
- Jilani, S., & Khan, M. A. (2006). Biodegradation of Cypermethrin by pseudomonas in a batch activated sludge process *international Journal of Environmental Science and Technology*, 3(4), 371-380.
- Jones, D. (1995). Environmental Fate of Cypermethrin. *Environmental Monitoring and Pest Management*.
- Jung, Y., Hong, E., Kwon, M., & Kang, J. W. (2017). A kinetic study of ozone decay and bromine formation in saltwater ozonation: Effect of O₃dose, salinity, pH, and temperature. *Chemical Engineering Journal*, 312, 30-38. <https://doi.org/10.1016/j.cej.2016.11.113>
- Kahla, O., Garali, S. M. B., Karray, F., Abdallah, M. B., Kallel, N., Mhiri, N., Zaghden, H., Barhoumi, B., Pringault, O., Quéméneur, M., Tedetti, M., Sayadi, S., & Hlaili, A. S. (2021). Efficiency of benthic diatom-associated bacteria in the removal of benzo(a)pyrene and fluoranthene. *Science of the Total Environment*, 751. <https://doi.org/10.1016/j.scitotenv.2020.141399>
- Kanyika-Mbewe, C., Thole, B., Makwinja, R., & Kaonga, C. C. (2020). Monitoring of carbaryl and cypermethrin concentrations in water and soil in Southern Malawi. *Environmental Monitoring and Assessment*, 192, 595.

- Kapoor, R., Ghosh, P., & Vijay, V. K. (2021). *Emerging Technologies and Biological Systems for Biogas Upgrading, Chapter 4 - Factors affecting CO₂ and CH₄ separation during biogas upgrading in a water scrubbing process*. Academic Press.
- Karnib, M., Kabbani, A., Holail, H., & Olama, Z. (2014). Heavy metals removal using activated carbon, silica and silica activated carbon composite. *Energy Procedia*, 50, 113-120. <https://doi.org/10.1016/j.egypro.2014.06.014>
- Khuntia, S., Majumder, S. K., & Ghosh, P. (2015). Quantitative prediction of generation of hydroxyl radicals from ozone microbubbles. *Chemical Engineering Research and Design* 98, 231-239.
- Kim, S. W., Sohn, J. S., Kim, H. K., Ryu, Y., & Cha, S. W. (2019). Effects of Gas Adsorption on the Mechanical Properties of Amorphous Polymer. *Polymers*, 11(5), 817.
- Kishimoto, N. (2007). Applicability of Ozonation Combined with Electrolysis to 1,4-Dioxane Removal from Wastewater Containing Radical Scavengers. *Ozone: Science and Engineering*, 29(1).
- Kishimoto, N., & Nakamura, E. (2011). Effects of ozone-gas bubble size and pH on Ozone/UV treatment. *The Journal of the International Ozone Association*, 33(5), 396-402. <https://doi.org/10.1080/01919512.2011.603657>
- Koch, H. M., Drexler, H., & Angerer, J. (2003). An estimation of the daily intake of di(2-ethylhexyl)phthalate (DEHP) and other phthalates in the general population. *International Journal of Hygiene and Environmental Health*, 206(2), 77-83. <http://www.urbanfischer.de/journals/intjhyg>
- Koch, H. M., Preuss, R., Angerer, J., Foster, P., Sharpe, R., & Toppari, J. (2006). Di(2-ethylhexyl)phthalate (DEHP): Human metabolism and internal exposure - An update and latest results. *International Journal of Andrology*, 29(1), 155-165. <https://doi.org/10.1111/j.1365-2605.2005.00607.x>
- Kohout, J. (2021). Modified Arrhenius Equation in Materials Science, Chemistry and Biology. *Molecules*, 26, 7162.
- Kurian, M. (2021). Advanced oxidation processes and nanomaterials -a review. *Cleaner Engineering and Technology*, 2. <https://doi.org/10.1016/j.clet.2021.100090>
- Kutt, A., Selberg, S., Kaljurand, I., Tshepelevitsh, S., Heering, A., Darnell, A., Kaupmees, K., Piirsalu, M., & Leito, I. (2018). pKa values in organic chemistry – Making maximum use of the available data. *Tetrahedron Letters*, 59, 3738-3748.
- Laidler, K. J. (1984). The Development of the Arrhenius Equation. *Journal of Chemical Education*, 61(6).
- Lapointe, M., Farner, J. M., Hernandez, L. M., & Tufenkji, N. (2020). Understanding and Improving Microplastic Removal during Water Treatment: Impact of Coagulation and Flocculation. *Environmental Science and Technology*, 54(14), 8719-8727. <https://doi.org/10.1021/acs.est.0c00712>
- Lau, R., Peng, W., Velazquez-Vargas, G., Yang, G. Q., & Fan, L. S. (2004). Gas-Liquid Mass Transfer in High-Pressure Bubble Columns. *Industrial and Engineering Chemical Research*, 43, 1302-1311.
- Lei, A. P., Hu, Z. L., Wong, Y. S., & Tam, N. F. Y. (2007). Removal of fluoranthene and pyrene by different microalgal species. *Bioresource Technology*, 98(2), 273-280. <https://doi.org/10.1016/j.biortech.2006.01.012>
- Leusink, J. (2014). Oxidation Potential of Ozone. *Pxidation Technologies LLC*.
- LeVan, M. D., & Vermeulen, T. (1981). Binary Langmuir and Freundlich Isotherms for Ideal Adsorbed Solutions. *Journal of Physical Chemistry*, 85, 3247-3250.
- Li, C., Zhu, Y., Zhang, T., Nie, Y., Shi, W., & Ai, S. (2022). Iron nanoparticles supported on N-doped carbon foam with honeycomb microstructure: An efficient potassium peroxymonosulfate activator for the degradation of fluoranthene in water and soil. *Chemosphere*, 286. <https://doi.org/10.1016/j.chemosphere.2021.131603>

- Li, F., Luo, T., Rong, H., Lu, L., Zhang, L., Zheng, C., Yi, D., Peng, Y., Lei, E., Xiong, X., Wang, F., Garcia, J. M., & Chen, J. a. (2022). Maternal rodent exposure to di-(2-ethylhexyl) phthalate decreases muscle mass in the offspring by increasing myostatin. *Journal of Cachexia, Sarcopenia and Muscle*, 13(6). <https://doi.org/10.1002/jcsm.13098>
- Lin, L., Xie, M., Liang, Y., He, Y., Chan, G. Y. S., & Luan, T. (2012). Degradation of cypermethrin, malathion and dichlorovos in water and on tea leaves with O3/UV/TiO2 treatment. *Food Control*, 28, 374-379.
- Liu, G., Huang, H., Xie, R., Feng, Q., Fang, R., Shu, Y., Zhan, Y., Ye, X., & Zhong, C. (2017). Enhanced degradation of gaseous benzene by a Fenton reaction. *RSC Advances*, 7, 71-76. <https://doi.org/10.1039/c6ra26016k>
- Liu, J., Chen, J., Jiang, L., & Wang, X. (2014). Adsorption of fluoranthene in surfactant solution on activated carbon: equilibrium, thermodynamic, kinetic studies. *Environmental Science and Pollution Research*, 21, 1809-1818.
- Liu, J. N., Chen, Z., Wu, Q. Y., Li, A., Hu, H. Y., & Yang, C. (2016). Ozone/graphene oxide catalytic oxidation: A novel method to degrade emerging organic contaminant N, N-diethyl-m-toluamide (DEET). *Scientific Reports*, 6. <https://doi.org/10.1038/srep31405>
- Liu, Y. (2006). Some consideration on the Langmuir isotherm equation. *Colloids and Surfaces A: Physicochemical and Engineering Aspects*, 274(1-3), 34-36.
- Liu, Z., Demeestere, K., & Hulle, S. V. (2021). Comparison and performance assessment of ozone-based AOPs in view of trace organic contaminants abatement in water and wastewater: A review. *Journal of Environmental Chemical Engineering*, 9(4). <https://doi.org/10.1016/j.jece.2021.105599>
- Liu, Z., Wang, S., Ma, W., Wang, J., Xu, H., Li, K., Huang, T., Ma, J., & Wen, G. (2022). Adding CuCo2O4-GO to inhibit bromate formation and enhance sulfamethoxazole degradation during the ozone/peroxymonosulfate process: Efficiency and mechanism. *Chemosphere*, 286. <https://doi.org/10.1016/j.chemosphere.2021.131829>
- Luo, L., Wang, P., Lin, L., Luan, T., Ke, L., & Tam, N. F. Y. (2014). Removal and transformation of high molecular weight polycyclic aromatic hydrocarbons in water by live and dead microalgae. *Process Biochemistry*, 49(10), 1723-1732. <https://doi.org/10.1016/j.procbio.2014.06.026>
- Luo, S., & Wong, C. P. (2001). Effect of UV/ozone treatment on surface tension and adhesion in electronic packaging. *IEEE Transactions on Components and Packaging Technologies*, 24, 43-49. <https://doi.org/10.1109/6144.910801>
- Lutsinge, T. B., & Chirwa, E. M. N. (2018). Biosurfactant-Assisted Biodegradation of Fluoranthene in a Two-Stage Continuous Stirred Tank Bio-Reactor System using Microorganism *Chemical Engineering Transactions*, 64.
- Lyngsie, G., Krumin, L., Tunlid, A., & Persson, P. (2018). Generation of hydroxyl radicals from reactions between a dimethoxyhydroquinone and iron oxide nanoparticles. *Scientific Reports*, 8, 10834.
- Małachowska-Jutcz, A., & Niesler, M. (2015). The effect of calcium peroxide on the phenol oxidase and acid phosphatase activity and removal of fluoranthene from soil. *Water, Air and Soil Pollution*, 226. <https://doi.org/10.1007/s11270-015-2632-y>
- Mandavgane, S. A., & Yenkie, M. K. N. (2011). EFFECT OF pH OF THE MEDIUM ON DEGRADATION OF AQUEOUS OZONE. *Rasayan Journal of Chemistry*, 4(3), 544-547.
- Manikkam, M., Tracey, R., Guerrero-Bosagna, C., & Skinner, M. K. (2013). Plastics Derived Endocrine Disruptors (BPA, DEHP and DBP) Induce Epigenetic Transgenerational Inheritance of Obesity, Reproductive Disease and Sperm Epimutations. *PLoS ONE*, 8(1). <https://doi.org/10.1371/journal.pone.0055387>

- Marttinen, S. K., Hänninen, K., & Rintala, J. A. (2004). Removal of DEHP in composting and aeration of sewage sludge. *Chemosphere*, *54*(3), 265-272.
[https://doi.org/10.1016/S0045-6535\(03\)00661-1](https://doi.org/10.1016/S0045-6535(03)00661-1)
- Marttinen, S. K., Kettunen, R. K., Sormunen, K. M., & Rintala, J. A. (2003). Removal of bis(2-ethylhexyl) phthalate at a sewage treatment plant. *Water Research*, *37*, 1385-1393.
- Mautz, W. J. (2003). Exercising animal models in inhalation toxicology: Interactions with ozone and formaldehyde. *Environmental Research*, *92*(1), 14-26.
[https://doi.org/10.1016/S0013-9351\(02\)00024-5](https://doi.org/10.1016/S0013-9351(02)00024-5)
- Molina, L. T., & Molina, M. J. (1986). Absolute absorption cross sections of ozone in the 185- to 350-nm wavelength range. *Journal of Geophysical Research: Atmospheres*, *91*(D13), 14501-14508.
- Monroe, E. B., & Heien, M. L. (2013). Electrochemical Generation of Hydroxyl Radicals for Examining Protein Structure. *Analytical Chemistry*, *85*(13), 6185-6189.
- Mook, W. T., Chakrabarti, M. H., Aroua, M. K., Khan, G. M. A., Ali, B. S., Islam, M. S., & Hassan, M. A. A. (2012). Removal of total ammonia nitrogen (TAN), nitrate and total organic carbon (TOC) from aquaculture wastewater using electrochemical technology: A review. *Desalination*, *284*, 1-13.
- Mopoung, S., Moonsri, P., Palas, W., & Khumpai, S. (2015). Characterization and Properties of Activated Carbon Prepared from Tamarind Seeds by KOH Activation for Fe(III) Adsorption from Aqueous Solution. *Scientific World Journal*, 415961.
- Muruganandam, L., Kumar, M. P. S., Jena, A., Gulla, S., & Godhwani, B. (2017). Treatment of waste water by coagulation and flocculation using biomaterials. *IOP Conference Series: Materials Science and Engineering*, *263*(3). <https://doi.org/10.1088/1757-899X/263/3/032006>
- Nastuneac, V., Panainte-Lehadus, M., Mosnegutu, E. F., Gavrilas, S., Cioca, G., & Munteanu, F. D. (2019). Removal of Cypermethrin from Water by Using Fucus Spiralis Marine Alga. *International Journal of Environmental Research and Public Health*, *16*, 3663.
- Nave, F., Cabrita, M. J., & Costa, C. T. d. (2007). Use of solid-supported liquid-liquid extraction in the analysis of polyphenols in wine. *Journal of Chromatography A*, *1169*(1-2), 23-30. <https://doi.org/10.1016/j.chroma.2007.08.067>
- Nkansah, M. A., Christy, A. A., Barth, T., & Francis, G. W. (2012). The use of lightweight expanded clay aggregate (LECA) as sorbent for PAHs removal from water. *Journal of Hazardous Materials*, *217-218*, 360-365.
<https://doi.org/10.1016/j.jhazmat.2012.03.038>
- Nobbs, J., & Tizaoui, C. (2014). A Modified Indigo Method for the Determination of Ozone in Nonaqueous Solvents. *Ozone: Science and Engineering*, *36*, 110-120.
- Nosaka, Y., & Nosaka, A. (2016). Understanding Hydroxyl Radical ($\bullet\text{OH}$) Generation Processes in Photocatalysis. *ACS Energy Letters*, *1*(2), 356-359.
- Nunes, C. A., & Guerreiro, M. C. (2011). ESTIMATION OF SURFACE AREA AND PORE VOLUME OF ACTIVATED CARBONS BY METHYLENE BLUE AND IODINE NUMBERS. *Química Nova*, *34*(3), 472-476.
- Oliveira, G. A., Monje-Ramirez, I., Carissimi, E., Rodrigues, R. T., Velasquez-Orta, S. B., Mejía, A. C. C., & Ledesma, M. T. O. (2019). The effect of bubble size distribution on the release of microalgae proteins by ozone-flotation. *Separation and Purification Technology*, *211*, 340-347. <https://doi.org/10.1016/j.seppur.2018.10.005>
- Owen, L. J., & Keevil, B. G. (2013). Supported liquid extraction as an alternative to solid phase extraction for LC-MS/MS aldosterone analysis? *The Association for Clinical Biochemistry and Laboratory Medicine*, *50*(5), 489-491.
<https://doi.org/10.1177/0004563213480758>
- Oxford Dictionary of Chemistry. In. (2020). *Oxford Dictionary of Chemistry*.

- Pan, H., Ritter, J. A., & Balbuena, P. B. (1998). Examination of the Approximations Used in Determining the Isothermic Heat of Adsorption from the Clausius-Clapeyron Equation *Langmuir*, 14, 6323-6327.
- Papageorgiou, A., Stylianou, S. K., Kaffes, P., Zouboulis, A. I., & Voutsas, D. (2017). Effects of ozonation pretreatment on natural organic matter and wastewater derived organic matter – Possible implications on the formation of ozonation by-products. *Chemosphere*, 170, 33-40. <https://doi.org/10.1016/j.chemosphere.2016.12.005>
- Papageorgiou, A., Voutsas, D., & Papadakis, N. (2014). Occurrence and fate of ozonation by-products at a full-scale drinking water treatment plant. *Science of the Total Environment*, 481, 392-400. <https://doi.org/10.1016/j.scitotenv.2014.02.069>
- Petrović, M., Gonzalez, S., & Barceló, D. (2003). Analysis and removal of emerging contaminants in wastewater and drinking water. *TrAC Trends in Analytical Chemistry*, 22(10), 685-696. [https://doi.org/10.1016/S0165-9936\(03\)01105-1](https://doi.org/10.1016/S0165-9936(03)01105-1)
- Pollak, E., & Talkner, P. (2005). Reaction rate theory: what it was, where is it today, and where is it going? *Chaos*, 15(2).
- Poole, C. F. (2003). New trends in solid-phase extraction. *TrAC Trends in Analytical Chemistry*, 22(6), 362-373. [https://doi.org/10.1016/S0165-9936\(03\)00605-8](https://doi.org/10.1016/S0165-9936(03)00605-8)
- Prakash, N. B., Sockan, V., & Jayakaran, P. (2014). Waste Water Treatment by Coagulation and Flocculation. *International Journal of Engineering Science and Innovative Technology*, 3(2). <https://www.researchgate.net/publication/273638362>
- Presumido, P. H., Montes, R., Quintana, J. B., RODIL, R., Feliciano, M., Puma, G. L., Gomes, A. I., & Vilar, V. J. P. (2022). Ozone membrane contactor to intensify gas/liquid mass transfer and contaminants of emerging concern oxidation. *Journal of Environmental Chemical Engineering*, 10(6), 108671. <https://doi.org/10.1016/j.jece.2022.108671>
- Qiu, H., Lv, L., Pan, B. C., Zhang, Q. J., ZHANG, W. M., & Zhang, Q. X. (2009). Critical review in adsorption kinetic models. *Journal of Zhejiang University - Science A* 10, 716-724. <https://doi.org/10.1631/jzus.A0820524>
- Rababah, A., & Matsuzawa, S. (2002). Treatment system for solid matrix contaminated with Fluoranthene. I-Modified extraction technique. *Chemosphere*, 46(1). www.elsevier.com/locate/chemosphere
- Rekhate, C. V., & Srivastava, J. K. (2020). Recent advances in ozone-based advanced oxidation processes for treatment of wastewater- A review. *Chemical Engineering Journal Advances*, 3. <https://doi.org/10.1016/j.ceja.2020.100031>
- Rivas, J., Gimeno, O., Calle, R. D. d. I., & Beltran, F. J. (2009). Ozone treatment of PAH contaminated soils: Operating variables effect. *Journal of Hazardous Materials*, 169(1-3), 509-515.
- Rodionova, O. E., & Pomerantsev, A. L. (2005). Estimating the Parameters of the Arrhenius Equation. *Kinetics and Catalysis*, 46(3), 329-332.
- Rodriguez, I., Llompарт, M. P., & Cela, R. (2000). Solid-phase extraction of phenols. *Journal of Chromatography*, 885(1-2), 291-304. www.elsevier.com/locate/chroma
- Rosenfeldt, E. J., Linden, K. G., Canonica, S., & Gunten, U. v. (2006). Comparison of the efficiency of $\cdot\text{OH}$ radical formation during ozonation and the advanced oxidation processes $\text{O}_3/\text{H}_2\text{O}_2$ and $\text{UV}/\text{H}_2\text{O}_2$. *Water Research*, 40(20), 3695-3704. <https://doi.org/10.1016/j.watres.2006.09.008>
- Rostam, A. B., & Taghizadeh, M. (2020). Advanced oxidation processes integrated by membrane reactors and bioreactors for various wastewater treatments: A critical review. *Journal of Environmental Chemical Engineering*, 8(6). <https://doi.org/10.1016/j.jece.2020.104566>
- Rout, P. R., Zhang, T. C., Bhunia, P., & Surampalli, R. Y. (2021). Treatment technologies for emerging contaminants in wastewater treatment plants: A review. *Science of the Total Environment*, 753. <https://doi.org/10.1016/j.scitotenv.2020.141990>

- Roy, K., & Moholkar, V. S. (2020). Sulfadiazine degradation using hybrid AOP of heterogeneous Fenton/persulfate system coupled with hydrodynamic cavitation. *Chemical Engineering Journal*, 386. <https://doi.org/10.1016/j.cej.2019.03.170>
- Ruffino, B., Korshin, G. V., & Zanetti, M. (2020). Use of spectroscopic indicators for the monitoring of bromate generation in ozonated wastewater containing variable concentrations of bromide. *Water Research*, 182. <https://doi.org/10.1016/j.watres.2020.116009>
- Saha, S., & Kaviraj, A. (2008). Acute Toxicity of Synthetic Pyrethroid Cypermethrin to Some Freshwater Organisms. *Bulletin of environmental contamination and toxicology*, 80, 49-52.
- Salgado, P., Melin, V., Y. Durán, Y., Mansilla, H., & Contreras, D. (2017). The Reactivity and Reaction Pathway of Fenton Reactions Driven by Substituted 1,2-Dihydroxybenzenes. *Environmental Science Technology*, 51(7), 3687-3693. <https://doi.org/10.1021/acs.est.6b05388>
- Sanchez-Polo, M., Gunten, U. v., & Rivera-Utrilla, J. (2005). Efficiency of activated carbon to transform ozone into radical OH radicals: Influence of operational parameters. *Water Research*, 39(14), 3189-3198.
- Saritha, V., Srinivas, N., & Vuppala, N. V. S. (2017). Analysis and optimization of coagulation and flocculation process. *Applied Water Science*, 7, 451-460. <https://doi.org/10.1007/s13201-014-0262-y>
- Savun-Hekimoglu, B. (2020). A Review on Sonochemistry and Its Environmental Applications. *Acoustics*, 2, 766-775.
- Schollée, J. E., Bourgin, M., Gunten, U. v., McArdell, C. S., & Hollender, J. (2018). Non-target screening to trace ozonation transformation products in a wastewater treatment train including different post-treatments. *Water Research*, 142, 267-278. <https://doi.org/10.1016/j.watres.2018.05.045>
- Schollée, J. E., Hollender, J., & McArdell, C. S. (2021). Characterization of advanced wastewater treatment with ozone and activated carbon using LC-HRMS based non-target screening with automated trend assignment. *Water Research*, 200. <https://doi.org/10.1016/j.watres.2021.117209>
- Selcuk, H., Vitosoglu, Y., Ozaydin, S., & Bekbolet, M. (2005). Optimization of ozone and coagulation processes for bromate control in Istanbul drinking waters. *Desalination*, 176(1-3), 211-217. <https://doi.org/10.1016/j.desal.2004.10.017>
- Seybold, P., & Sheilds, G. C. (2015). Computational estimation of pKa values. *WIREs Computational Molecular Science*, 5, 290-297.
- Shafeeyan, M. S., Daud, W. M. A. W., Houshmand, A., & Shamari, A. (2010). A review on surface modification of activated carbon for carbon dioxide adsorption. *Journal of Analytical and Applied Pyrolysis*, 89(2), 143-151. <https://doi.org/10.1016/j.jaap.2010.07.006>
- Shahid, M. K., Kashif, A., Fuwad, A., & Choi, Y. (2021). Current advances in treatment technologies for removal of emerging contaminants from water – A critical review. *Coordination Chemistry Reviews* 442, 213993.
- Shi, Z., Wang, C., & Zhao, Y. (2020). Effects of surfactants on the fractionation, vermiaccumulation, and removal of fluoranthene by earthworms in soil. *Chemosphere*, 250. <https://doi.org/10.1016/j.chemosphere.2020.126332>
- Shukla, Y., Yadav, A., & Arora, A. (2002). Carcinogenic and cocarcinogenic potential of cypermethrin on mouse skin. *Cancer Letters*, 182, 33-41.
- Si, B., Yang, L., Zhou, X., Watson, J., Tommaso, G., Chen, W. T., Liao, Q., Duan, N., Liu, Z., & Zhang, Y. (2019). Anaerobic conversion of the hydrothermal liquefaction aqueous phase: Fate of organics and intensification with granule activated carbon/ozone

- pretreatment. *Green Chemistry*, 21, 1305-1318.
<https://doi.org/10.1039/c8gc02907e>
- Silvestre, C. I. C., Santos, J. L. M., Lima, J. L. F. C., & Zagatto, E. A. G. (2009). Liquid-liquid extraction in flow analysis: A critical review. *Analytica Chimica Acta*, 652(1-2), 54-65. <https://doi.org/10.1016/j.aca.2009.05.042>
- Skopp, J. (2009). Derivation of the Freundlich Adsorption Isotherm from Kinetics. *Journal of Chemical Education*, 86(11).
- Snyder, S. A., Wert, E. C., Rexing, D. J., Zegers, R. E., & Drury, D. D. (2006). Ozone oxidation of endocrine disruptors and pharmaceuticals in surface water and wastewater. *The Journal of the International Ozone Association*, 28(6), 445-460.
<https://doi.org/10.1080/01919510601039726>
- Sohn, S., & Kim, D. (2005). Modification of Langmuir isotherm in solution systems— definition and utilization of concentration dependent factor. *Chemosphere*(58), 115-123.
- Somtrakoon, K., Chouychai, W., & Lee, H. (2014). Phytoremediation of anthracene-and fluoranthene-contaminated soil by *Luffa acutangula*. *Maejo International Journal of Science and Technology*, 8(3), 221-231. www.mijst.mju.ac.th
- Srividhya, J., & Schnell, S. (2006). Why substrate depletion has apparent first-order kinetics in enzymatic digestion. *Computational Biology and Chemistry*, 30(3), 209-214.
- Sun, Y., Angelotti, B., Brooks, M., Dowbiggin, B., Evans, P. J., Devins, B., & Wang, Z. W. (2018). A pilot-scale investigation of disinfection by-product precursors and trace organic removal mechanisms in ozone-biologically activated carbon treatment for potable reuse. *Chemosphere*, 210, 539-549.
<https://doi.org/10.1016/j.chemosphere.2018.06.162>
- Sunta, C. M., Ayta, W. E. F., Chubaci, J. F. D., & Watanabe, S. (2001). A critical look at the kinetic models of thermoluminescence: I. First-order kinetics. *Journal of Physics D: Applied Physics*, 34(17), 2690.
- Taheran, M., Naghdi, M., Brar, S. K., Verma, M., & Surampalli, R. Y. (2018). Emerging contaminants: Here today, there tomorrow! *Environmental Nanotechnology, Monitoring and Management*, 10, 122-126.
<https://doi.org/10.1016/j.enmm.2018.05.010>
- Tawabini, B., & Zubair, A. (2011). Bromate control in phenol-contaminated water treated by UV and ozone processes. *Desalination*, 267(1), 16-19.
<https://doi.org/10.1016/j.desal.2010.08.039>
- Tay, K. S., N. A. R., & Abas, M. R. B. (2013). Ozonation of metoprolol in aqueous solution: Ozonation by-products and mechanisms of degradation. *Environmental Science and Pollution Research*, 20, 3115-3121. <https://doi.org/10.1007/s11356-012-1223-3>
- The-Metabolomics-Innovation-Centre. *Di(2-ethylhexyl)phthalate (T3D0076)*.
- Tickner, J. A., Schettler, T., Guidotti, T., McCally, M., & Rossi, M. (2001). Health risks posed by use of di-2-ethylhexyl phthalate (DEHP) in PVC medical devices: A critical review. *American Journal of Industrial Medicine*, 39(1), 100-111.
[https://doi.org/10.1002/1097-0274\(200101\)39:1<100::AID-AJIM10>3.0.CO;2-Q](https://doi.org/10.1002/1097-0274(200101)39:1<100::AID-AJIM10>3.0.CO;2-Q)
- Tizaoui, C., & Grima, N. (2011). Kinetics of the ozone oxidation of Reactive Orange 16 azo-dye in aqueous solution. *Chemical Engineering Journal*, 173, 463-473.
- Tizaoui, C., Grima, N. M., & Dardar, M. Z. (2009). Effect of the radical scavenger t-butanol on gas-liquid mass transfer. *Chemical Engineering Science*, 64(21), 4375-4382.
- Toor, R., & Mohseni, M. (2007). UV-H₂O₂ based AOP and its integration with biological activated carbon treatment for DBP reduction in drinking water. *Chemosphere*, 66(11), 2087-2095. <https://doi.org/10.1016/j.chemosphere.2006.09.043>

- Toth, J. (2000). Calculation of the BET-compatible surface area from any Type I isotherms measured above the critical temperature. *Journal of Colloid and Interface Science*, 225(2), 378-383. <https://doi.org/10.1006/jcis.2000.6723>
- Tran, N. H., Reinhard, M., & Gin, K. Y. H. (2018). Occurrence and fate of emerging contaminants in municipal wastewater treatment plants from different geographical regions-a review. *Water Research*, 133, 182-207. <https://doi.org/10.1016/j.watres.2017.12.029>
- Tran, N. H., Urase, T., Ngo, H. H., Hu, J., & Ong, S. L. (2013). Insight into metabolic and cometabolic activities of autotrophic and heterotrophic microorganisms in the biodegradation of emerging trace organic contaminants. *Bioresource Technology*, 146, 721-731. <https://doi.org/10.1016/j.biortech.2013.07.083>
- Tsani, S., Koundouri, P., & Akinsete, E. (2020). Resource management and sustainable development: A review of the European water policies in accordance with the United Nations' Sustainable Development Goals. *Environmental Science and Policy*, 114, 570-579. <https://doi.org/10.1016/j.envsci.2020.09.008>
- Ullah, S., Zuberi, A., Alagawany, M., Farag, M. R., Dadar, M., Karthik, K., Tiwari, R., Dhama, K., & Iqbal, H. M. N. (2018). Cypermethrin induced toxicities in fish and adverse health outcomes: Its prevention and control measure adaptation. *Journal of Environmental Management*, 206, 863-871.
- Valdes, H., Sanchez-Polo, M., Rivera-Ultrilla, J., & Zaror, C. A. (2002). Effect of ozone treatment on surface properties of activated carbon. *Langmuir*, 18(6), 2111-2116. <https://doi.org/10.1021/la010920a>
- Van, E., Titus, M. S., & Johan, A. (2011). A standardization for BET fitting of adsorption isotherms. *Microporous and Mesoporous Materials*, 145(1-3), 188-193. <https://doi.org/10.1016/j.micromeso.2011.05.022>
- Velisek, J., Wlasow, T., Gomulka, P., Svobodova, Z., Dobsikova, R., NOVotny, L., & Dudzik, M. (2006). Effects of cypermethrin on rainbow trout. *Veterinarni Medicina*, 51(10), 469-476.
- Visco, G., Campanella, L., & Nobili, V. (2005). Organic carbons and TOC in waters: an overview of the international norm for its measurements. *Microchemical Journal*, 79(1-2), 185-191.
- Wang, B., Shi, W., Zhang, H., Ren, H., & Xiong, M. (2021). Promoting the ozone-liquid mass transfer through external physical fields and their applications in wastewater treatment: A review. *Journal of Environmental Chemical Engineering*, 9(5). <https://doi.org/10.1016/j.jece.2021.106115>
- Wang, Y., Yu, G., Deng, S., Huang, J., & Wang, B. (2018). The electro-peroxone process for the abatement of emerging contaminants: Mechanisms, recent advances, and prospects. *Chemosphere*, 208, 640-654. <https://doi.org/10.1016/j.chemosphere.2018.05.095>
- Wei, X., Shi, Y., Fei, Y., Chen, J., Lv, B., Chen, Y., Zheng, H., Shen, J., & Zhu, L. (2016). Removal of trace phthalate esters from water by thin-film composite nanofiltration hollow fiber membranes. *Chemical Engineering Journal*, 292, 382-388. <https://doi.org/10.1016/j.cej.2016.02.037>
- Wu, J., Rudy, K., & Spark, J. (2000). Oxidation of aqueous phenol by ozone and peroxidase. *Advances in Environmental Reserach* 4, 339-346.
- Wu, J. G., Luan, T. G., Lan, C. Y., Lo, W. H., & Chan, G. Y. S. (2007). Efficacy evaluation of low-concentration of ozonated water in removal of residual diazinon, parathion, methyl-parathion and cypermethrin on vegetable. *Journal of Food Engineering*, 79, 803-809.
- Xiong, W., Cui, W., Li, R., Feng, C., Liu, Y., Ma, N., Deng, J., Xing, L., Gao, Y., & Chen, N. (2020). Mineralization of phenol by ozone combined with activated carbon:

- Performance and mechanism under different pH levels. *Environmental Science and Ecotechnology*, 1. <https://doi.org/10.1016/j.es.2019.100005>
- Yang, C. (1998). Statistical Mechanical Study on the Freundlich Isotherm Equation. *Journal of Colloid and Interface Science*, 208(2), 379-387.
- Yao, H., Sun, P., Minakata, D., Crittenden, J. C., & Huang, C. H. (2013). Kinetics and modeling of degradation of ionophore antibiotics by UV and UV/H₂O₂. *Environmental Science and Ecotechnology*, 47(9), 4581-4589. <https://doi.org/10.1021/es3052685>
- Yilmaz, O., & Tas, B. (2021). Feasibility and assessment of the phytoremediation potential of green microalga and duckweed for zeta-cypermethrin removal. *Desalination and Water Treatment*, 3209, 131-143.
- Yousef, M. I., El-Demerdash, F. M., Kamel, K. I., & Al-Salhen, K. S. (2003). Changes in some hematological and biochemical indices of rabbits induced by isoflavones and cypermethrin. *Toxicology*, 189, 223-234.
- Zarean, M., Bina, B., & Ebrahimi, A. (2017). The influence of zero-valent iron on the photodegradation ozonation of di 2-ethyl hexyl phthalate in aqueous solution. *Desalination and Water Treatment*, 78, 321-329.
- Zarean, M., Bina, B., Ebrahimi, A., Pourzamani, H., & Esteki, F. (2015). Degradation of di-2-ethylhexyl phthalate in aqueous solution by advanced oxidation process. *International Journal of Environmental Health Engineering*, 4(3).
- Zeng, Y., & Hong, P. K. A. (2002). Slurry-Phase Ozonation for Remediation of Sediments Contaminated by Polycyclic Aromatic Hydrocarbons. *Journal of the Air and Water Management Association*, 52(1), 56-68.
- Zhang, C., Wu, L., Cai, D., Zhang, C., Wang, N., Zhang, J., & Wu, Z. (2013). Adsorption of polycyclic aromatic hydrocarbons (fluoranthene and anthracenemethanol) by functional graphene oxide and removal by pH and temperature-sensitive coagulation. *ACS Applied Materials and Interfaces*, 5(11), 4783-4790. <https://doi.org/10.1021/am4002666>
- Zhang, S., Sun, M., Hedtke, T., Deshmukh, A., Zhou, X., Weon, S., Elimelech, M., & Kim, J. H. (2020). Mechanism of Heterogeneous Fenton Reaction Kinetics Enhancement under Nanoscale Spatial Confinement. *Environmental Science and Ecotechnology*, 54(17), 10868-10875. <https://doi.org/10.1021/acs.est.0c02192>
- Zhang, W., Zheng, N., Sun, S., An, Q., Li, X., Li, Z., Ji, Y., Li, Y., & Pan, J. (2023). Characteristics and health risks of population exposure to phthalates via the use of face towels. *Journal of Environmental Sciences*, 130, 1-13. <https://doi.org/10.1016/j.jes.2022.10.016>
- Zhang, X., Echigo, S., Lei, H., Smith, M., Minear, R., & Talley, J. (2005). Effects of temperature and chemical addition on the formation of bromoorganic DBPs during ozonation. *Water Research*, 39(2-3), 423-435. <https://doi.org/10.1016/j.watres.2004.10.007>
- Zhao, G., Lu, X., Zhou, Y., & Gu, Q. (2013). Simultaneous humic acid removal and bromate control by O₃ and UV/O₃ processes. *Chemical Engineering Journal*, 232, 74-80. <https://doi.org/10.1016/j.cej.2013.07.080>
- Zhou, H., & Smith, D. W. (2000). Ozone mass transfer in water and wastewater treatment: experimental observations using a 2D laser particle dynamics analyzer. *Water Research*, 34(3), 909-921. www.elsevier.com/locate/watres
- Zhou, Y., Zhao, B., Wang, L., Li, T., Ye, H., Li, S., Hunag, M., & Zhang, X. (2022). Adsorption of Phthalate Acid Esters by Activated Carbon: The Overlooked Role of the Ethanol Content. *Foods*, 11, 2114.
- Ziembowicz, S., Kida, M., & Kpszelnik, P. (2017). Sonochemical Formation of Hydrogen Peroxide 2nd International Electronic Conference on Water Sciences

Zwir-Ferenc, A., & Biziuk, M. (2015). Solid phase extraction technique-Trends, opportunities and applications. *Polish Journal of Environmental Studies*, 15, 677-690.
<https://www.researchgate.net/publication/279597851>

Glossary

aqueous	describing a solution in water ("Oxford Dictionary of Chemistry," 2020)
biosorption	a property by which certain types of microbial biomass can absorb contaminants from the environment ("Collins English Dictionary ", 2023)
biotransformation	the metabolising of some substance in the body ("Collins English Dictionary ", 2023)
carcinogen	any agent that produces cancer ("Oxford Dictionary of Chemistry," 2020)
coagulation	the process in which colloidal particles come together irreversibly to form larger masses ("Oxford Dictionary of Chemistry," 2020)
degradation	a type of chemical reaction where a compound is converted into a simpler compound ("Oxford Dictionary of Chemistry," 2020)
deionised water	water from which ionic salts have been removed by ion-exchange ("Oxford Dictionary of Chemistry," 2020)
electrophile	an ion or molecule that is electron deficient and can accept electrons ("Oxford Dictionary of Chemistry," 2020)
emissivity	the ability of an object to emit heat, compared to the heat emitted by a black object of the same temperature ("Cambridge Dictionary," 2023)
endocrine disruptors	a chemical that can affect the systems in the body that produce and control hormones ("Cambridge Dictionary," 2023)
flocculation	the process in which particles in a colloid aggregate into larger clumps ("Oxford Dictionary of Chemistry," 2020)
heteroatoms	an odd atom in the ring of a heterocyclic compound ("Oxford Dictionary of Chemistry," 2020)
heterogenous	relating to two or more phases ("Oxford Dictionary of Chemistry," 2020)

isotherm	a curve on a graph representing readings taken at constant temperature ("Oxford Dictionary of Chemistry," 2020)
leaching	extraction of soluble compounds of a solid mixture by percolating a solvent through it ("Oxford Dictionary of Chemistry," 2020)
lipophilic	lipophilic substances are attracted to lipids ("Cambridge Dictionary," 2023)
moiety	a characteristic part of a molecule ("Oxford Dictionary of Chemistry," 2020)
ozonation	the formation of ozone ("Oxford Dictionary of Chemistry," 2020)
ozone	a colourless gas, soluble in cold water and alkalis ("Oxford Dictionary of Chemistry," 2020)
photolysis	a chemical reaction produced by exposure to light or ultraviolet radiation ("Oxford Dictionary of Chemistry," 2020)
phthalate	a chemical compound used in making plastics, which is believed to be dangerous to health ("Cambridge Dictionary," 2023)
pyrethroids	any of various chemical compounds having similar insecticidal properties to pyrethrin ("Collins English Dictionary ", 2023)
reagent	a substance reacting with another substance ("Oxford Dictionary of Chemistry," 2020)
solvent	a liquid that dissolves another substance or substances to form a solution ("Oxford Dictionary of Chemistry," 2020)
stoichiometric	describing chemical reactions in which the reactants combine in simple whole number ratios ("Oxford Dictionary of Chemistry," 2020)

Appendices

Appendix 1 – Iodine Number Calculations

Standardisation of 0.100 N Sodium Thiosulfate

$$N_1 = \frac{P \times R}{S}$$

Where:

N_1 = sodium thiosulfate, N

P = potassium iodate, mL

R = potassium iodate, N

S = sodium thiosulfate, mL

Standardisation of 0.100 N Iodine Solution

$$N_2 = \frac{S \times N_1}{I}$$

Where:

N_2 = iodine, N

S = sodium thiosulfate, mL

N_1 = sodium thiosulfate, N

I = iodine, mL

Calculating the iodine number

$$A = (N_2)(12693.0)$$

Where:

N_2 = iodine, N

$$B = (N_1)(126.93)$$

Where:

N_1 = sodium thiosulfate, N

$$DF = \frac{I + H}{F}$$

Where:

DF = dilution factor

I = iodine, mL

H = 5 % hydrochloric acid used, mL

F = filtrate, mL

$$\frac{X}{M} = \frac{[A - (DF)(B)(S)]}{M}$$

Where:

$\frac{X}{M}$ = iodine absorbed per gram of carbon, mg/g

S = sodium thiosulfate, mL

M = carbon used, g

Calculating the carbon dosage

$$M = \frac{[A - (DF)(C)(126.93)(50)]}{E}$$

Where:

M = carbon, g

$A = (N_2)(12693.0)$

DF = dilution factor

C = residual iodine

E = estimated iodine number of the carbon

Appendix 2 – deriving the equation relating C_{AL} and $k_L a$

$$N_A \times a \times V_L = V_L \frac{d C_{AL}}{d t}$$

$$N_A = k_L (C_{AL}^* - C_{AL})$$

$$k_L a V_L (C_{AL}^* - C_{AL}) = V_L \frac{d C_{AL}}{d t}$$

$$\int_{C_{AL0}}^{C_{AL}} \frac{d C_{AL}}{C_{AL}^* - C_{AL}} = \int_0^t k_L a d t$$

$$\int_{C_{AL0}}^{C_{AL}} \frac{d C_{AL}}{C_{AL} - C_{AL}^*} = - \int_0^t k_L a d t$$

$$\ln \left(\frac{C_{AL} - C_{AL}^*}{C_{AL0} - C_{AL}^*} \right) = - k_L a t$$

$$\frac{C_{AL} - C_{AL}^*}{C_{AL0} - C_{AL}^*} = \exp(-k_L a t)$$

Assuming $C_{AL0} = 0$

$$C_{AL} - C_{AL}^* = - C_{AL}^* \exp(-k_L a t)$$

$$C_{AL} = C_{AL}^*(1 - \exp(-k_L a t))$$

Where:

N_A = Avogadro constant

V_L = volume of liquid

C_{AL} = ozone concentration in the liquid phase

t = time

$k_L a$ = mass transfer coefficient